UNIVERSITY OF CALIFORNIA,
IRVINE

Assessing the Benefits of Incorporating Soil Moisture Observations into a Distributed Hydrologic Model

DISSERTATION

Submitted in partial satisfaction of the requirements
for the degree of

DOCTOR OF PHILOSOPHY

in Civil Engineering

by

Andrea Rose Thorstensen

Dissertation Committee:
Professor Soroosh Sorooshian, Co-Chair
Professor Kuolin Hsu, Co-Chair
Professor Amir AghaKouchak
Professor Russell Detwiler

2016

DEDICATION

To

My loving parents,

My wonderful siblings, Dan and Karen,

and

My love, Andy

Their love, motivation, kindness, and sacrifice
made the completion of this dissertation possible.

TABLE OF CONTENTS

LIST OF FIGURES

LIST OF TABLES

ACKNOWLEDGMENTS

I would like to sincerely thank my advisor Professor Soroosh Sorooshian for giving me the priceless opportunity to become a member of the Center for Hydrometeorology and Remote Sensing (CHRS) at UCI. Not only did he welcome me into the highly supportive, collaborative, and productive environment that he has cultivated within CHRS, but he also consistently encouraged me to learn from new experiences that fell outside of my comfort zone. Because of this, my personal and professional growth during my time at UCI has far exceeded my expectations. For this, I am forever grateful. I want to acknowledge and thank my co-advisor, Professor Kuolin Hsu, who put in tireless hours of guidance during the course of my studies. His passion for research is highly contagious, and his work ethic and selflessness are truly inspirational.

Many thanks go to my committee members, Professor Amir AghaKouchak and Professor Russell Detwiler. Dedication of their valuable time and effort helped to improve the quality of this dissertation. I would like to thank Dr. Xiaogang Gao for his support throughout my time at CHRS. I am also very grateful to Dr. Jialun Li for dedicating a great deal of his time to helping me in the early stages of my research.

My sincerest gratitude goes to my dear friends at CHRS: Wei, Ali, Alex, Joey, Nasrin, Jinging, Hamed, Scott, Phu, Hao, Sepideh, Tiantian, Negar, Yumeng, Hoang, Ata, Baoxiang, Raied, Mohammad, and Negin. Time spent with you has been a highlight for me and I am truly amazed and inspired by the talented people I am fortunate enough to call my friends. I would like to give special acknowledgement to Phu, who adopted me as a little sister from the moment I arrived at UCI and who continues to be a wonderful role model and research partner.

Special thanks go to Diane Hohnbaum, who keeps CHRS running like a well-oiled machine, and to Dan Braithwaite, who is truly the heartbeat of the center.

Thanks to my undergraduate advisors, Rodney Kubesh, Juan Fedele, and Anthony Hansen, who first encouraged me to pursue an advanced degree and have continued to be some of the loudest voices on my cheering squad. Thanks to Robert Zamora, who continues to be a cherished mentor.

I would not be where I am let alone who I am without the love and support of my family. To my parents, my brother Dan, and sister Karen, thank you for the unconditional love you have given me my entire life. Sincere gratitude to my dear Andy, for loving me the way I am, for sharing in my joys, and for keeping me sane when times were hard. Thank you to all my friends and family all over the world. Though we may sometimes be far apart, I always keep you close in my heart.

IFloodS data was provided by Dr. Witold Krajewski and the Iowa Flood Center team and SMOS data from the European Space Agency. Primary funding for this work was provided by the Department of Defense through the National Defense Science and Engineering Graduate fellowship program and the National Oceanic and Atmospheric Administration's National Weather Service.

CURRICULUM VITAE

Andrea Rose Thorstensen

Education

Ph.D., Civil Engineering, University of California, Irvine, May 2016

M.S., Civil Engineering, University of California, Irvine, June 2013

B.S., Meteorology & Hydrology (summa cum laude), St. Cloud State University, May 2011

Research Interests

Surface hydrology, rainfall-runoff modeling, model calibration, data assimilation, water resources management, remote sensing, flood forecasting/prediction, and hydroclimate analysis

Research Experience

2011-2013	Graduate Student Researcher, Center for Hydrometeorology and Remote Sensing, The Henry Samueli School of Engineering, University of California, Irvine
2013	Student Intern, DEVELOP National Program, Jet Propulsion Laboratory, National Aeronautics and Space Administration, Pasadena, California
2010	Student Intern, David Skaggs Research Center, National Oceanic and Atmospheric Administration, Boulder, Colorado
2009	Student Intern, National Weather Service, National Oceanic and Atmospheric Administration, Juneau, Alaska

Fellowships and Awards

- Department of Defense National Defense Science and Engineering Graduate Fellowship, 2013-2016
- American Meteorological Society 29th Conference on Hydrology 2nd place Student Oral Presentation, Phoenix, AZ, 2015
- American Meteorological Society Hydrology Section Student Travel Grant, 2015 & 2016

- University of California Graduate Student Research and Travel Grant, 2014
- University of California Associated Graduate Students Travel Grant, 2014, 2015 & 2016
- American Meteorological Society Student Travel grant, 2013
- National Oceanic and Atmospheric Administration 2009 Ernest F. Hollings Scholar, 2009-2011
- St. Cloud State University Honors Program, 2007-2011
- Alworth Memorial Scholarship, 2007-2011
- Northeast Minnesota Scholarship, St. Cloud State University, 2008
- Founders Scholarship, St. Cloud State University, 2008

Publications

2016 **Thorstensen, A**., P. Nguyen, K. Hsu, and S. Sorooshian. "Using Densely Distributed Soil Moisture Observations for Calibration of a Hydrologic Model," *Journal of Hydrometeorology, 17*

2016 **Thorstensen, A**., P. Nguyen, K. Hsu, and S. Sorooshian. "Assessment of Assimilating SMOS Soil Moisture Information into a Distributed Hydrologic Model," *ESA SP-740* (CD-ROM), ESA Publications Division, European Space Agency

2016 Nguyen, P., **A. Thorstensen**, K. Hsu, A. AghaKouchak, B. Sandres, M. Smith, V. Koren, and S. Sorooshian. "A high resolution coupled hydrologic/hydraulic model (HiResFlood-UCI) for flash flood modeling." *Journal of Hydrology* (in press)

2015 Nguyen, P., **A. Thorstensen**, S. Sorooshian, K. Hsu, and A. Aghakouchak. "Flood forecasting and inundation mapping using HiResFlood-UCI and near real-time satellite precipitation data: the 2008 Iowa flood," *Journal of Hydrometeorology, 16(3)*

2015 Nguyen, P., **A. Thorstensen**, H. Ashouri, S. Sellars, K. Hsu, A. AghaKouchak, D. Braithwaite, and S. Sorooshian. "Tutorial on CHRS-UCI's Satellite Data Products." *Proceedings of the U.S.-Iran Symposium on Climate Change: Impacts and Mitigation.*

2015 Zamora, R. J., **A. R. Thorstensen**, A. B. White, C. W. King, and C. Shobe. "The Influence of Soil Texture on Soil Water Storage in the North Fork American River Basin," *Journal of Hydrometeorology* (in review)

2015 Ashouri, H., P. Nguyen, **A. Thorstensen**, K. Hsu, and S. Sorooshian. "Long-Term historical rainfall-runoff modeling using high-resolution satellite-based precipitation products," *Journal of Hydrometeorology* (in review)

2014 Nguyen, P., S. Sellars, **A. Thorstensen**, Y. Tao, H. Ashouri, D. Braithwaite, K. Hsu, and S. Sorooshian. "Satellites Track Precipitaiton of Super Typhoon Haiyan," *Eos, Transactions American Geophysical Union. 95(16)*

Presentations

2016 **Thorstensen, A**., P. Nguyen, K. Hsu, and S. Sorooshian. "Assessment of Assimilating SMOS Soil Moisture Information into a Distributed Hydrologic Model," Poster Presentation, Living Planet Symposium 2016, European Space Agency, Prague, Czech Republic

2016 **Thorstensen, A**., P. Nguyen, R. Zamora, K. Hsu, and S. Sorooshian. "Using the Ensemble Kalman Filter Recursively to Update Soil Moisture Estimates in a Conceptually-Based Distributed Hydrologic Model," Oral Presentation, American Meteorological Society Annual Meeting, New Orleans, LA

2015 **Thorstensen, A**., P. Nguyen, K. Hsu, R. Zamora, and S. Sorooshian. "Data Assimilation of Soil Moisture in a Distributed Hydrologic Model: A Case Study over the Russian River Basin," Oral Presentation, American Meteorological Society Annual Meeting, Phoenix, AZ

2015 Nguyen, P., **A. Thorstensen**, H. Liu, S. Sellars, H. Ashouri, D. Braithwaite, K. Hsu, X. Gao, and S. Sorooshian, "CHRS Connect – a global extreme precipitation event database using object-oriented approach," 5th Annual Meeting of NSF Expeditions in Computing, Minneapolis, MN

2015 Hsu, K., P. Nguyen, **A. Thorstensen**, H Ashouri, D. Braithwaite, and S. Sorooshian. "Development of Satellite-based PERSIANN Precipitation Retrieval," Telecon Presentation, ASEAN Network Workshop on Satellite-based Rainfall Application, Bangkok, Thailand

2015 Hsu, K., P. Nguyen, **A. Thorstensen**, H Ashouri, D. Braithwaite, and S. Sorooshian. "Development of Satellite-based PERSIANN Precipitation Retrieval," ICIWaRM Partners Meeting, Lakewood, CO

2014 **Thorstensen, A**., P. Nguyen, K. Hsu, and S. Sorooshian. "Calibration of a Hydrologic Model via Densely Distributed Soil Moisture Observations," Poster Presentation, American Geophysical Union Fall Meeting, San Francisco, CA

2014 Nguyen, P., **A. Thorstensen**, K. Hsu, A. Aghakouchak, B. Sanders, and S. Sorooshian. "Simulation of the 2008 Iowa Flood using HiResFlood-UCI Model with Remote Sensing Data," Poster Presentation, American Geophysical Union Fall Meeting, San Francisco, CA

2014 Ashouri, H., P. Nguyen, **A. Thorstensen**, K., Hsu, and S. Sorooshian. "Long-Term Historical Rainfall-Runoff Modeling Using High-Resolution Satellite-based Precipitation Products," Oral Presentation, American Geophysical Union Fall Meeting, San Francisco, CA

2013 **Thorstensen, A**., P. Nguyen, K. Hsu, W. Krajewski, and S. Sorooshian. "Comparison of Multiple Precipitation Products over a Densely Gauged Basin through Distributed Hydrologic Modeling," Poster Presentation, American Geophysical Union Fall Meeting, San Francisco, CA

2011 **Thorstensen, A**. "Influence of soil moisture on dry down patterns of the North Fork of the American River," Poster Presentation, American Meteorological Society Annual Meeting, Seattle, WA

Training Courses

2015 American Meteorological Society Summer Policy Colloquium, Washington, DC

2015 Predictive Modeling with Python – Data Science Initiative, Irvine, CA

2014 NASA Jet Propulsion Lab Center for Climate Sciences Summer School, Pasadena, CA

2013 American Meteorological Society Short Course: A Beginner's Course to Using Python in Climate and Meteorology, Austin, TX

Conferences and Meetings Attended Without Presentation

2015 Drought Response Workshop, Irvine, CA

2014 California Council on Science and Technology Meeting, Sacramento, CA

2014 UNESCO G-WADI Meeting, Irvine, CA

2013 American Meteorological Society Annual Meeting, Austin, TX

2012 IUGG GRC Conference on Extreme Natural Hazards and Risk, Orange, CA

2012 3rd SMAP Calibration/Validation Workshop, Oxnard, CA

2009 2009 Severe Storms & Doppler Radar Conference, Des Moines, IA

Service and Volunteering

2016 Reviewer of Journal of Hydrology: Regional Studies

2015 & 2016 Served as judge for Junior Science and Humanities Symposium, Irvine, CA

2015 Guest lecturer for UC Irvine undergraduate/graduate Hydrology class, Irvine, CA

2015 Volunteer for NASA Data Intensive Research and Education Center in Science, Technology, Engineering, and Math workshop, Irvine, CA

2014 Graduate Student Representative for UCI Academic Senate Council on Research, Computing, and Libraries, Irvine, CA

2014 Student Volunteer for American Geophysical Union Fall Meeting, San Francisco, CA

2010 Weather Briefing, Northern Plains Winter Storm Conference, St. Cloud, MN

2009 Session Chair, Northern Plains Winter Storm Conference, St. Cloud, MN

Professional And Academic Memberships

American Geophysical Union

American Meteorological Society

American Society of Civil Engineers

Associated Graduate Students – UCI (Council Member 2014-2015)

National Weather Association (President of Student Chapter 2010-2011)

Society of Women Engineers

Graduate Women in Engineering

Earth Science Women's Network

Golden Key International Honour Society

Tutorials

G-WADI GeoServer Tutorial (English version), 2012. Available at: http://persiann.eng.uci.edu/gwadi_tutorial_videos.html

RainSphere Tutorial, 2016, Available at: http://rainsphere.eng.uci.edu/

ABSTRACT OF THE DISSERTATION

Assessing the Benefits of Incorporating Soil Moisture Observations into a Distributed Hydrologic Model

by

Andrea Rose Thorstensen

Doctor of Philosophy in Civil Engineering

University of California, Irvine, 2016

Professor Soroosh Sorooshian, Co-Chair

Professor Kuolin Hsu, Co-Chair

Soil moisture is a vital component of the hydrologic cycle. It modulates the partitioning of infiltration and runoff as well as controls surface moisture and energy fluxes. Until recent years, it has also been one of the most overlooked components because of the difficulty to effectively measure and model it at scales most relevant to the hydrologic community. With a rise of new observation technologies and a growth in modeling efforts, this dissertation aims to investigate and establish the most useful ways to incorporate observed soil moisture information into a conceptually-based distributed hydrologic model developed for operational streamflow prediction by the U.S. National Weather Service. A common platform of soil saturation ratios for comparison between observations and model simulations of soil moisture is established using past observations mindfully combined with calculations of soil hydraulic properties based on readily available characteristics

from soil surveys. Data assimilation using an Ensemble Kalman Filter is used to update conceptual model storages with observed volumetric soil moisture. The assimilation is modified to address underdispersiveness that occurs following a precipitation event and after prolonged dry periods. A second filtering step is developed to spread innovation at pixels collocated with observations to model pixels that are not "observed." The use of soil moisture observations as a tool for calibration is also investigated, and a new two-step hybrid calibration scheme that utilizes both soil moisture observations and observed streamflow is introduced. The effects of soil moisture data assimilation and soil moisture-based calibration on simulated streamflow are also analyzed.

Development of soil saturation ratio comparison efforts and data assimilation techniques are conducted in the Russian River Basin in northern California. Both *in situ* soil moisture probes and Soil Moisture Ocean Salinity (SMOS) surface soil moisture estimates are tested in the data assimilation experiments. The soil moisture-based calibration development takes place in the Turkey River Basin in northeastern Iowa, and is further tested in the Russian River Basin. Results show that while both uses of soil moisture are effective in improving estimates of the soil moisture state, the calibration scheme is more stable and necessary to improve simulated streamflow.

Chapter 1. Introduction

1.1 Importance of Soil moisture Characterization

Soil moisture is a key element to consider when modeling catchment scale water balance and predicting extreme weather events as processes including evaporation, infiltration, and runoff are driven by it (Kerr *et al.*, 2001). It follows that timely access to soil moisture data can lead to better forecasts of flooding from rainstorms. Additionally, evidence of soil moisture-precipitation feedback has been presented in several studies (Alfieri *et al.*, 2007; Frye and Mote, 2009; Ford *et al.*, 2015), suggesting its importance as both an initiator and inhibitor of convective activity. Accurate knowledge of soil moisture conditions also has direct applicability to agricultural practices. Irrigation planning (especially for arid regions) is crucial for optimal economic use of water for farming, and soil moisture monitoring is a promising contributor for such planning (Kerr *et al.*, 2010). The aforementioned topics call for soil moisture information on a variety of timescales, even as frequent as daily to sub-daily. This is particularly true in dry regions, where the soil moisture dynamic signal can change rapidly during and immediately following a precipitation event.

As valuable as knowledge of the soil moisture state in high spatio-temporal resolution is, modeling and/or measuring soil moisture remains a challenge. Obtaining this data has been investigated in a number of ways including back-tracking from other observed quantities such as streamflow (Komma *et al.*, 2008) as well as direct measurements from soil moisture probes. Jin and Henderson (2011) mention how traditional methods for

measuring soil moisture such as airborne measurements and *in situ* observations are often limited in their spatial and temporal coverage, and that methods that improve on these deficiencies are required for measured soil moisture to be able to achieve the potential benefits within the scope of agriculture, rainfall-runoff modeling, large vehicle trafficability, and soil moisture/precipitation feedback.

1.2 Research Motivation

As soil moisture observation techniques and technology matures, so do the possibilities of providing reliable estimates of the soil moisture state within the aforementioned applications. Retrieval of surface soil moisture is now possible globally thanks to the efforts of several missions launched within the last decade. This opens a new realm in which information about ungauged basins or those with limited observations is now available, and a new piece of the hydrologic cycle can be more accurately accounted for. It follows that improved estimation of this storage component of the hydrologic cycle may provide valuable added information to help better characterize additional constituents such as streamflow.

This new suite of information has the potential to improve hydrologic modeling capabilities if handled properly. To this end, careful consideration should be taken of spatial and temporal scales (both of the model and the observations), associated uncertainties, and effective strategies to meld observations with model predictions.

1.3 Objectives

In this dissertation, methods designed to fully exploit the distributed nature of soil moisture data are developed and tested for fruitfulness in the scope of distributed hydrologic modeling. The role that soil moisture plays in the realm of hydrologic modeling is two-fold. The first is to serve as the observations necessary for a Monte Carlo data assimilation process to update predicted model states. The second seeks to assess how information from soil moisture observations can be used to constrain model parameters, especially those that are commonly grouped together and calibrated using observed streamflow. Use of both *in situ* and satellite-based soil moisture retrievals are investigated, assuming that the highly localized *in situ* data serve as a "best case" representation of the quality and temporal frequency of what satellite retrievals could hope to achieve (with the limitation of less spatial coverage than that which the satellite-based estimates offer).

This study attempts to incorporate soil moisture observations of various scales into a conceptual distributed hydrologic model through a newly developed calibration scheme that focuses on capturing soil moisture dynamics, as well as a two-step data assimilation procedure. Proper treatment of soil moisture observations/simulations prior to comingling them is investigated, and a scalable approach for describing soil properties is introduced. As the model utilized in this dissertation is intended as a hydrologic model, the final stage is to investigate any enhancement of streamflow characterization/prediction that results from the potentially improved description of the soil moisture state.

The specific objectives are as follows:

1) Establish a common ground on which highly localized in situ observations, large-scale satellite-based estimates (10's of km), and medium-scale model pixels (~4km) representations of soil moisture can be compared.

2) Construct an effective assimilation framework suitable for updating conceptual model states using observed soil moisture.

3) Assess the value that comes with incorporating soil moisture information into the calibration processes of a distributed hydrologic model.

4) Investigate what improvements (if any) can be achieved in terms of streamflow prediction when soil moisture observations are assimilated into a distributed hydrologic model.

1.4 Organization of the Dissertation

The remainder of this dissertation is organized into six additional chapters. Chapter 2 describes current representations of soil moisture via modeling efforts and observation strategies. Chapter 3 introduces a method to address the spatial discrepancies of the soil moisture estimates investigated in this work. Chapter 4 discusses strategies for and implications of soil moisture data assimilation on state estimation in a conceptual distributed hydrologic model. Chapter 5 is dedicated to describing a newly developed calibration strategy that utilizes soil moisture observations. Chapter 6 investigates the individual (and combined) effects that using soil moisture for data assimilation and for calibration have on simulated streamflow. Finally, Chapter 7 presents a summary and relevant future work.

Chapter 2. Model and Data for Soil Moisture Estimation

2.1 Background

The "Holy Grail" for soil moisture data is such that both the spatial and temporal resolutions are fine enough to capture the processes of interest and that information on the entire soil column can be characterized. In situ soil moisture measurements may capture temporal variability, and possibly the vertical variability with the implementation of multiple probes, but are restricted to the location of the instrument. When it comes to satellite retrievals there is yet to be a single method for observation that satisfies the requirements either. Optical methods provide spatial fine-scale potential but have drawbacks such as timing limitations and cloud dependence (Scott *et al.*, 2003). On the other hand, microwave systems have a more coarse spatial resolution but provide a nearly direct measurement of soil moisture, have the advantage of being all-weather, and when the frequency is low enough (ideally the L-band) attenuation from vegetation and the atmosphere is significantly reduced (Kerr *et al.* 2010). As there is no complete end-all solution to achieve the desired resolutions, the realm of data assimilation, where observations fuse with modeling, becomes an attractive option. Furthermore, calibration using soil moisture observations has the potential to add internal basin information that calibration with outlet streamflow (the traditional calibration strategy) simply cannot capture.

2.2 Soil Moisture Observations

When it comes to soil moisture observations, the two categories that represent extremes both spatially and temporarily are the focus of this dissertation. On one hand, soil moisture probes (particularly permanent and automatically sampling *in situ* instruments) provide frequent, continuous monitoring of a highly localized area. The space represented by these instruments is often on the order of the volume of a pop can with the temporal frequency as high as sub-minute. On the other end of the spectrum, satellite retrieved soil moisture tends to represent spatial resolutions around 10's of km and several cm deep with a return period of several days. Measurement methods on intermediate scales do exist (for example, see Desilets *et al.*, 2010 for information on the Cosmic Ray Soil Moisture Observing System), but such systems are currently less common globally compared to the other two methods.

2.2.1 *In Situ* Measurements

Several *in situ* soil moisture monitoring networks have been providing local soil moisture measurements for years. As part of the Oklahoma Mesonet (Brock *et al*., 1995), soil moisture monitoring instruments have been deployed since 1996 (Scott *et al*., 2013). The NOAA Hydrometeorology Testbed (HMT) program has developed soil moisture observation networks in the Russian River and North Fork of the American River Basins in California as well as the San Pedro River Basin in Arizona (Zamora *et al*., 2011). Since the 1990's, U.S. Department of Agriculture (USDA) Natural Resources Conservation Service has hosted the Soil Climate Analysis Network (SCAN), a continental-scale network with over 100 stations across the United States (Schaefer *et al.*, 2007). The Walnut Gulch

Experimental Watershed housed 19 near surface soil moisture measurement instruments from 2002 to 2006 in addition to a select few sites with deeper soil profile measurements and longer record periods (Keefer *et al*. 2008).

2.2.2 Satellite Estimates

Recent years have witnessed the extension from ground-based observations to retrievals from satellites. While satellite-based soil moisture estimation has been investigated as an additional post-launch capability in several missions, highlighted here are two satellite missions with at least a portion of the mission objectives specifically dedicated to the retrieval of soil moisture. The European Space Agency's Soil Moisture and Ocean Salinity (SMOS) satellite mission was launched in 2009 with the purpose of measuring sea surface salinity over the world's oceans and surface soil moisture over land (Kerr *et al.*, 2010). NASA's recently launched Soil Moisture Active Passive (SMAP) mission utilizes a passive L-band radiometer combined with active L-band radar. Like its European counterpart, SMAP has a revisit time on the order of 3 days. The mission requirements for SMAP are such that L-band brightness temperature and backscatter are retrieved for both the active and passive component at the same time. The passive radiometer measurements have a resolution of approximately 40 km with the active radar component making measurements of approximately 3 km. By combining the accuracy of passive L-band microwave measurements with heterogeneity patterns offered by active measurements, the benefits of both methods are utilized (Entekhabi *et al.*, 2010). These benefits were somewhat short-lived, as the active radar instrument failed several months after the mission launched in January, 2015. Nonetheless, distributed hydrologic modeling lends itself nicely to such

observations, as their relatively extensive spatial coverage can account for the sub-basin soil moisture variations.

ESA's SMOS is a passive microwave sensor that makes retrievals at a spatial resolution of approximately 50 km. The instrument utilizes synthetic aperture radiometry in order to make measurements in the L-band while overcoming the need for a large antenna (Kerr *et al.*, 2010). The accuracy requirement for the soil moisture component of this mission is to be within 0.04 m^3/m^3 of the true soil moisture state to ensure its usefulness in hydrologic and meteorological models. It provides global coverage of surface soil moisture with a revisit time of 2-3 days to be able to capture important information on hydrologic processes such as post-rain dry downs (Kerr *et al.*, 2001).

Since the launch of SMOS, it has been discovered that significant Radio Frequency Interference (RFI) has polluted much of the data (Figure 2-1). Even though the radiometer measures frequencies that are in a restricted band (1.4-1.427 GHz), unforeseen sources of RFI including militant, commercial, and private sources have caused severe problems with satellite soil moisture retrievals, particularly in Europe and Asia (Castro *et al.,* 2012; Camps *et al*., 2011). Taking careful consideration to decrease or at least flag high RFI signals (Kerr *et al.*, 2012) has subsequently resulted in successful applications of data in these problem areas (Wanders *et al.,* 2014).

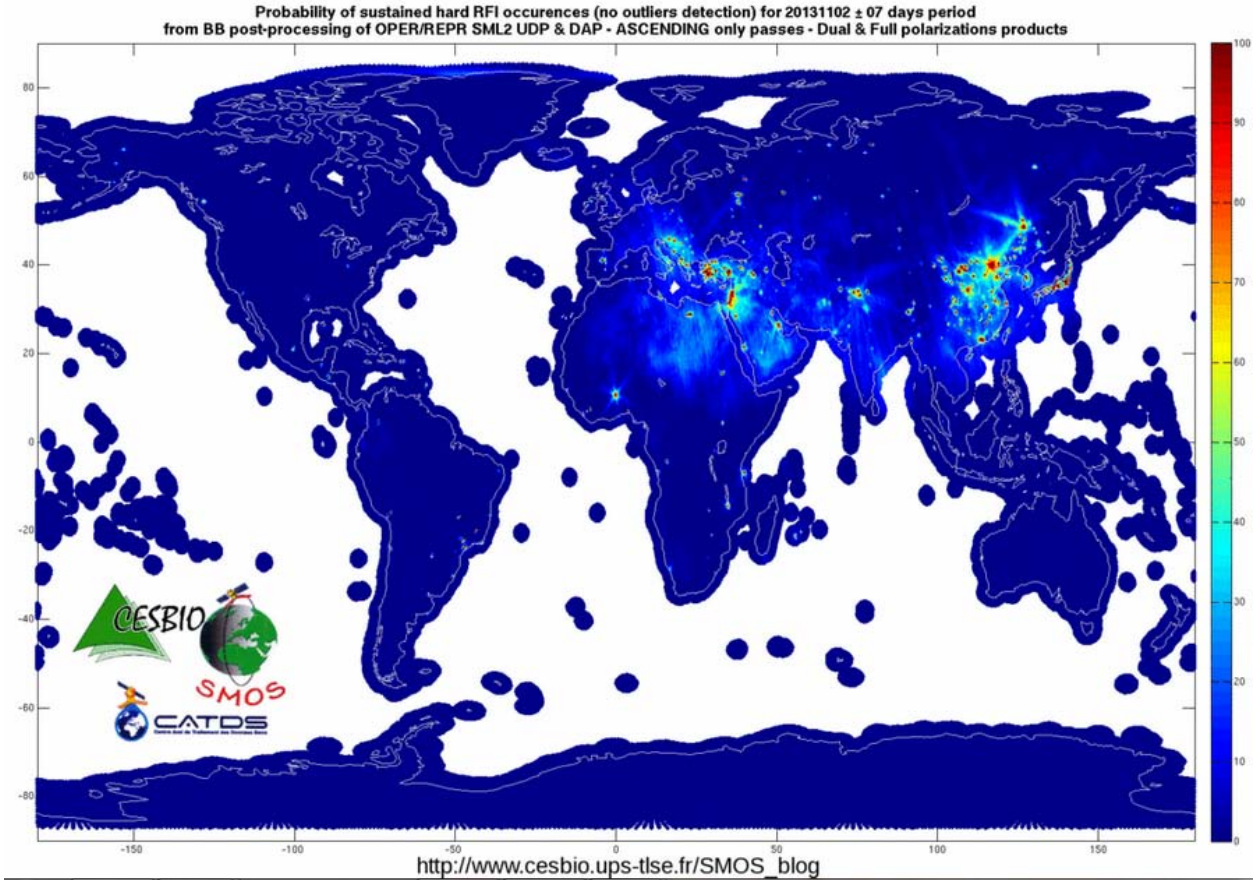

Figure 2-1 Probability of sustained RFI from early November, 2013. This area will use SMOS data for applications in the United States, which has less RFI occurrences compared to areas like Europe and Asia.

2.3 Model Simulated Soil Moisture

2.3.1 Overview of Models for Soil Moisture

In an effort to accommodate the ever-growing need to represent sub-basin processes, the development of distributed hydrologic and land surface models has become an area of great interest. Some of these models are physically based, with a realistically meaningful structure of soil layers. Such models include the Noah Land Surface Model (Chen *et al.,* 1996) and the Soil-Water-Atmosphere-Plant (SWAP) model (Van Dam *et al.,* 1997). Others

feature a more conceptual representation of soil layers in the rainfall-runoff generation process such as the Variable Infiltration Capacity (VIC; Wood *et al.,* 1992), NOAA's HL-RDHM (Koren *et al.,* 2004), the U.S. Army Corps of Engineers' Gridded Surface Subsurface Hydrologic Analysis model (Downer and Ogden, 2004), and the LISFLOOD model (Van Der Knijff, 2010). As they are distributed in nature, all of these models have the opportunity to incorporate soil moisture information to improve representation of internal basin processes. Several studies have investigated use of soil moisture observations in distributed models for this very purpose (Das *et al.,* 2008; Hsu *et al.,* 2012; Wanders *et al.,* 2014; among others). Those models that are conceptually-based and rely on parameterizations of soil processes may also benefit from soil moisture observations as a way to calibrate those parameters that control sub-basin mechanisms.

2.3.2 Hydrology Laboratory Research Distributed Hydrologic Model (HL-RDHM)

HL-RDHM was developed by the National Weather Service (NWS) Office of Hydrologic Development (OHD). Detailed information can be found in Koren *et al.* (2004), NWS (2011) and Smith *et al.* (2012). HL-RDHM is a distributed hydrologic model which was designed and implemented for the entire CONUS (Contiguous United States) at three spatial resolutions of 1 HRAP (Hydrologic Rainfall Analysis Project, ~4 km), 1/2 HRAP and 1/4 HRAP. HL-RDHM structure can also be applied for any cell resolution and time step length (NWS, 2011). The heart of the model is the Sacramento Soil Moisture Accounting (SAC-SMA) model (Figure 2-2).

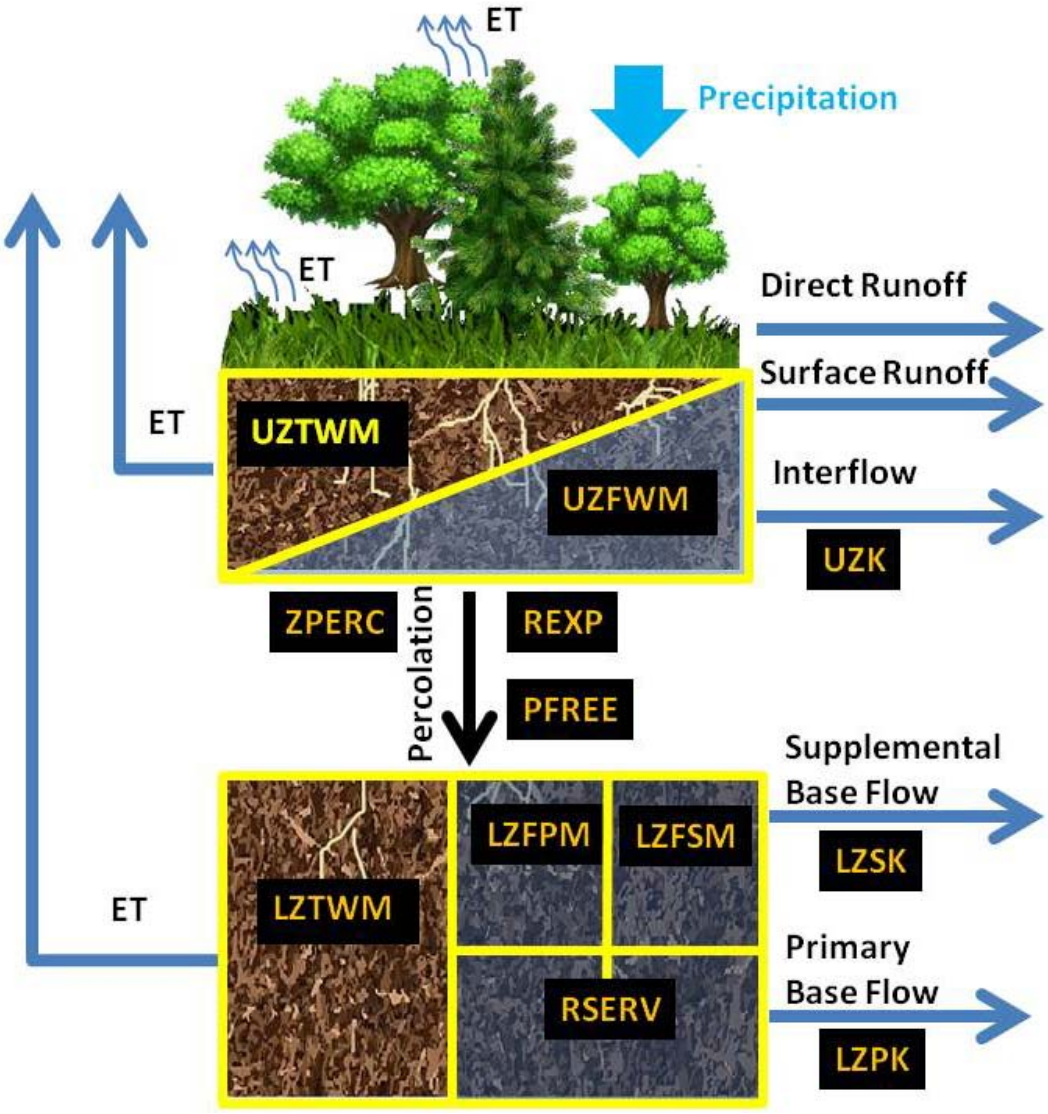

Figure 2-2 Formulation of basic SAC-SMA model and its parameters (black boxes) that are most relevant to soil moisture.

Within HL-RDHM, unlike other distributed models with fixed values for sub-domains or the entire domain, an advanced algorithm was designed to derive *a priori* parameters from soil and land use data for each SAC-SMA sub model at every pixel. Recent enhancements to the basic SAC-SMA model include the use of Noah Land Surface Model-based physics to estimate a physically meaningful soil moisture profile as well as evapotranspiration from

the soil column. This is accomplished through the conversion of SAC-SMA conceptual soil water storages into physical soil layers. Once this is done, a heat transfer component accounting for frozen ground processes allows the soil liquid and solid water contents at each soil layer to be estimated (Koren *et al.* 2007).

Utilizing the Noah Land Surface Model vegetation-soil moisture interaction parameterization as well as data sets regarding vegetation activities, Koren *et al.* (2010) have further adjusted SAC-HT soil moisture estimations at different physical layers through advancing the ET estimation in SAC-HT by accounting for the effects of photosynthetically active radiation, soil moisture and vapor pressure deficits, and air temperature on ET. Empirical relationships are used to estimate these additional variables in an effort to reduce input data requirements to a level consistent with what is available for River Forecast Center operations. This new version is referred to as the Sacramento Soil Moisture Accounting Heat Transfer component for Enhanced Evapotranspiration (SAC-HTET) and is included in version 3.2.1 of HL-RDHM (used in this study). After the soil moisture is adjusted at different physical layers, it is shuffled backed to SAC-SMA conceptual layers (see Figure 2-3) where adjustments due to free water exchange and removal from runoff are made. For a detailed procedure on the conversion from conceptual storages to physical soil layers, readers are referred to Koren *et al.* (2007 and 2014).

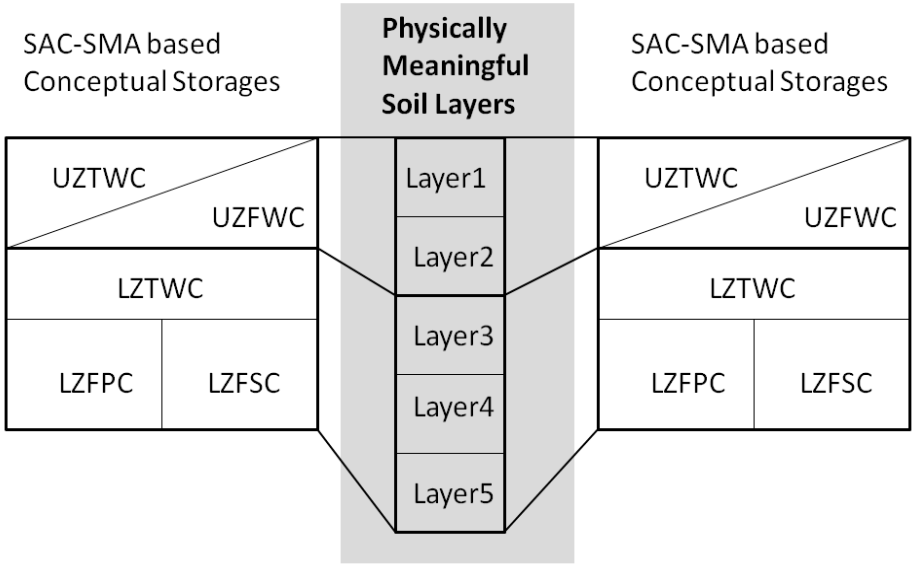

Figure 2-3 Example conversion of SAC conceptual storages to model-prescribed physically meaningful soil layers (number of layers varies from pixel to pixel).

An optional HL-RDHM routine that was utilized in this study is the rutpix9 routing module. This module has a hillslope component, where surface and subsurface flows are routed over a uniform conceptual hillslope. In the channel routing component of rutpix9, water moves from cell-to-cell according to a predefined cell connectivity sequence. This sequence is topography-based such that at each cell, fast runoff routed over the hillslope of that cell is combined with the subsurface flow and streamflow routed from the upstream pixels (NWS, 2011).

Sections of this dissertation also employ the snow component in HL-RDHM known as SNOW17. This routine uses empirical relationships to calculate heat storages, liquid water storages, and snowpack melt to represent snow accumulation and ablation (Anderson, 1973). Although all evaluation periods of the segments of the research that utilize the

SNOW17 module occur during spring/summers that are snow-free, some model spin-up periods include the preceding winters of evaluation events. No parameters from the SNOW17 module were included in the calibration process, as the focus of this study is to investigate the potential of soil moisture. Because soil water is likely to be frozen during the time periods when SNOW17 would be activated, soil moisture evolution is rendered unusable for calibration of the snow module parameters in this research.

The 11 SAC-HTET storage and release parameters and 4 rutpix9 routing parameters that are calibrated for this study are presented in Table 2-1. The feasible ranges for the storage and release parameters proposed by Koren *et al.* (2008) are also provided in this table. These ranges were used as bounds during calibration. The model was run at an hourly time step, with a 1 HRAP spatial resolution (~4 km).

Table 2-1 HL-RDHM parameters considered for calibration and feasible ranges as provided by Koren et al. (2008)

Parameters	Description	Range
SAC-HTET		
UZTWM	Upper zone tension water maximum (mm)	10-300
UZFWM	Upper zone free water maximum (mm)	5-150
UZK	Upper zone free water depletion rate due to interflow (day^{-1})	0.10-0.75
ZPERC	Maximum and minimum percolation rate ratio	5-350
REXP	Percolation curve shape parameter	1-5
LZTWM	Lower zone tension water maximum (mm)	10-500
LZFSM	Lower zone supplemental free water maximum (mm)	5-400
LZFPM	Lower zone primary free water maximum (mm)	10-1000
LZSK	Lower zone supplemental free water depletion rate due to interflow (day^{-1})	0.01-0.35
LZPK	Lower zone primary free water depletion rate due to interflow (day^{-1})	0.001-0.05
PFREE	Fraction of percolated water that goes straight to lower zone free storage	0.0-0.8
rutpix9		
Q0CHN	Channel specific discharge (m/s)	
QMCHN	Power value for discharge-cross section relationship	
ROUGH	Hillslope roughness coefficient	
SLOPH	Hillslope slope	

2.4 Discussion

With each method for representing soil moisture come advantages and disadvantages. For the observation methods discussed, users are provided with hints of the "true" moisture state. However, this may be a limited picture of the truth due to constraints on the soil layer being observed, the time frequency of an observation, or the spatial representativeness of the observation. When it comes to modeled estimates of soil moisture, a continuous picture of soil moisture can be generated virtually on any land mass, anywhere on the globe, and at any desired level/resolution. The limitations with modeled soil moisture is the reliability due to uncertainties in model assumptions/structure and input forcing data quality. The remainder of this dissertation attempts to leverage the advantages of each to provide means of obtaining a more accurate and complete picture of soil moisture.

2.5 Chapter 2 Synopsis

- Soil moisture observations range from highly localized *in situ* probes to satellite estimates that generalize areas of ~25 km^2.
- The model of choice for this dissertation is the National Weather Service's HL-RDHM, which is a distributed, conceptually based hydrologic model that features a meaningful connection to physical soil layers.
- Combining soil moisture observations with a distributed hydrologic model has perceived benefits, but also challenges that must be met.

Chapter 3. Transforming into Saturation Ratio Space

3.1 Introduction

Particularly for shorter time scales, and depending on the spatial scale of interest, many factors begin to influence soil moisture. As scale increases from a single point to a watershed scale, heterogeneity of characteristics including soil type/texture, vegetation, and terrain (among others) begin to complicate the representativeness of observed soil moisture signals and model simulations. For the work conducted here, three main spatial scales are taken into consideration: 1) highly localized observations from *in situ* soil moisture probes 2) HL-RDHM grids (~4 km^2) and 3) satellite-based retrievals (10s of km^2). SMOS data is regridded into the HRAP domain using the nearest neighbor method. This means that for each HRAP pixel, the SMOS retrieved value with a latitude/longitude center closest to that of the HRAP pixel is assigned to that HRAP location. This approach is stable, as all HRAP pixels in this study domain have a side length of ~6 km and the SMOS pixel center geolocation has an accuracy of slightly better than 500 m and is fixed for all passes (Kerr *et al.,* 2012).

As an anecdotal example of soil moisture estimation discrepancies, Figure 3-1 highlights the challenge of directly comparing volumetric soil moisture values between the 3 spatial scales in question. With the upper and lower bounds for the model's dynamic space marked, an immediate issue of both observation sources falling outside of these bounds becomes apparent.

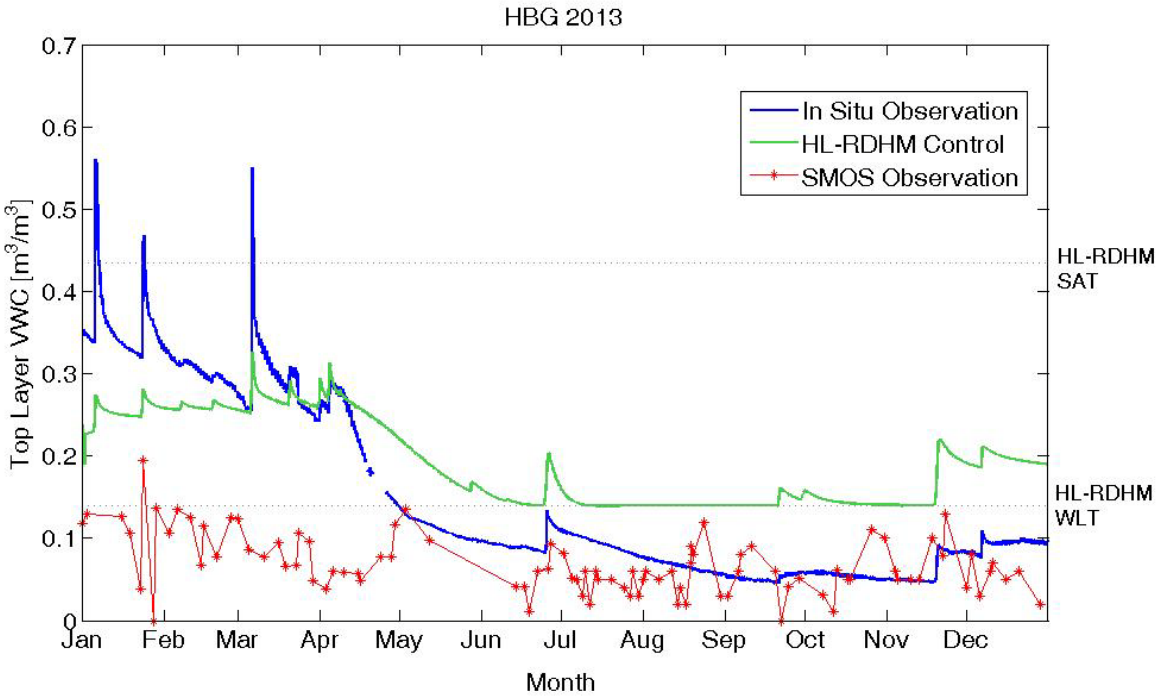

Figure 3-1 Sample discrepancy between 3 soil moisture estimation sources collocated with NOAA HMT site HBG. HL-RDHM SAT and HL-RDHM WLT mark the bounds of the HL-RDHM soil moisture dynamic space for this particular model pixel.

It follows that in order to adequately compare observations and model simulations of varying scales, certain measures must be taken. For the data assimilation studies in this dissertation, much of the work is performed in the HL-RDHM spatial domain/projection. Therefore, the two observation sources are manipulated into the model HRAP space.

The first step in maintaining a consistent comparison realm follows the lead of Brocca *et al.* (2010), Wanders *et al.* (2014), Sutanudjaja *et al.* (2014) and others by converting actual volumetric soil moisture to a soil saturation ratio. Koren *et al.* (2008) also perform this transformation specifically for the lumped version of SAC-HT, and recommend this

procedure when comparing model estimates to observed soil moisture. This is performed according to

$$\theta_{SR} = \frac{\theta_{Vol} - \theta_{WLT}}{\theta_{SAT} - \theta_{WLT}} \qquad (3\text{-}1)$$

where θ_{SR} is the calculated saturation ratio, θ_{Vol} is the volumetric soil moisture estimate/observation to be converted, θ_{WLT} is the volumetric soil moisture at wilting point, and θ_{SAT} is the volumetric soil moisture content at saturation.

From Equation 3-1, it becomes apparent that a representative value for θ_{WLT} and θ_{SAT} should be established for each scale under consideration. In the case of HL-RDHM, these values are predefined *a priori* and calculated from soil survey data for the dominant soil type within each model pixel (Koren *et al.,* 2003). These soil parameters are adopted for use in this work and are left unchanged.

The issue of scaling soil hydraulic properties has received a large amount of attention in the soil science and hydrology communities. Specifically, a large amount of focus has been placed on methods of developing and scaling soil moisture characteristic curves (conceptualization provided in Figure 3-2). This may be in the form of using various functional models (for example Warrick *et al.,* 1977; Simmons *et al.* 1979, and Clausnitzer *et al.,* 1992) or physically-based scaling parameters (Kosugi and Hopmans, 1988). All of these methods require use of a reference soil's water retention curve, which by itself requires rigorous laboratory work and/or field samples.

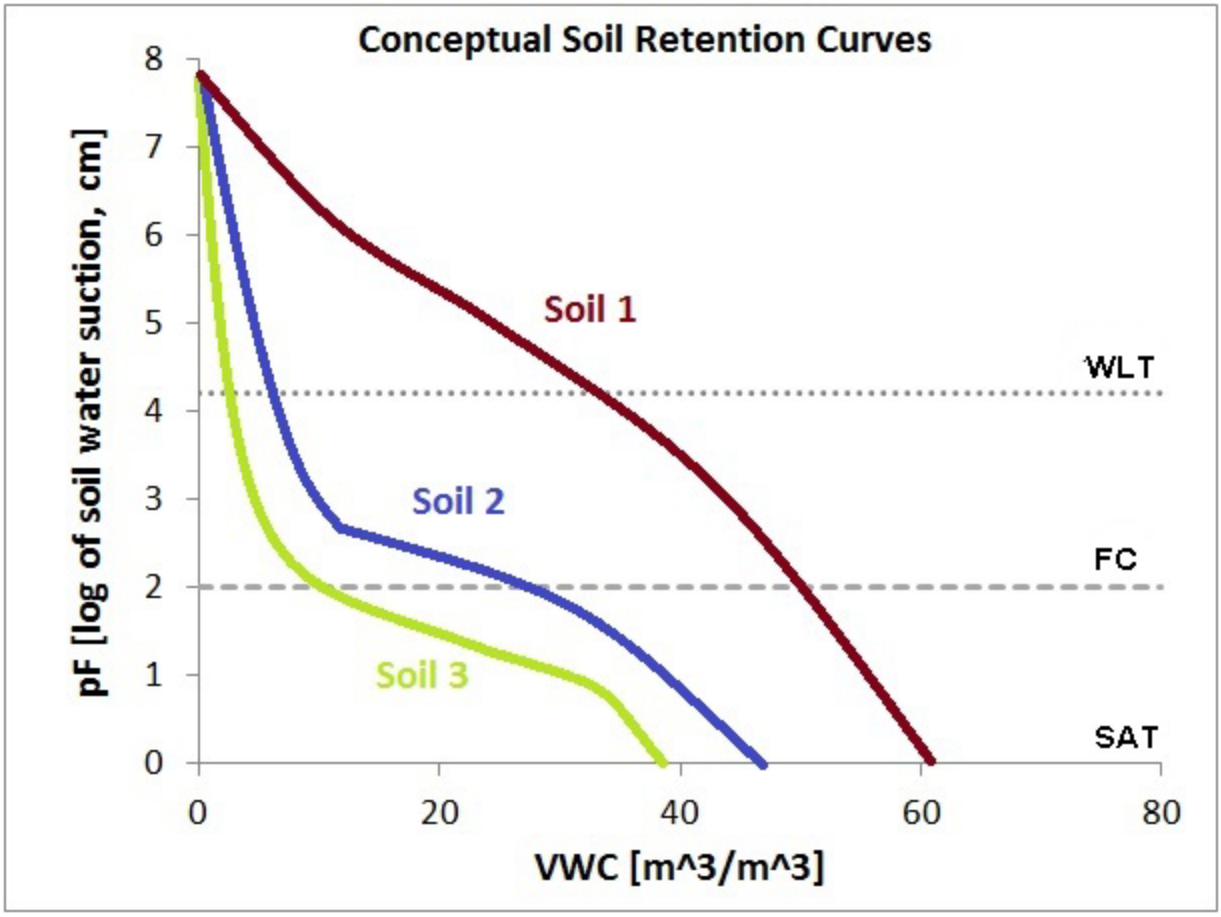

Figure 3-2 Illustration of soil retention curves from three hypothetical soil types typical of those from laboratory samples.

While scaling of these curves would result in the ability to identify θ_{WLT} and θ_{SAT}, these methods typically rely on detailed laboratory measurements that may not be readily available (Gijsman *et al.,* 2002; Saxton and Rawls, 2006). Gijsman *et al.* (2002) express the need to characterize soil properties at coarse scales (even as coarse as regional or continental) in a generalized form, as systematic fine spatial resolution sampling of characteristics at these scales is all but impossible. In their study, an evaluation of methods catered to identifying soil properties using only properties readily available via soil surveys was conducted. They found that of the 8 current strategies examined, the one proposed by

Saxton *et al.* (1986) performed the best. This set of equations/assumptions was therefore adopted and built upon in this work to keep the flexibility of scaling soil characteristics in regions that lack the luxury of extensive laboratory samples.

3.2 Methods for Defining Soil Properties

3.2.1 Soil Plant Air Water Tool

To easily put the characterization by Saxton *et al.* (1986) to work, the Soil Water Characteristics Program within the Soil Plant Air and Water (SPAW) tool (Saxton and Rawls 2006) was employed. Inputs for this tool include % clay, % sand, and % organic matter and relationships are based on an expanded version of the equations initially proposed in the work by Saxton *et al.* (1986). A visualization of the SPAW tool is provided in Figure 3-3.

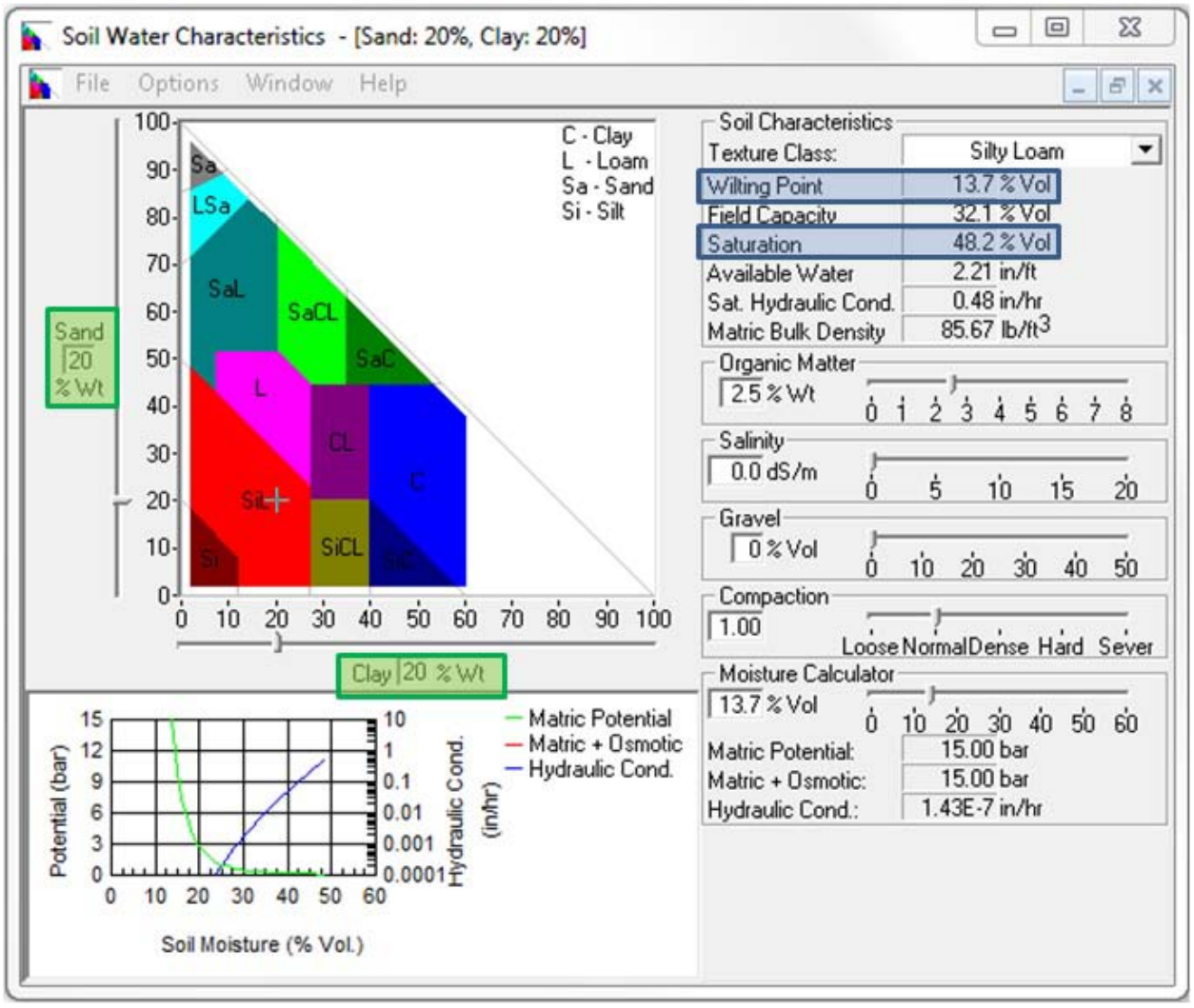

Figure 3-3 Screenshot of SPAW Soil Water Characteristics tool. Inputs highlighted in green rectangles, desired outputs for this work are highlighted in blue rectangles.

3.2.2 Observation-Based Estimates

Estimates of soil properties can be extracted from soil moisture observations themselves in the absence of thorough laboratory measurements. It is necessary that the observation period is sufficiently long (at *least* one year to experience a full wet and dry cycle) and that observations are taken with adequate frequency such that highly dynamic events (i.e.

gravitational drainage after rainfall with time scales on the order of several days) are not missed. If these conditions are met, the upper and lower bounds of the dynamic soil moisture range can be estimated as the observed maximum and minimum soil moisture values.

3.3 Strategies for Each Observation Type

For both the *in situ* soil moisture measurements and the satellite soil moisture estimates, a unique procedure that combines the use of observed soil moisture values with parameters calculated from soil properties is developed for each measurement type. Computed values for θ_{WLT} and θ_{SAT} are obtained using the SPAW tool. Soil textural properties were gathered from the United States Department of Agriculture (USDA) Natural Resources Conservation Service (NRCS) Web Soil Survey (WSS) (available at: http://websoilsurvey.sc.egov.usda.gov/App/HomePage.htm).

Data from NOAA HMT-West *in situ* sites of the Russian River Basin are used in this chapter and are available from 2010 to spring 2014, with a few sites having fewer observations due to instrument installations/updates. For each site, the observed maximum (θ_{Obmax}) and minimum (θ_{Obmin}) volumetric soil moisture value of the entire observation record of the site is retrieved. These, along with the wilting point and soil saturation level calculated with the SPAW tool (θ_{WLT_SPAW} and θ_{SAT_SPAW}, respectively) are used to develop the following scheme to represent the HMT wilting point (θ_{WLT_HMT}) and soil saturation level (θ_{SAT_HMT})

$$\theta_{WLT\_HMT} = \min\left(\theta_{Obmin}, \theta_{WLT\_SPAW}\right) \qquad (3\text{-}2)$$

$$\theta_{SAT\_HMT} = \max\left(\theta_{Obmax}, \theta_{SAT\_SPAW}\right) \qquad (3\text{-}3)$$

This scheme works under the rational that the SPAW tool will not be completely perfect and, given the reliability of this particular type of data, if an observation falls above (below) θ_{SAT_SPAW} (θ_{WLT_SPAW}), that observation should be considered the level of the new bound of the plausible soil moisture dynamical space. Conversely, the SPAW calculations are necessary in the case that either bound has not been reached during the observation record.

In the case of normalizing SMOS soil moisture to saturation ratios, a similar process is developed with extra considerations being taken to account for soil type/texture complexity at this larger spatial scale and lower observation frequency. Given that ~12 HRAP pixels fall under the coverage of a single SMOS pixel, the representativeness of the dominant soil type may deteriorate (save for particularly homogenous conditions) and along with it, the reliability of the calculated θ_{WLT} and θ_{SAT} values. Similarly, there are far fewer SMOS observations available to capture the appropriate bounds, thus further complicating the transformation. In fact, if a SMOS node cannot meet the accuracy requirements of the mission (due to complexity of surface features, RFI, or other flags) it is not retrieved at all (Kerr *et al.,* 2012). If the frequency of observations for a given location is particularly low, this becomes an indicator of poor reliability of an observation-based defined boundary.

Taking the two aforementioned limitations into account yields the following weighting scheme for SMOS soil moisture wilting point θ_{WLT_SMOS} and θ_{SAT_SMOS} and soil saturation level

$$\theta_{WLT\_SMOS} = \text{average}(\theta_{WLT\_ObFreq}, \theta_{WLT\_CV}) \quad (3\text{-}4)$$

$$\theta_{SAT\_SMOS} = \text{average}(\theta_{SAT\_ObFreq}, \theta_{SAT\_CV}) \quad (3\text{-}5)$$

Subscripts *ObFreq* and *CV* represent two distinct weighting schemes to consolidate wilting point estimates and soil saturation estimates from SMOS observations and SPAW calculated values. First, estimates for $\theta_{Obmin}/\theta_{Obmax}$ and $\theta_{WLT\_SPAW}/\theta_{SAT\_SPAW}$ are calculated similarly to the case of the HMT *in situ* observations. Because of the complications associated with both estimation methods, these are weighted according to:

- *ObFreq (Observation Frequency)* – places heavier weight to $\theta_{Obmin}/\theta_{Obmax}$ if the frequency of observations at the given SMOS "pixel" is high, defaults closer to $\theta_{WLT\_SPAW}/\theta_{SAT\_SPAW}$ if the frequency of observations is low.

$$\theta_{WLT\_ObFreq} = w_{ObFreq} * \theta_{Obmin} + \left(1 - w_{ObFreq}\right) * \theta_{WLT\_SPAW} \quad (3\text{-}6)$$

$$\theta_{SAT\_ObFreq} = w_{ObFreq} * \theta_{Obmax} + \left(1 - w_{ObFreq}\right) * \theta_{SAT\_SPAW} \quad (3\text{-}7)$$

w_{ObFreq} is weight given to $\theta_{Obmin}/\theta_{Obmax}$ calculated according to

$$w_{ObFreq} = \frac{N_{Obthrex}}{N_{Obthr}} \quad (3\text{-}8)$$

where N_{Obthr} is a user-defined number of thresholds for a specified range of observation frequencies (defined ad-hoc in this study) and $N_{Obthrex}$ is the number of said thresholds exceeded at a given SMOS "pixel."

- *CV (Coefficient of Variation)* – places heavier weight to $\theta_{WLT\_SPAW}/\theta_{SAT\_SPAW}$ if the complexity of the soil composition is low, defaults closer to $\theta_{Obmin}/\theta_{Obmax}$ if the complexity is high.

$$\theta_{WLT\_CV} = w_{CV} * \theta_{WLT\_SPAW} + (1 - w_{CV}) * \theta_{Obmin} \quad (3\text{-}9)$$

$$\theta_{SAT\_CV} = w_{CV} * \theta_{SAT\_SPAW} + (1 - w_{CV}) * \theta_{Obmax} \quad (3\text{-}10)$$

w_{CV} is weight given to $\theta_{WLT\_SPAW}/\theta_{SAT\_SPAW}$ calculated according to

$$w_{CV} = \frac{N_{CVthrex}}{N_{CVthr}} \quad (3\text{-}11)$$

where N_{CVthr} is a user-defined number of thresholds for a specified range for the inverse of coefficient of variation and $N_{CVthrex}$ is the number of said thresholds exceeded at a given SMOS "pixel." The coefficient of variation (*CV)* is defined as

$$CV = \frac{\sigma}{\mu} \quad (3\text{-}12)$$

where σ is the standard deviation and μ is the mean. To quantify complexity of soil composition under a SMOS pixel, the *CV* is calculated for the %clay/%sand ratio between all soil units in a SMOS pixel area.

This scheme allows for the dominant estimation method (observation based or calculated) to prevail if one truly is dominant, but also compensates if equal faith should be placed in both methods (i.e. frequently observed, homogenous soils). For this study, observation frequency ranged from 45 to 750 within the 2010 to 2014 time frame and a threshold

interval size of 100 was chosen, yielding 8 bins (weights ranging from 0 to 7) for the *ObFreq* method.

3.4 Bias adjusting SMOS saturation ratio

Even though the transformation from soil moisture to saturation ratio mitigates the impacts of scale differences, the bias between SMOS observations and HL-RDHM model has not yet been accounted for. From Figure 3-4, it can be seen that seasonality plays a role in the bias behavior for SMOS-based soil saturation ratios in the Russian River Basin. For use in the Ensemble Kalman filter, it is a prerequisite that the observations be unbiased to the model. Removal of soil moisture bias prior to assimilation has been addressed using model climatology (e.g. Lee *et al.*, 2011 and Wanders *et al.,* 2014). This work utilizes the CDF mapping method, where a CDF for both the ranked soil moisture observations and ranked modeled soil moisture are constructed (Brocca *et al.,* 2011, Drusch *et al.*, 2005, Reichle and Koster 2004).

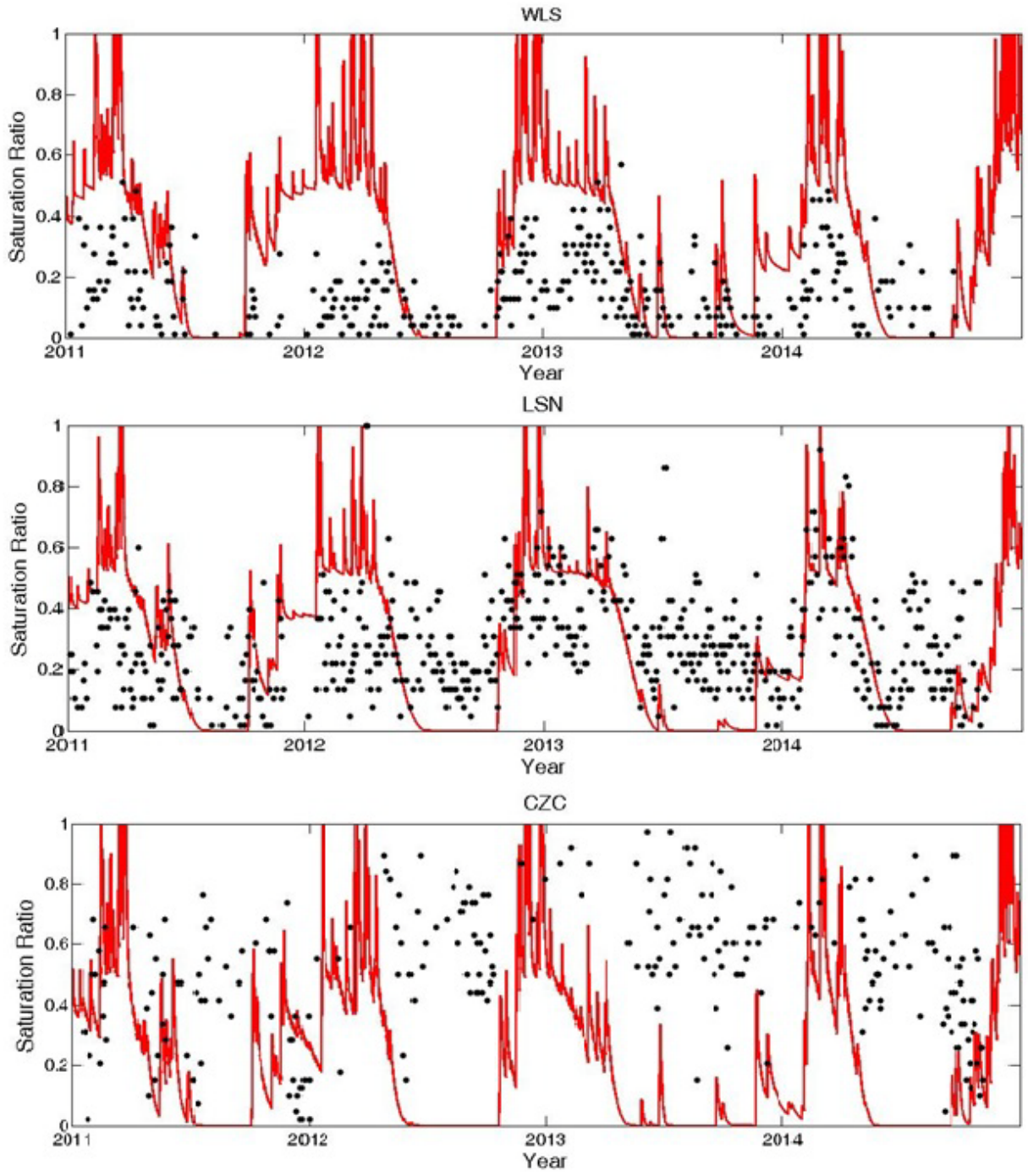

Figure 3-4 Examples of seasonally dependant bias from HMT stations WLS (top), LSN (middle), and CZC (bottom). Model control runs are red lines and black dots are SMOS observations after transformation to a saturation ratio.

The Russian River Basin has a distinct wet and dry season, with most of the precipitation falling from November-April. A reconstruction of the average monthly precipitation for the

Russian River Basin from 1983-2015 based on estimates from CHRS RainSphere (*rainsphere.eng.uci.edu*) is provided in Figure 3-5.

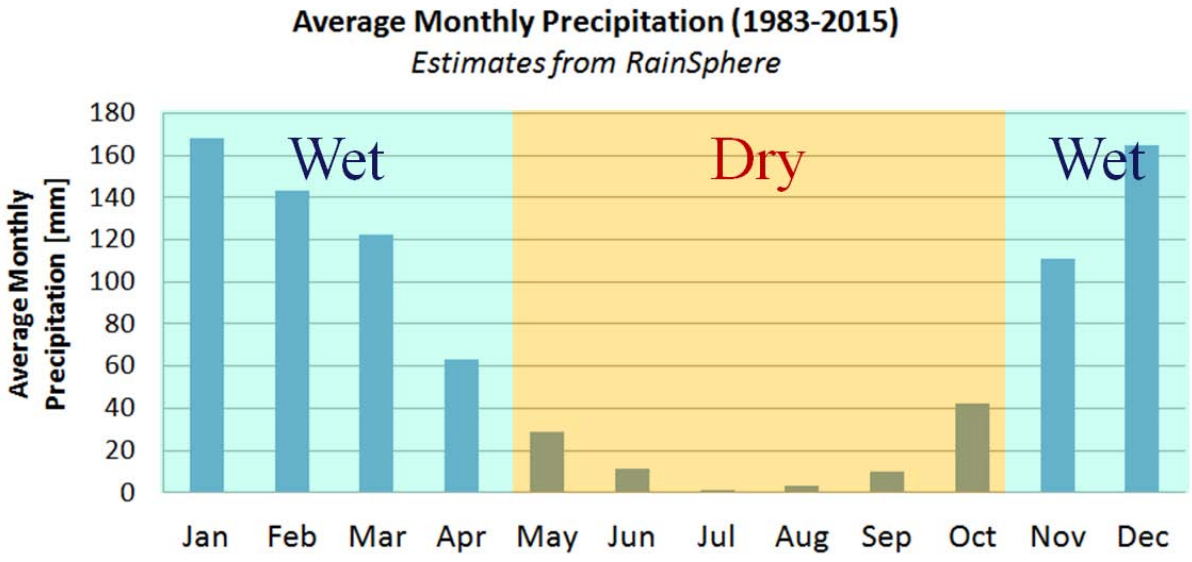

Figure 3-5 Separation of months for the Russian River Basin into "wet" and "dry" periods. Wet months were taken as the 6 months with the highest average monthly precipitation.

Drusch *et al.* (2005) point to the possible necessity of computing multiple CDF's in such a way to account for interannual variability associated with seasonality. Since the seasonality is quite strong for the California basin being examined, two CDF's were constructed for each SMAP "pixel" location with the wet season defined as November through April and the dry season defined as May through October. The SMOS observations are adjusted according to the solution to

$$CDF_m(\theta') = CDF_s(\theta) \qquad (3\text{-}12)$$

where CDF_m and CDF_s are the CDF's for the modeled soil moisture and satellite-based estimates respectively and θ and θ' are the unadjusted SMOS soil moisture (or soil

saturation ratio) and corresponding transformed soil moisture (or soil saturation ratio). Examples of dry and wet season CDF curves for two HMT sites in the Russian River Basin are illustrated in Figure 3-6.

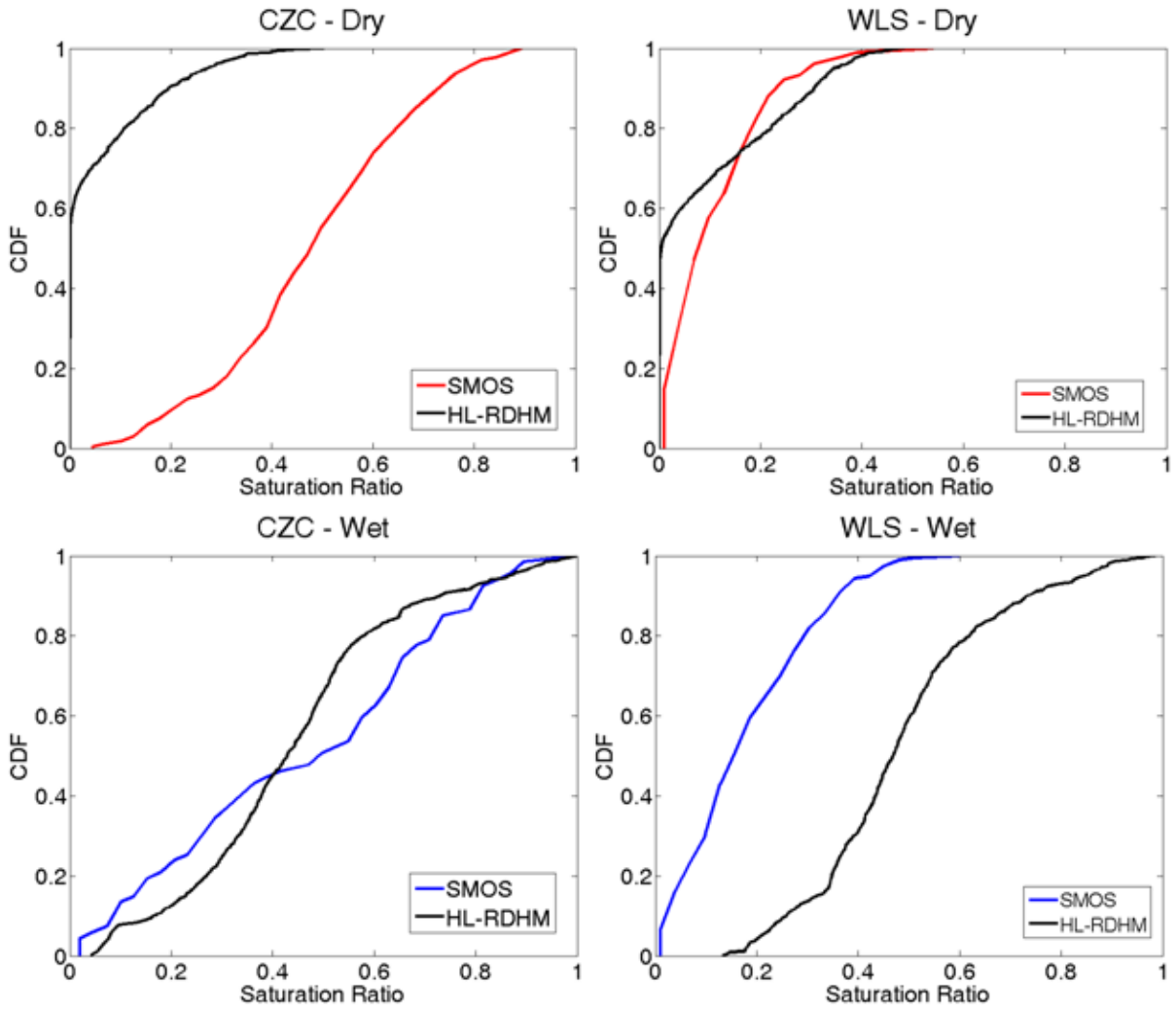

Figure 3-6 Sample CDF curves for two observation sites in the Russian River Basin: CZC (left) and WLS (right) for dry (top) and wet (bottom) seasons.

Reichle and Koster (2004) recommend a minimum threshold of at least 100 observations for the CDF matching to be performed. Of the 29 SMOS pixels under consideration for the Russian River Basin study area, only 6 of them do not meet this criterion after dividing into

wet and dry seasons. Of these 6, only 2 had less than 66 samples. Although the solution provided by Reichle and Koster (2004) that suggests using a moving spatial window does increase the number of samples, it also relies on an assumption of ergodicity within the window. Due to an interest in maintaining relatively high spatial resolution for this study, it was decided that it is more important to minimize the error introduced by the ergodicity assumption than to increase the sample size for a select few pixels. It should also be noted that 6 of the 7 pixels that are collocated with the HMT *in situ* observations exceed the 100 sample criterion, therefore, the *in situ*-based validations are not compromised.

To construct the CDF's the HL-RDHM model was run for 2011 to 2014, plus a 1 year spinup period in 2010 that was disregarded for the analysis. CNRFC precipitation and temperature were used as forcing of these control runs. Following the lead of Reichle and Koster (2004), the model simulations selected corresponded to the date and time of each available SMOS observation to maximize the compatibility of the two datasets. The model was run with a resolution of 1 HRAP, so the values used for CDF construction were obtained by taking the arithmetic mean of all HRAP pixels under the coverage their nearest neighbor SMOS retrieval.

3.5 Discussion

In this chapter, several measures were taken to compensate for spatial scale discrepancies amongst the 3 representations of soil moisture under consideration in this dissertation (*in situ* point measurements, HRAP model pixels, and SMOS satellite estimates). The first strategy was to transform each of the volumetric soil moisture measurements/simulations into a soil saturation ratio. While the HL-RDHM simulations can be and were normalized to

a saturation ratio internally within the model, the two observation sources require defining representative upper and lower bounds (saturation and wilting point, respectively) of the dynamic soil moisture space. Due to an apparent seasonal bias in the SMOS data, a second preprocessing step of CDF matching was performed.

Although estimates of soil properties are just that, and limitations are anticipated, the proposed method allows for a transformation from volumetric soil moisture to soil saturation ratio requiring very little information. Since this is the case for many places around the world, the simplicity of this strategy lends itself nicely to potential studies in poorly studied remote regions across the globe.

3.6 Chapter 3 Synopsis

- Spatial scale discrepancies between 3 soil moisture representation methods are partially resolved by mapping each from volumetric water content to soil saturation ratio, and from native resolution to the HRAP model spatial resolution.
- Soil saturation ratios for each observation type were defined in way that rewards observation frequency, and penalizes soil lateral heterogeneousness.
- SMOS – based retrievals were bias corrected (seasonally) relative to HL-RDHM model.

Chapter 4. Soil Moisture Data Assimilation to Improve Soil Moisture State

4.1 Introduction

Several studies have already made efforts to examine how the incorporation of soil moisture observations through data assimilation into hydrologic, land surface, and hillslope models improves estimates and predictions of the soil moisture state. Using a distributed soil-vegetation-atmosphere transfer (SVAT) model and Ensemble Kalman Filter (EnKF), Merlin *et al.* (2006b) found that all data assimilation runs in their study provide an improvement over non assimilation runs, even when observation frequency was reduced from daily to once every 5 days. This result is particularly encouraging for satellite based soil moisture applications, since these observations may only be available every 1-3 days for a given location. Reichle *et al.* (2002a) also employ the EnKF but use a synthetic experiment with a land surface model. These results yield reasonable soil moisture estimates even with relatively few ensemble members, suggesting a perhaps computationally efficient method. Using the Noah LSM, Hsu *et al.* (2012) express improvement, especially in the top soil layer estimates by incorporating AMSR-E surface soil moisture retrievals in a semi-arid region. Flores *et al.* (2012) show significant reduction of surface soil moisture bias with some reduction of RMSE for over half the watershed in the hillslope tRIBS-VEGGIE model, which they use for assimilation of synthetic 3 km Soil Moisture Active Passive (SMAP) radar data.

Previous investigations attempt to improve other pieces of the hydrologic cycle, via the improvement of surface soil moisture through data assimilation. Chen *et al.* (2011) and Han *et al.* (2012) both explore assimilation of upper layer soil moisture into the Soil and Water Assessment Tool (SWAT) through use of the EnKF. These studies report limited success when considering improvements on streamflow, but show that upper layer (and profile according to Han *et al.*, 2012), soil moisture is improved. Through a variational assimilation (VAR) method, Lee *et al.* (2011) assimilate soil moisture and basin interior streamflow simultaneously in HL-RDHM. They found that while incorporating soil moisture observations does not improve streamflow estimates beyond what assimilating streamflow alone could do, the soil moisture bias is significantly reduced. Crow *et al.* (2009) demonstrated some success in improving streamflow when internal soil moisture and external rainfall forcing are simultaneously updated through their assimilation framework into the Sacramento model, but mostly for large-scale flooding situations and when rainfall errors are high.

4.2 Overview of the Ensemble Kalman Filter

The standard Kalman Filter is one of many data assimilation methods used in hydrologic applications to combine imperfect models estimates with uncertain observations (Walker and Houser, 2005). It is a sequential assimilation method suitable for linear dynamic systems, and forms the basis for the application of the Ensemble Kalman Filter (EnKF), used for the nonlinear application in this work. The EnKF introduced in Evensen (1994), belongs to a family of ensemble-based methods that rely on the propagation of individual

ensemble members through the nonlinear system to obtain an approximation of the state probability density function. A brief overview of the EnKF process is provided below.

Consider the nonlinear state equation:

$$x_k = f(x_{k-1}, u_{k-1}) + w_{k-1} \qquad (4\text{-}1)$$

where x_k is the state variable at step k, u_k is the input at step k, and w_k is the processes noise sampled from a zero-mean normal distribution with covariance Q_k, and corresponding measurement equation:

$$y_k = h(x_k) + v_k \qquad (4\text{-}2)$$

where y_k is the predicted measurement at step k and v_k is the processes noise sampled from a zero-mean normal distribution with covariance R_k.

An ensemble of N states is generated from a prior distribution to obtain $X_k = [x_1, x_2 \ldots x_N]$. When an observation is available at step k, a corresponding N replicates of true observation z is generated according to:

$$Z = [z_1, \ldots z_i, \ldots z_N],\ z_i = z + v_i,\ v_i \sim N(0, R) \qquad (4\text{-}3)$$

As per the standard Kalman filter, the predicted state variable is updated to a posterior estimate, $\hat{x}_k$ when there is an observation at step k, except this is done for each member in the ensemble according to:

$$\hat{X}_k = X_k + K_k(Z_k - HX_k) \qquad (4\text{-}4)$$

where H is the transformation matrix (analogous to h(x), but presented as a matrix here for simplicity), and K is the K Kalman gain calculated as:

$$K_k = C_k H^T (H C_k H^T + R_k)^{-1} \quad (4\text{-}5)$$

where C is the covariance matrix calculated from X.

Following the state update, the mean of the ensemble is taken as the best estimate for the state. The EnKF has the advantage of handling highly nonlinear systems at a low computational cost.

One issue that arises when using the EnKF for soil moisture data assimilation is the notion of filter divergence. With filter divergence, the model ensemble begins to drift so far from the truth that the observations have less and less impact until finally they become completely trivial. This may arise due to model error, but as shown in Whitaker and Hamill (2002), the EnKF can underestimate state uncertainty even when considering a perfect model.

There are two primary situations under which filter divergence becomes an issue in this work (Figure 4-1). The first scenario is the case such that immediately following a precipitation event, the observational dry down curve is considerably steeper than that of the model. While it is both expected and desired that the model variance be relatively small after an intense precipitation event (i.e. high confidence that the soil moisture should be approaching saturation), if the observed dry down is too rapid relative to observation frequency, the ensemble effectively looses the influence of the observation. The second scenario of filter degeneration occurs after a prolonged dry period. Again, a small variance

is desirable in this case, as the longer the dry spell, the more confident one can be that the system is at or approaching the wilting point. Furthermore, a precipitation event that occurs immediately after a prolonged dry period may not be sufficient to reestablish the ensemble spread, particularly if the model underestimates the precipitation-induced soil moisture spike by a large margin.

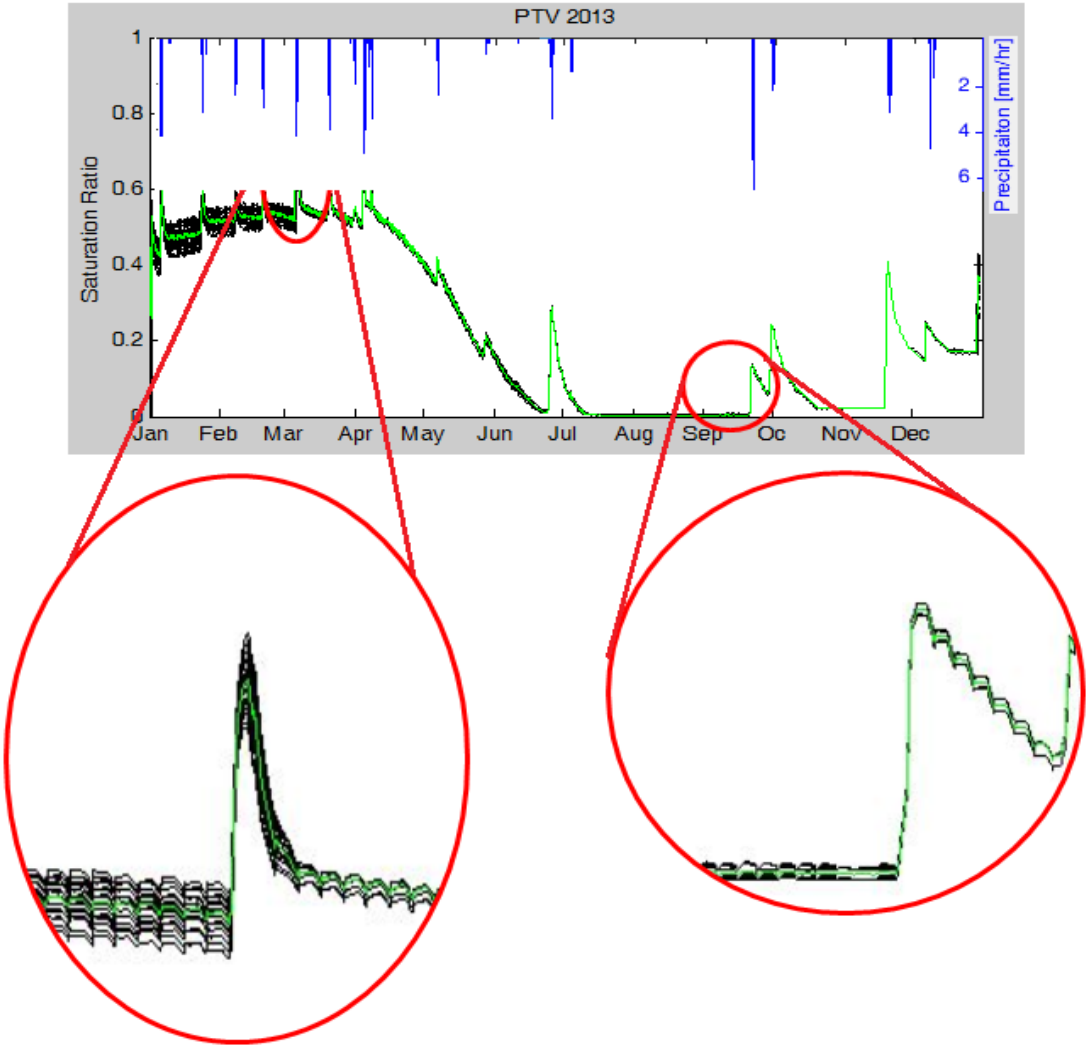

Figure 4-1 Example of ensemble member (black lines) underdispersiveness that occurs after precipitation event (left circle) or after prolonged dry period (right circle). Ensemble mean is shown in green.

Anderson and Anderson (1999) offer a simple method to circumvent filter divergence in which the covariance matrix calculated for the prior distribution is inflated by a modest multiplier, γ, and the ensemble is redefined to fit this new covariance accordingly. A suitable value of γ is established heuristically (Petrie, 2008), and for this study γ =1.2 was found. This value was found via manual adjustments and subjectively examining the effects on the ensemble at 7 model pixels collocated with *in situ* soil moisture observations. Therefore, the reader is cautioned against using this value for other basins/applications without prior testing of a suitable value. The redefined ensemble is defined as

$$X' = \sqrt{\gamma}(X - \bar{X}) + \bar{X} \qquad (4\text{-}6)$$

where X' is the new ensemble member value, X is the initial ensemble member value, and $\bar{X}$ is the ensemble mean.

While the implementation of this method is simple and has shown merit (particularly in atmospheric model applications), it suffers deficiencies for the hydrological application presented here. This is particularly true in the problematic conditions highlighted above, where the variance has collapsed to nearly zero. Figure 4-2 shows an example of an attempt to employ the inflation factor, and showcases areas where the strategy has failed.

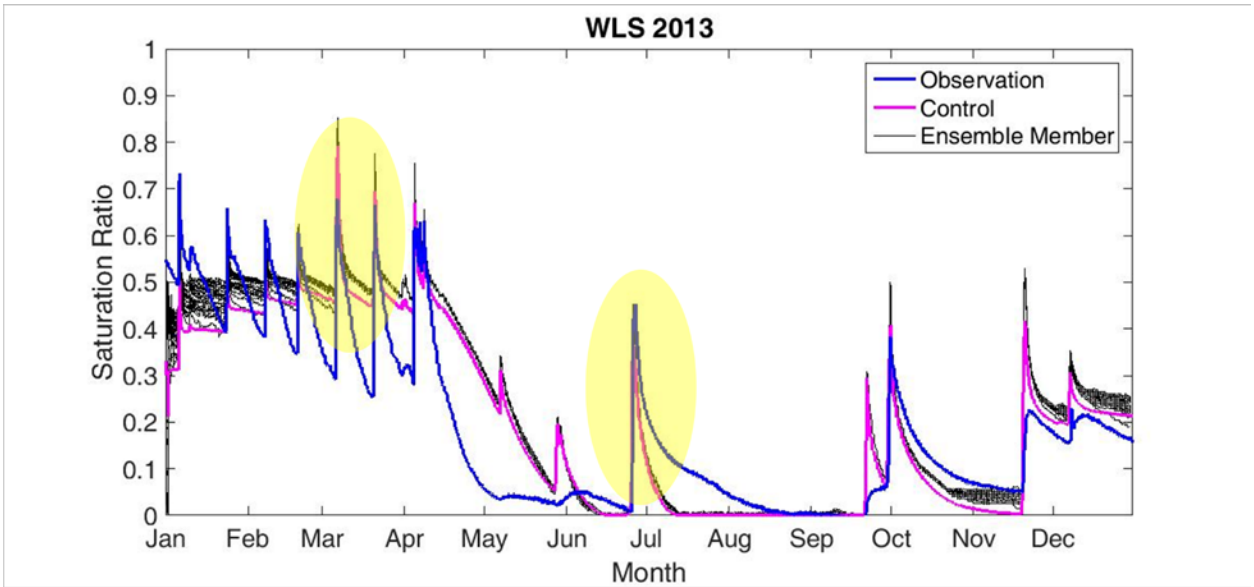

Figure 4-2 Example of limitation of using a simple inflation factor for deterring filter divergence. Areas of insufficient ensemble spread following precipitation events are highlighted in shaded circles.

To avoid a nearly complete ensemble member collapse during occurrences of rapid soil moisture dynamics (i.e. an intense precipitation event followed by a rapid drydown), an ensemble member tracking mechanism is developed and implemented. In this method, the influence of an observation on the adjusted states is tested after each assimilation step. To continue to the next prediction step with no further modifications, the condition must be met such that at least one observation member (ensemble generated from observation plus noise) is above and one is below either the maximum or minimum predicted observation. In the event that this condition is not met, the model ensemble is resampled from a distribution that keeps the original mean, but increases the variance in attempt to recapture the lost influence of the observation. A hypothetical example with a 3 member ensemble of model predicted observations and noisy observations is shown in Figure 4-3

to illustrate a case for resampling and not resampling when an observation is available at a given time *t*.

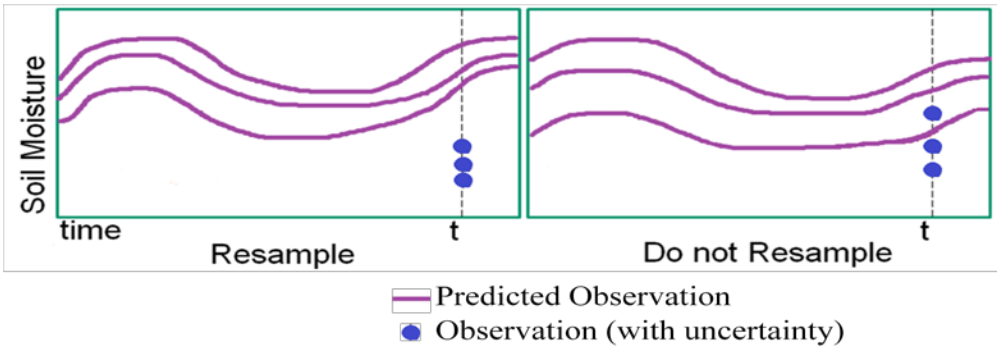

Figure 4-3 Toy example of conditions to resample during an assimilation time step (left) and when not to resample (right).

Selection of an appropriate variance size for ensemble resampling may vary by application. However, for circumstances in which the observation space and state spaces are bounded from 0 to 1 (and normalized if they are not), the following formula is recommended:

$$V_E = \frac{|\overline{y_f} - Y|}{2} \qquad (4\text{-}7)$$

where V_E is the expansion variance, $\overline{y_f}$ is the predicted observation mean, and Y is the observation. This formulation allows for the expansion size to be proportional to how far the ensemble has diverged from the observation, preventing overexpansion in the event that the ensemble has only slightly fallen outside the reach of influence of the observation.

4.3 Strategy for a Double Ensemble Kalman Filter

In the case of both *in situ* observations and satellite-based estimates, observations are not available at all locations within the basin at every observation time step (Figure 4-4). Therefore, a recursive EnKF strategy is developed to update all pixels in the study basin in

a manner that is respectful of the spatially heterogeneous nature of soil moisture dynamics. This is in contrast to previous studies that have (or assume) observations available at all locations (i.e. Flores *et al.,* 2012, Han *et al.,* 2012, Sutanudjaja *et al.,* 2014, Wanders *et al.,* 2014) or assign the same observation to all pixels but assign varying degrees of uncertainty according to spatial variations in soil moisture (Lee *et al.*, 2011).

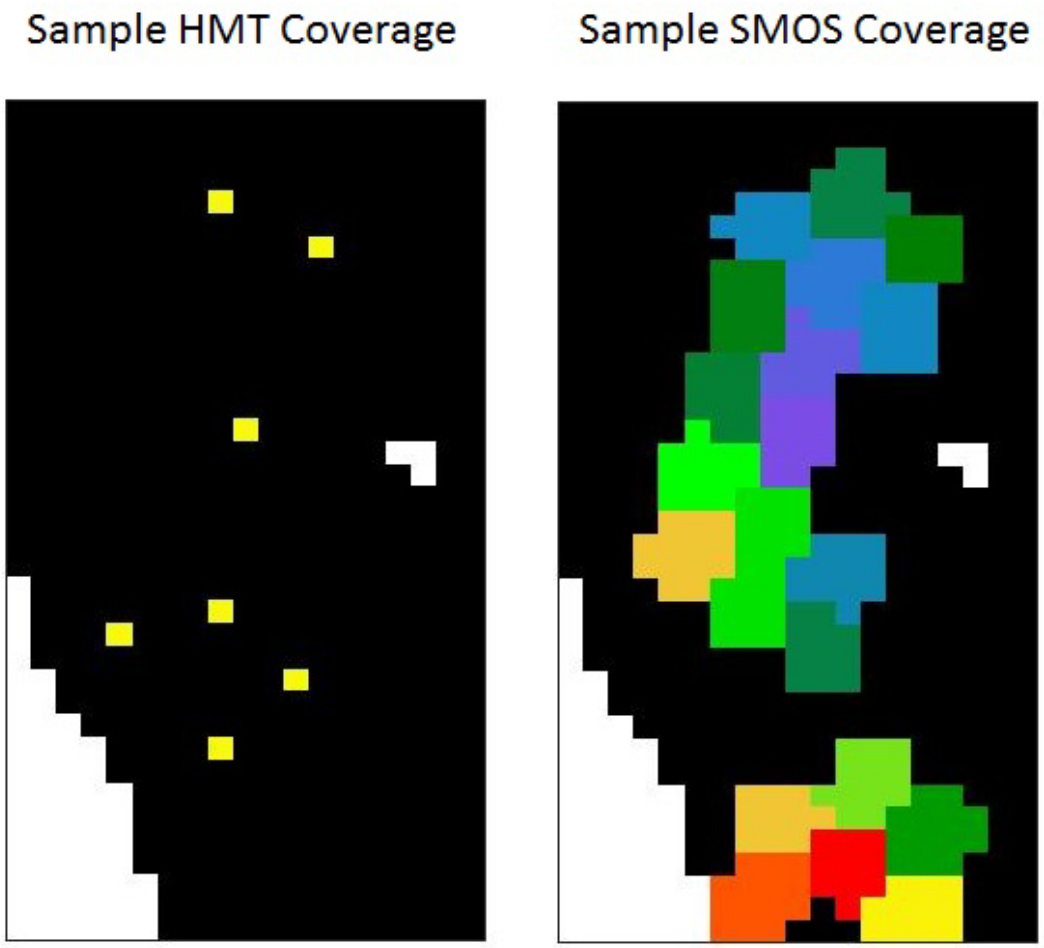

Figure 4-4 Sample coverage (colored areas) for a single time step of HMT stations (left) and SMOS coverage (right) in the Russian River Basin. Black area represents entire land domain that is being modeled but not observed, white areas represent water features that produce no simulation.

Considering a single observed model pixel, the state equation in the EnKF for this work is the running of HL-RDHM to project conceptual states to the next time step. The observations represent soil moisture estimates either from *in situ* HMT soil moisture probes or SMOS observations disaggregated to the HRAP scale. However, to reach the point of the conceptual storages at all simulated pixels being updated by the soil moisture data assimilation process, a second filtering step in which there is a shift in the observation equation is proposed. For this second step, the states are now the conceptual storages of the "unobserved" pixels and the observations are changed to be the ensemble of updated conceptual storages at model locations collocated with observations.

4.4 In Situ Studies

The double EnKF procedure is tested over the Russian River Basin in Northern CA and utilizes the NOAA HMT program *in situ* measurements (Zamora *et al*., 2011). The network provides observations of soil moisture and temperature at several depths, but this study makes use of only the 10 cm depth (the shallowest layer for most of the sites). Using only the topmost observation layer is done to mimic what is captured by satellite-based retrievals. Sites are dispersed throughout the approximately 3,800 km^2 basin and include Willits (WLS) and Potter Valley (PTV) in the upper basin, Hopland (HLD) and Lake Sonoma (LSN) in the central basin, and Cazadero (CZC), Rio Nido (ROD), and Healdsburg (HBG) in the lower basin (Figure 4-5). Although the CZC site does not properly sit within the drainage area of the Russian River Basin, the observations from this site are still useful during the second filtering step, to spread innovation to pixels that are within the basin boundaries.

Figure 4-5 Russian River Basin and location of HMT soil moisture observation sites (green circles).

To evaluate the impact and practicality of soil moisture assimilation with the proposed double EnKF, the model is run for a 1-year spinup period (2012) and a 1-year data assimilation period (2013). Precipitation and temperature data for model forcing come from the California-Nevada River Forecast Center. A 25 member ensemble is generated by sampling a Gaussian distribution with a mean equal to that of the states at the end of the 1-year spinup period, and a variance of 0.25 $(m^3/m^3)^2$. This sizeable variance was chosen to represent a large initial uncertainty in the possible range of 0 to 1 and approaches a "worst case" scenario for prior understanding of the state. Ensemble members are sustained by perturbing the precipitation and temperature forcing data with noise sampled from a

normal distribution. Similarly, Gaussian noise that reflects uncertainty associated with the soil moisture probe is added to the soil moisture observations.

The evaluation is performed at the 7 HL-RDHM pixels collocated with the HMT observation sites in two phases. The first phase uses the same observation set for the assimilation and the assessment to test the impact of the first filtering step in which the observations come from the soil moisture probe. In this case, the states being estimated are the SAC-SMA upper zone conceptual storages at the pixels collocated with the volumetric soil moisture observations. For the second phase, only 6 of the 7 observation sites are used in the complete double EnKF process, with the 7th saved for a validation of the spreading of the innovation to "unobserved" pixels. For both parts, the RMSE, correlation, bias, and NSE are used as performance metrics. Figures 4-6, 4-7, and 4-8 feature results from both phases of the evaluation for the upper, central, and lower basin sites respectively.

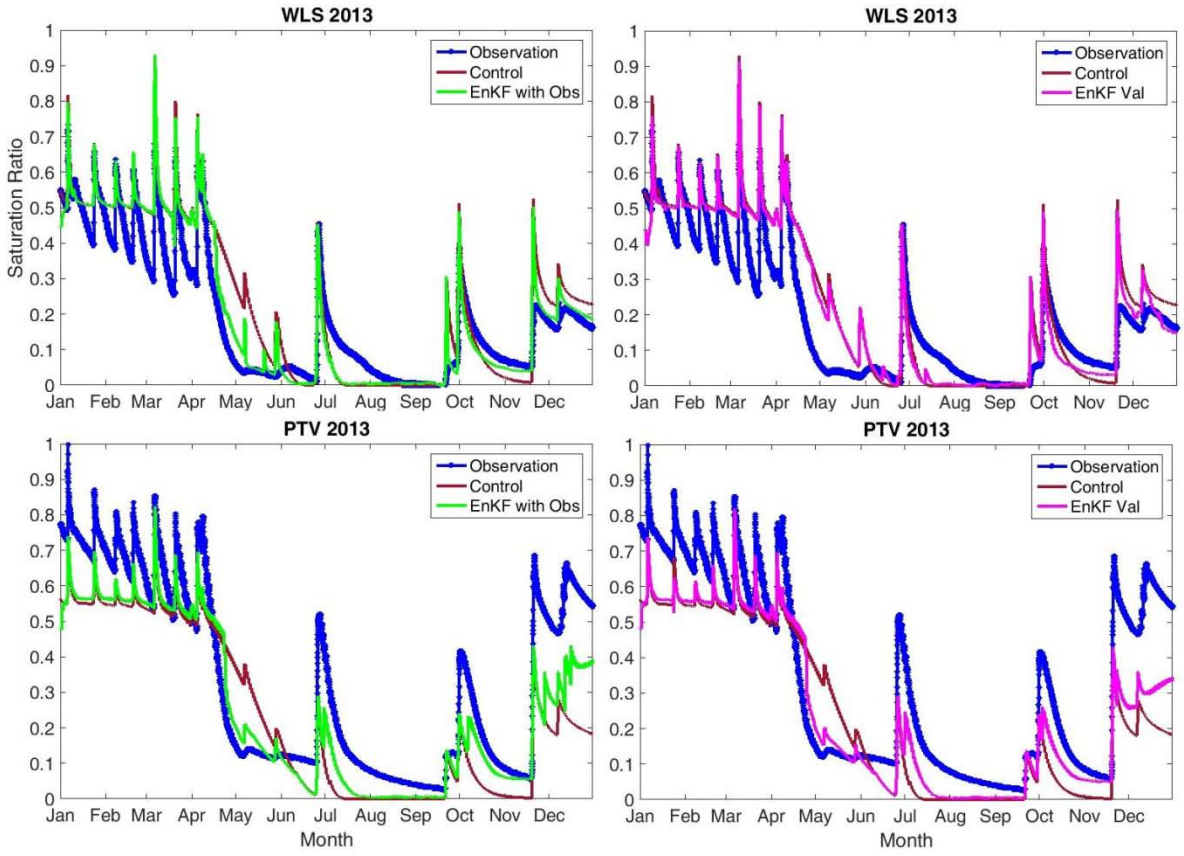

Figure 4-6 Double EnKF soil saturation ratio results at 10 cm for upper basin observation sites in the Russian River Basin. Left: Results with observations collocated at the site assimilated. Right: Validation of the second filter step with collocated observations removed from the assimilation

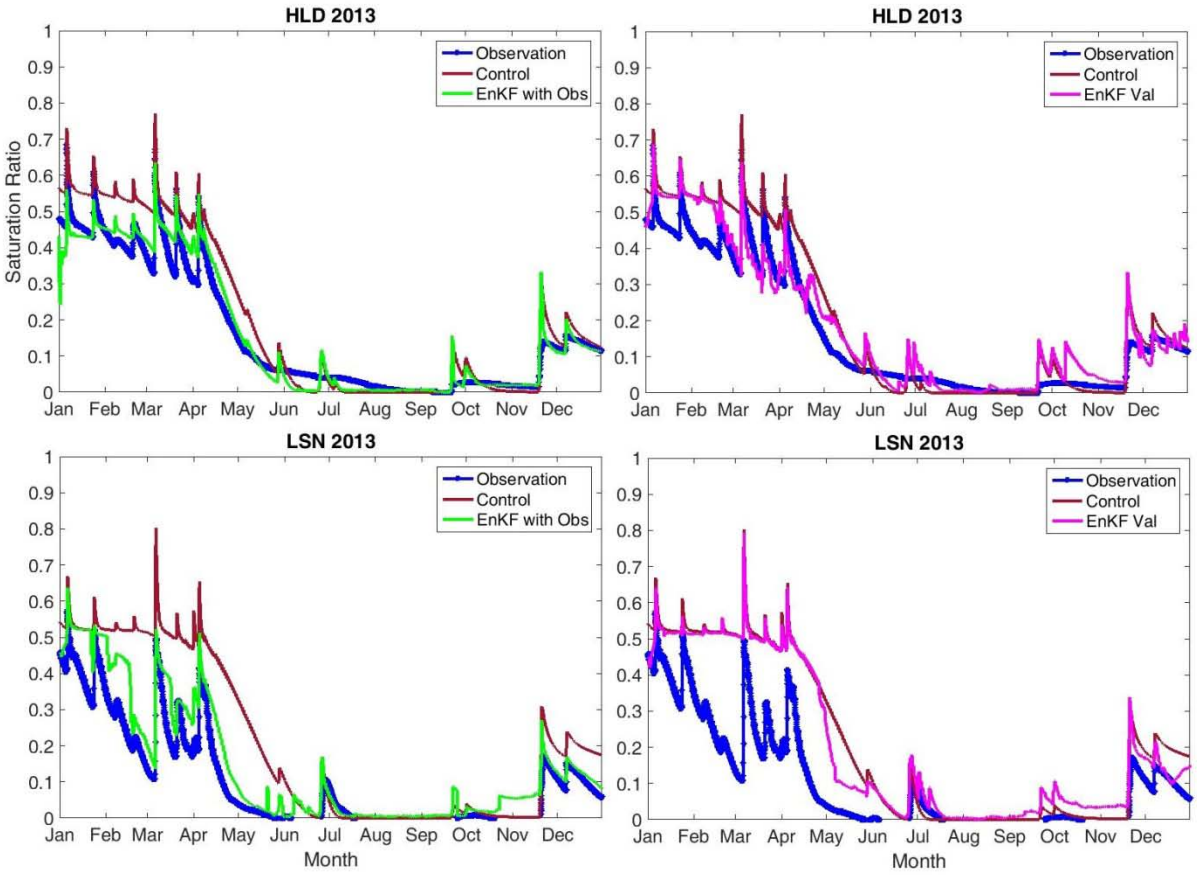

Figure 4-7 Same as Figure 4-6, but for 2 central basin stations.

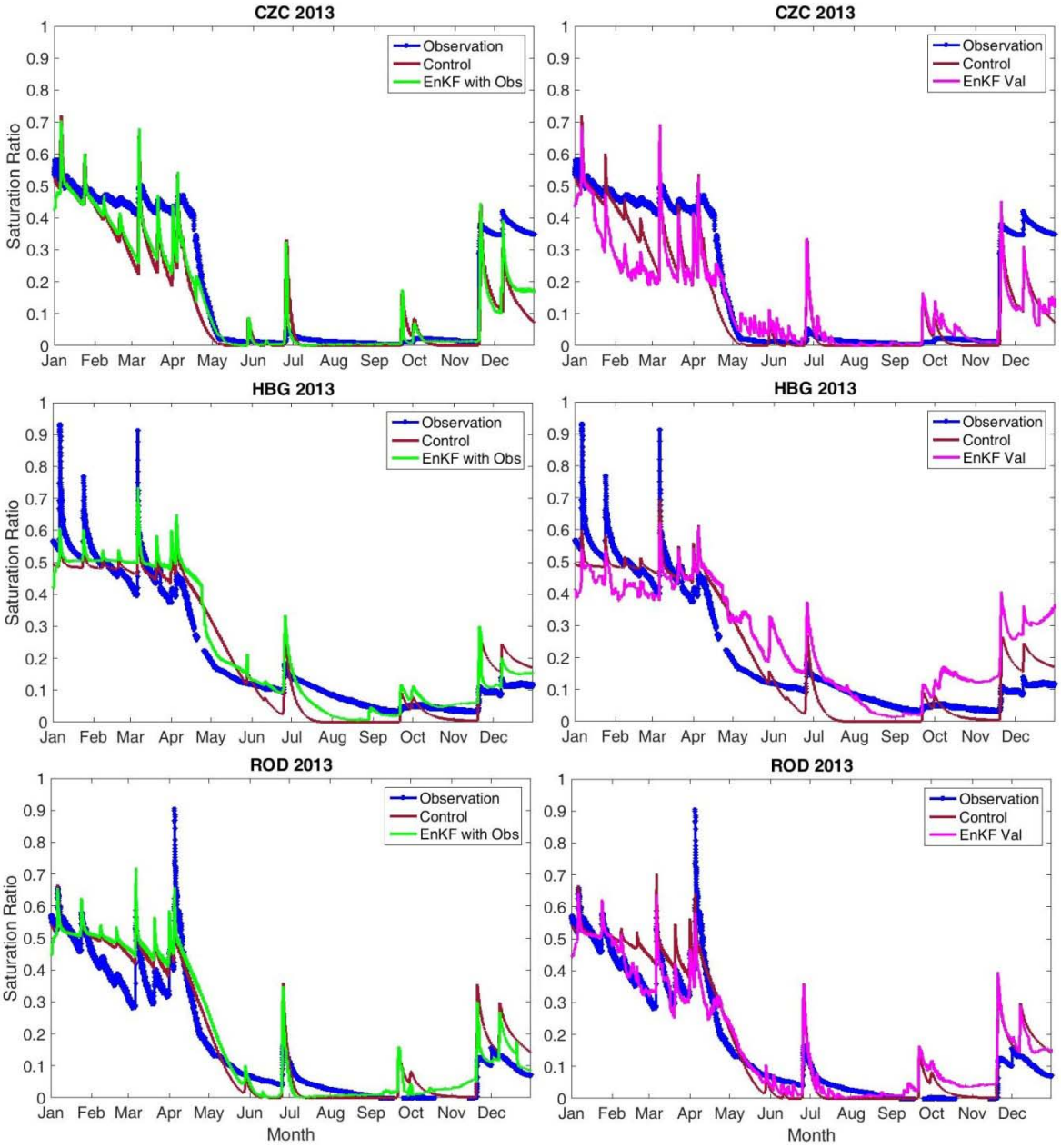

Figure 4-8 Same as Figure 4-6, but for 3 lower basin stations.

From Table 4-1, it can be seen that 5 of the 7 sites showed at least some improvement across all statistics for the experiment that included collocated observations. The exceptions came from ROD and HBG, which show a slight degradation in bias. It is worth noting here that the control runs at these two sites were already performing high across all

statistics, and even though the bias suffered mildly, the predictive capability in the form of NSE was unchanged at ROD and even had a modest 3% improvement at HBG. For the remaining sites, a 3-61% RMSE reduction, a 0-16% correlation increase, a 4-66% bias decrease, and a 1-186% NSE increase is seen. The site that clearly benefited the most from data assimilation of its collocated observation was LSN, which went from -0.84 NSE to 0.72 in addition to dramatic improvement in the other three metrics as well.

Table 4-1 Statistical summary for in situ double EnKF tests

SITE ID	MODEL RUN	RMSE	CORR	BIAS	NSE
WLS	Control	0.10	0.91	0.21	0.70
	EnKF with Obs	0.08	0.95	0.10	0.83
	EnKF Validation	0.09	0.91	0.15	0.73
PTV	Control	0.17	0.86	-0.29	0.61
	EnKF with Obs	0.12	0.95	-0.24	0.80
	EnKF Validation	017	0.85	-0.27	0.59
HLD	Control	0.07	0.98	0.26	0.82
	EnKF with Obs	0.07	0.98	0.25	0.83
	EnKF Validation	0.06	0.97	0.16	0.90
LSN	Control	0.20	0.83	1.00	-0.84
	EnKF with Obs	0.08	0.97	0.34	0.72
	EnKF Validation	0.018	0.84	0.90	-0.59
CZC	Control	0.10	0.91	-0.29	0.75
	EnKF with Obs	0.09	0.94	-0.24	0.82
	EnKF Validation	0.13	0.87	-0.31	0.63
HBG	Control	0.07	0.94	-0.02	0.88
	EnKF with Obs	0.06	0.96	0.06	0.91
	EnKF Validation	0.11	0.85	0.22	0.67
ROD	Control	0.07	0.95	0.12	0.87
	EnKF with Obs	0.07	0.96	0.13	0.87
	EnKF Validation	0.06	0.95	0.05	0.90

Where the experiments that use collocated observations for the assimilation and evaluation provide valuable insight as a sanity check/general proof of concept, their impact basin-wide is minimal unless the innovation spreading step can be demonstrated to be

effective. This is especially true given the relatively sparse nature of the *in situ* observation network of this basin. Removing one station at a time to treat its corresponding HL-RDHM pixel as "unobserved" allows for validation of the second spreading step. Right panels in Figures 4-6 through 4-8 permit visualization of each station's validation simulation, with a statistical summary provided in Table 4-1.

It is expected that a pixel collocated with an observation will exhibit improvement in soil moisture simulation, however, the minimalist goal for unobserved pixels after assimilation is that performance is not worse than the control run. The results for the validation are mixed in this case with 4 sites (WLS, HLD, LSN, and ROD) outperforming the control run, 1 site (PTV) left largely unchanged from the control run, and 2 sites (CZC and HBG) performing measurably worse than the control run. Even though the two sites downgraded, they still outperformed the LSN site validation, which even after the assimilation has an unacceptable NSE of -59 (due to a large bias), and even slightly edged out the PTV site in terms of NSE. For this reason, the validation experiments are still crowned "more successful than detrimental" overall.

4.5 SMOS Studies

The double EnKF test is repeated using SMOS observations for assimilation rather than HMT station observations. There is no separate validation stage for these observations, as each SMOS pixel is not necessarily retrieved at the same locations for at each observation time. That is, at some assimilation time steps, a given pixel might be collocated with an observation and at others it may not be and must rely on the second filtering step. Although SMOS observations are viable for the ~5 cm depth and are assimilated into HL-

RDHM accordingly, they are compared to the same observations sets as in section 4.4. The control run is now also evaluated at the 5 cm depth to highlight any changes resulting from the assimilation.

Simulation results are presented in Figures 4-9 through 4-11 and are separated by upper, central, and lower basin station sites respectively. The 5 cm depth model control run and 10 cm depth HMT observations are provided in each plot. Noteworthy is the model tendency to overestimate soil moisture during the first large spring-time dry down period (April and May), especially at WLS, PTV, HLD, LSN, and HBG. Generally, the SMOS assimilation is able to push the ensemble mean toward the observation in this case. Improvement is also visible at sites with a control model run that overestimates in the first four months of the year (WLS, HLD, LSN, and ROD).

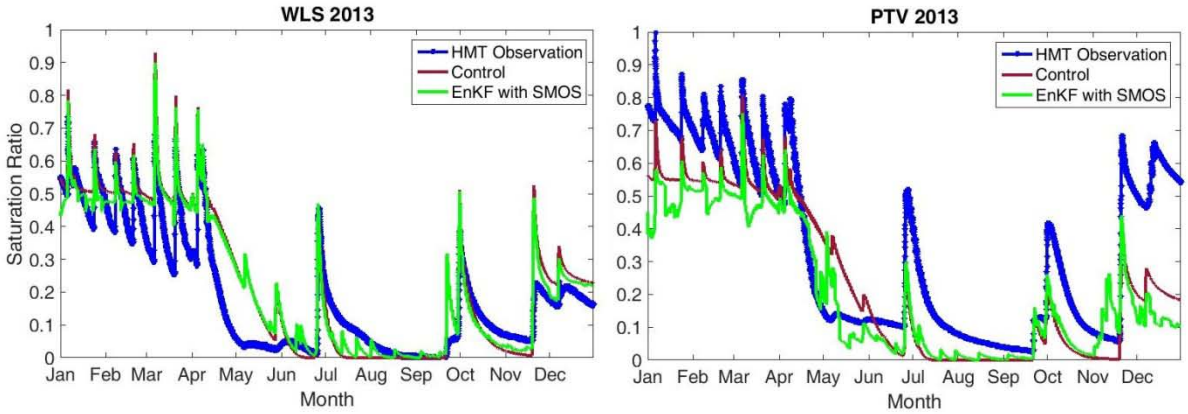

Figure 4-9 Double EnKF soil saturation ratio results at 5 cm for upper basin observation sites in the Russian River Basin using SMOS observations for assimilation.

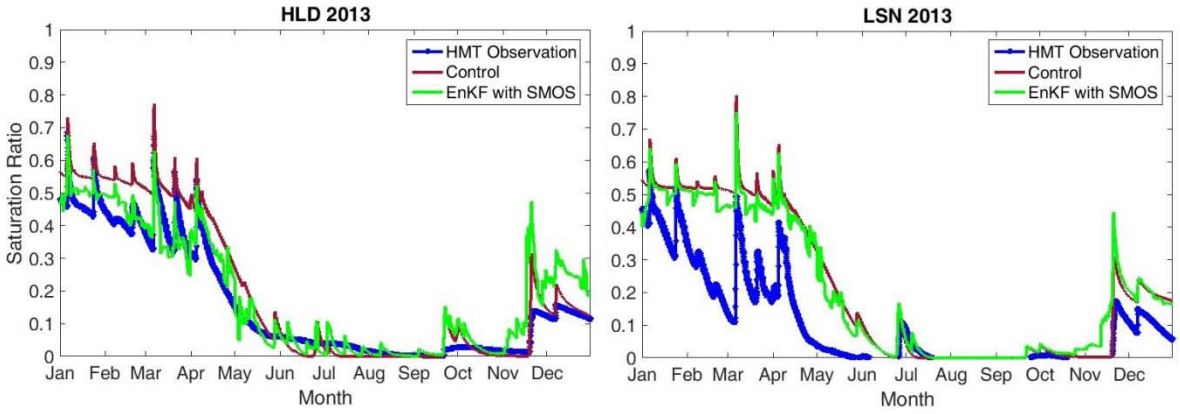

Figure 4-10 Same as Figure 4-9, but for 2 central basin stations.

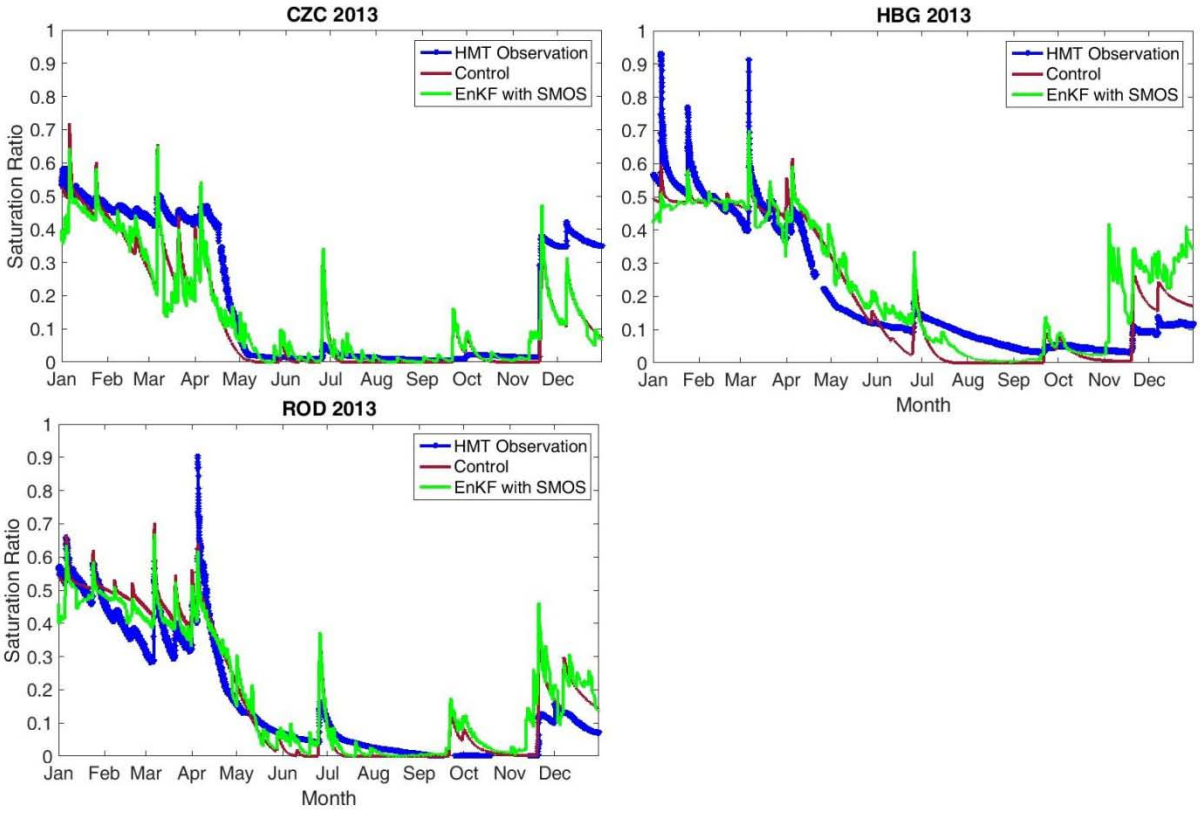

Figure 4-11 Same as Figure 4-9, but for 3 lower basin stations.

Several striking pessimistic features appear in the assimilation runs as well. At PTV for example, a large dip in soil saturation ratio appears at the end of February, despite the

control run already underestimating at that site. Similarly, the SMOS assimilation simulation at HBG jumps in early November and remains higher than the control run even though the control run overestimates this for most of this period. These features could be due to a number of factors including spurious correlations with observations not located at the pixel site, issues with SMOS observations at the pixel location, or even improper model parameter specification.

A statistical summary of the 5 cm depth control run along with simulations assimilated with SMOS saturation ratios are presented in Table 4-2. Again it is stressed that the catch with these results is that the HMT observations are used as a baseline and are at a 10 cm depth rather than 5 cm.

Table 4-2 Statistical summary for SMOS double EnKF tests

SITE ID	MODEL RUN	RMSE [fraction]	CORR	BIAS	NSE
WLS	Control	0.10	0.91	0.20	0.70
	EnKF with SMOS	0.09	0.90	0.13	0.75
PTV	Control	0.17	0.86	-0.30	0.60
	EnKF with SMOS	0.17	0.88	-0.30	0.61
HLD	Control	0.07	0.98	0.25	0.83
	EnKF with SMOS	0.06	0.97	0.22	0.87
LSN	Control	0.19	0.83	0.99	-0.81
	EnKF with SMOS	0.18	0.85	0.90	-0.49
CZC	Control	0.11	0.91	-0.31	0.73
	EnKF with SMOS	0.10	0.92	-0.29	0.75
HBG	Control	0.07	0.94	-0.03	0.88
	EnKF with SMOS	0.10	0.87	0.14	0.72
ROD	Control	0.07	0.95	0.11	0.87
	EnKF with SMOS	0.06	0.96	0.15	0.89

With the exception of HBG, all sites showed an RMSE decrease (or remained unchanged at PTV). Correlation results were mixed, with three sites showing a decrease in correlation

and four showing an increase. With the exception of HBG, changes in either direction were less than 2.5%. Correlations for all simulations (with SMOS soil moisture assimilation or not) were high with the minimum value of 0.83 belonging to the control run of LSN. While bias results for HBG and ROD increased and PTV remained unchanged, improvement at the other stations ranged from 6% to 35%. NSE improved at all sites except for HBG with improvement ranging from 2% to 40%. It should be noted that although LSN enjoyed the largest improvement in NSE through assimilation of SMOS soil moisture information, the simulation still produced a value of -0.49, which indicates no predictive ability.

4.6 Discussion

A strategy to address ensemble member underdispersiveness was developed to allow small variances when desired and expected (i.e. prolonged dry periods and precipitation events) but to resample state values when the influence of the observation is no longer effective. This is done through a mechanism that checks whether or not the maximum or minimum value for ensemble members is in the region of the noisy observation. If the resampling is deemed necessary, the ensemble is resampled from a distribution with the same mean and with a variance that is proportional to the distance between the predicted and observed observation. There are further possible enhancements to consider for the resampling strategy. First, since the variance inflation essentially is adding uncertainty to the simulation without attributing it to a particular source, a restriction may be added to only resample immediately after a precipitation event. This can be justified in that precipitation remains arguably the most uncertain component in rainfall-runoff modeling. Such a restriction was not included in this work, particularly because the model was not yet

calibrated to correct for improper specifications of PET or wilting point so as to allow the assimilation process to attempt to catch problems in the drydown signal. Also worth noting is that using selective variance expansion compliments the use of an inflation factor with the inflation factor modulating ensemble spread and the variance expansion and resampling picking up the slack for rapidly changing soil moisture conditions. It is also likely that the frequency of variance resampling will decrease with a larger ensemble size.

A double EnKF technique was introduced as a means to update the conceptual storages at every pixel within the model domain without assuming observations are available at every location, and without having to rely on interpolation of soil moisture observations prior to assimilation. In the first step of the assimilation, conceptual model states at "observed" pixels are updated with observed near surface soil moisture observations. In the second step, the remaining pixels are update by treating the ensemble of the adjusted states from step one as the observations in the EnKF process. Tests with the HMT sites show consistent improvement for step one of the procedure, and the validation phase with station removal revealed mostly favorable results over the control run.

While it is expected that the more observations to contribute to the update of an unobserved state the better, given the formulation of this second EnKF step, there must be a correlation between the observation and unobserved state in order for it to be useful. Therefore, strategies related to maximizing the benefit of the most relevant observations to a particular unobserved state could be further investigated. This notion of data selection is discussed in Houtekamer and Mitchell (1998), who utilize a cutoff radius to distinguish which analyzed points should be considered impacted by each observation in an

atmospheric model. They also stress that the further a point becomes from an observation, the potential positive impact from updating can be expected to be small. The analogy to the hydrologic application in this sense is that the more dissimilar an observation location is (due to distance from the observation, physical properties leading to different drying rates, or differences in recent meteorological influences), the less of a positive impact that observation will have on an analyzed pixel. Although not fully examined here since performance in the *in situ* validation investigation was largely positive, localization techniques may be beneficial in preventing detrimental prediction skill results as seen at the HBG and CZC sites during the validation period.

The double EnKF procedure was also tested using SMOS satellite-based estimates and evaluated against the HMT observations. Overall, the improvement over the control run was largely underwhelming. Nonetheless, with the exception of the HBG site, all of the sites experienced minor improvement in predictive capability as expressed by the NSE. Of the cases that did outperform the control run, bias showed the largest degree of improvement. The slight decrease in correlation at some sites (and large decrease at the HBG site) may be attributed to the frequency of assimilation time steps, which was slightly lower than the HMT study. Although improvement may be slight, this study suggests there is valuable information contained in the SMOS soil moisture retrievals for the Russian River Basin, despite the fairly complex terrain challenging the capabilities of the retrieval.

It is anticipated that localization techniques (not employed here) could also benefit the SMOS experiments, since there are generally more observations for each retrieved time step compared to the HMT experiment (increasing the chances for spurious correlations). If

the detrimental features of the assimilation runs at PTV in February and at HBG in Nov – Dec are, in fact, due to spurious correlations with other observations and not due to problems with collocated observations or model parameterizations, then localization could help to eliminate these features. Otherwise, model calibration or further preprocessing of the SMOS retrievals may be required to get rid of these features.

4.7 Chapter 4 Synopsis

- A new strategy to resolve ensemble member underdispersiveness for soil moisture was developed and tested.
- A double EnKF approach, featuring a state to observation shift, was used to update conceptual storages collocated with observations then subsequently spread the innovation to remaining pixels.
- The double EnKF approach was validated using HMT *in situ* soil moisture measurements and tested with SMOS satellite-based measurements over the Russian River Basin.
- Assimilation of both types of observations showed improvement in soil moisture simulations, with the *in situ* data vastly outperforming the satellite data.

Chapter 5. Soil Moisture for Calibration of a Distributed Hydrologic Model

5.1 Introduction

For many years, calibration of hydrologic models has been a crucial step in identifying parameters used to represent mechanisms that are either poorly understood, too computationally expensive to resolve, or even unnecessary for a given application. Calibration of hydrologic models has traditionally been performed by adjusting model parameters such that the simulated hydrograph best fits an observed hydrograph. This framework is often limited in that the observed outlet hydrograph is the result of a collection of many internal basin processes (Ivanov *et al.,* 2010; Liang and Xie, 2001). Several studies have pointed to soil moisture as a possible vehicle for describing these heterogeneous sub-basin processes, particularly in respect to how streamflow is modulated (Santanello Jr. *et al.*, 2003; Campo *et al.,* 2006; Wanders *et al.*, 2014; Zamora *et al.,* 2014). Some have turned to other variables such as evapotranspiration (Rientjes *et al.,* 2013; Immerzeel and Droogers, 2008; Cao *et al.,* 2006), snow covered area (Isensteirn *et al.*, 2015; Franz and Karsten 2013), and nitrogen concentration (Bergström *et al.*, 2002) either in lieu of, or as a compliment to calibrating to discharge. While significant progress has been made from these studies, challenges still remain regarding how best to leverage available observations for calibration.

Utilization of soil moisture observations as a tool for calibrating hydrologic models has been explored in several studies. Wanders *et al.* (2014) propose the use of satellite-based

surface soil moisture observations in conjunction with discharge observations in a dual state/parameter estimation of the LISFLOOD model in the Upper Danube. This study found an improvement of discharge simulations when both observations were used for calibration over using discharge-only based calibration and that there was the added benefit of improved soil moisture simulation throughout the catchment. Campo *et al.* (2006) use synthetic aperture radar data to infer information about soil moisture at bare soil pixels to use for calibration of the distributed hydrologic model called MOBIDIC. Although restricted to areas with little to no vegetation cover, results of this work also demonstrate improvement in simulated discharge with the addition of soil moisture-based calibration. Studies using limited *in situ* observations for basin calibration have found some improvement in discharge simulations. Koren *et al.* (2008) explore the calibration of basin average soil moisture for a lumped version of SAC-HT. Using daily, basin average soil moisture calibration, simulated discharge improvement was achieved by defining an objective function that took into account the RMSE of outlet streamflow at four different time scales combined with RMSE of two soil moisture layers.

In this chapter, using the NWS HL-RDHM model, a distributed calibration approach based on soil moisture is developed. This approach allows the loosening of the assumption in Koren *et al.* (2003) that states *a priori* parameter grid cell values are correctly proportioned relative to one another. This soil moisture-based calibration is tested alongside the traditional discharge-based calibration, and a two-step hybrid scheme is introduced. Pixel scale synthetic studies are carried out to identify appropriate parameters for soil moisture-based calibration, and to evaluate performance under ideal conditions (all inputs and outputs are known as well the corresponding parameter sets that produce

them). These single pixel experiments are then expanded to the full basin scale for a basin that is included in the Iowa Flood Studies (IFloodS) experiment domain. This chapter aims to 1) determine which HL-RDHM parameters are most identifiable when calibrating to soil moisture, 2) test how to best spread calibration information from isolated pixels to the full basin scale so that internal basin process representation is enhanced, and 3) examine if the inclusion of soil moisture observations in the calibration process provides additional improvement to streamflow simulations or if it can improve streamflow simulations as a standalone under the circumstance that streamflow observations are unavailable. For all simulations, calibration or validation, a 1-year spin-up period was used.

5.2 Calibration Scheme

Calibration of HL-RDHM was performed with the global search algorithm, Shuffled Complex Evolution-University of Arizona (SCE-UA) (Duan *et al.*, 1992). Use of SCE-UA and its subsequent variations have been extensively used in hydrologic modeling (Sorooshian *et al.*, 1993; Duan *et al.*, 1994; Gan and Biftu, 1996; Cooper *et al.* 1997, 2007; Hogue *et al.*, 2000, 2003; Vrugt *et al.*, 2003; Chu *et al.* 2010). The notion of multi-objective strategies for hydrologic modeling has been highlighted in Gupta *et al.* (1998), Yappo *et al.* (1998), Vrugt *et al.* (2003), and Shafii and De Smedt (2009) (among others). These studies emphasize the need to exploit as much useful information as possible from observations rather than relying on a single objective. This can be in the form of calibrating to multiple variables, or calibrating to multiple signals of the same variable. For example, Gutpa et al. (1999) highlight effective constraining of parameters in a complex land surface scheme when calibrating to heat flux data in addition to an available state variable. With this in mind, the

calibration scheme here focuses on soil moisture and discharge as the two calibration variables. For the soil moisture-based calibration of this work, SCE-UA was applied at the single model pixel scale, wherever *in situ* soil moisture observations were available. The objective function to minimize in this case was the combined root mean square error (RMSE) of four observed soil moisture layers. For discharge-based calibration in this study, the objective function that SCE-UA sought to minimize was the RMSE of simulated discharge.

Hogue *et al.* (2000, 2003) introduced an automatic calibration scheme for the lumped version of SAC-SMA and SNOW17 that was designed to mimic the manual calibration approach of NWS. This method featured two objective functions used in successive calibration with each objective function targeting specific parameters (i.e. baseflow parameters with one objective function, upper zone parameters with the second). Franz and Karsten (2013) explore a multistep calibration process that targets parameters in the SNOW17 model where three parameters are first optimized to snow covered area followed by an additional parameter being optimized via streamflow observations and simulations from the lumped SAC-SMA. The work presented here similarly explores stepwise calibration of a watershed that focuses on relevant parameters by following the example of Franz and Karsten (2013) of targeting certain parameter groups with different variables. Soil moisture observations from the IFloodS experiment are used to calibrate a specific parameter group followed by discharge-based calibration of the remaining parameters. The effects of only using soil moisture-based calibration and discharge-based only calibration are also investigated.

The framework for the soil-moisture based calibration of this study relies on calibrating single pixels within the distributed model domain, but dispersing the calibration to the rest of the model pixels. In order to apply parameter adjustment of the individually calibrated parameters to the rest of the pixels in the basin, 3 different distribution schemes were investigated:

- Inverse distance weighting (**InvDist**): Inverse distance weighting of parameters was used to distribute calibrated values to neighboring pixels according to physical proximity. Weights for InvDist are calculated as

$$w_i(\mathbf{x}) = \frac{1}{d(\mathbf{x},\mathbf{x}_i)^p} \qquad (5\text{-}1)$$

$$d(\mathbf{x},\mathbf{x}_i) = \sqrt{\sum_{j=1}^{n}(x_j - x_{ij})^2} \qquad (5\text{-}2)$$

where w_i is the weight of the ith calibrated pixel given to the unknown pixel $\mathbf{x}$, based on the distance (d), between pixel $\mathbf{x}$ and calibrated pixel $\mathbf{x}_i$, and p is the power parameter (chosen as 2 for this study). Parameter values are then assigned to pixel $\mathbf{x}$ as

$$\theta(\mathbf{x}) = \begin{cases} \dfrac{\sum_{i=1}^{N} w_i(\mathbf{x})\theta(\mathbf{x}_i)}{\sum_{i=1}^{N} w_i(\mathbf{x})} & \text{if } d(\mathbf{x},\mathbf{x}_i) \neq 0 \\ \theta(\mathbf{x}_i) & \text{if } d(\mathbf{x},\mathbf{x}_i) = 0 \end{cases} \qquad (5\text{-}3)$$

where $\boldsymbol{\theta}(\mathbf{x})$is a vector of parameters at pixel $\mathbf{x}$, $\boldsymbol{\theta}(\mathbf{x}_i)$ and is a vector of parameters at calibrated pixel $\mathbf{x}_i$.

- Similarity of pixels weighting (**SimPix**): SimPix is a distribution method based on the similarity of pixel characteristics and was created following the InvDist method with the exception that the distance is now defined as the Euclidean distance in parameter space rather than in 2-D physical space

$$d(\boldsymbol{\theta}'_{\mathbf{x}}, \boldsymbol{\theta}'_{\mathbf{x}i}) = \sqrt{\sum_{k=1}^{m}\left(\frac{\theta_{\mathbf{x}k} - \theta'_{\mathbf{x}ik}}{\theta_{kMAX} - \theta_{kMIN}}\right)^2} \qquad (5\text{-}4)$$

where $\boldsymbol{\theta}'_{\mathbf{x}}$ is the uncalibrated parameter vector at pixel $\mathbf{x}$, $\boldsymbol{\theta}'_{\mathbf{x}i}$ is the uncalibrated parameter vector at calibrated pixel $\mathbf{x}_i$, and θ_{kMAX} and θ_{kMIN} are the maximum and minimum value of the kth parameter respectively. The $(\theta_{kMAX} - \theta_{kMIN})$ term is a necessary regularization provision that prevents the magnitude of a given parameter from dominating the similarity measure. This method was developed using the *a priori* parameter grids provided by the NWS as the metric of similarity, given that these parameter grids are derived from soil surveys (Koren *et al.,* 2003). It is assumed that if a specific pixel requires calibration, those pixels that are physically similar according to the *a priori* parameters will need to be calibrated similarly. This has the potential advantage over the InvDist method in that the unobservable pixels do not need to be in the near vicinity of the observable pixels, and that a landscape with drastically changing soil characteristics in space will not become smoothed by the InvDist process.

- Basic average of scalar multipliers (**BaseAve**): The BaseAve method follows the same assumptions as the original calibration method outlined in NWS (2011). In this method, scalar multipliers are identified and applied to the *a priori* parameter grids while presupposing the spatial relationship of the parameters is correct and only their average magnitude requires adjustment. To identify basin multipliers in this study, a multiplier is calculated for each parameter at every observation station pixel, and the average of the multipliers is taken and applied to the original grids basin-wide. Like its discharge-based calibration counterpart that is traditionally used and is discussed in NWS (2011), this distribution method will see no changes in the description of basin heterogeneity beyond what has already been established in the *a priori* parameter grids.

5.3 Data and Study Area

The Turkey River (Figure 5-1) is a 246 km tributary of the upper Mississippi River covering a drainage area of 4,384 km^2 in Iowa. The region is comprised primarily of non-irrigated farmland (corn and soybeans). Northeastern Iowa, where the Turkey River Basin is located, hosts an area characterized by a karstic and high relief landscape. These complex systems allow for the rapid transmission of groundwater through broken rocks, eventually leading to steeply-banked streams through seeps and springs (Libra, 2005). While the conceptual rainfall-runoff scheme doesn't explicitly represent a water table, the lower zone incorporates the saturated zone (Brazil and Hudlow, 1981), which may be influenced by the karst formations. The sinkholes that pepper this region allow surface runoff to directly infiltrate to the water table (Libra, 2005). This particular geological formation is not

directly accounted for in HL-RDHM and adds a unique complication to the experiment, particularly in the southeastern region of the basin, where there is a concentration of known sinkholes.

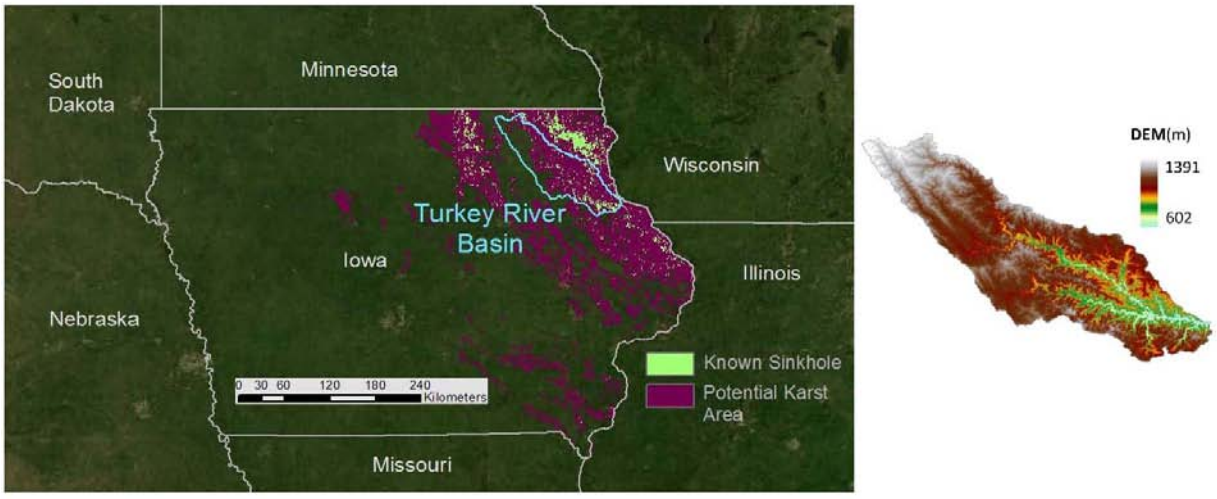

Figure 5-1 Left: Turkey River Basin and Iowa's karstic regions. Right: Topography of Turkey River Basin derived from 30m DEM.

In support of the National Aeronautics and Space Administration (NASA) Global Precipitation Measurement (GPM) validation efforts, the Iowa Flood Center (IFC) launched the IFloodS field campaign in the spring of 2013 (Krajewski *et al.,* 2013; Demir *et al.*, 2015; Schwaller and Morris, 2011, Tapiador *et al.*, 2012). As part of the comprehensive collection of hydrometeorological instrumentation used for IFloodS, provides multiple real-time observed hydrometeorological data during spring of 2013 from tipping-bucket rain gauges, weather radars, stream flow and stage gauges, and soil moisture probes (Krajewski *et al.*, 2013). While limited in observation period length, these observations are rich in terms of spatial density.

The two primary data components required for this study were soil moisture and discharge. The soil moisture data used is from the IFloodS field campaign. These data are available at 5, 10, 20, and 50 cm depths at 20 *in situ* locations throughout the Turkey River Basin during the spring of 2013. Figure 5-2 depicts the layout of the IFloodS soil moisture network. Station soil moisture time series were averaged from 15 minute to hourly observations for use in this study. Basin outlet discharge data used were from the USGS streamflow gauge number 05412500 at Garber, Iowa. These too were averaged from 15 minute to hourly data to remain consistent with model simulations. All non-synthetic experiments for calibration and soil moisture-based validation in this study are set up from 24 April – 24 June 2013, a time period in which data is available from the IFloodS campaign.

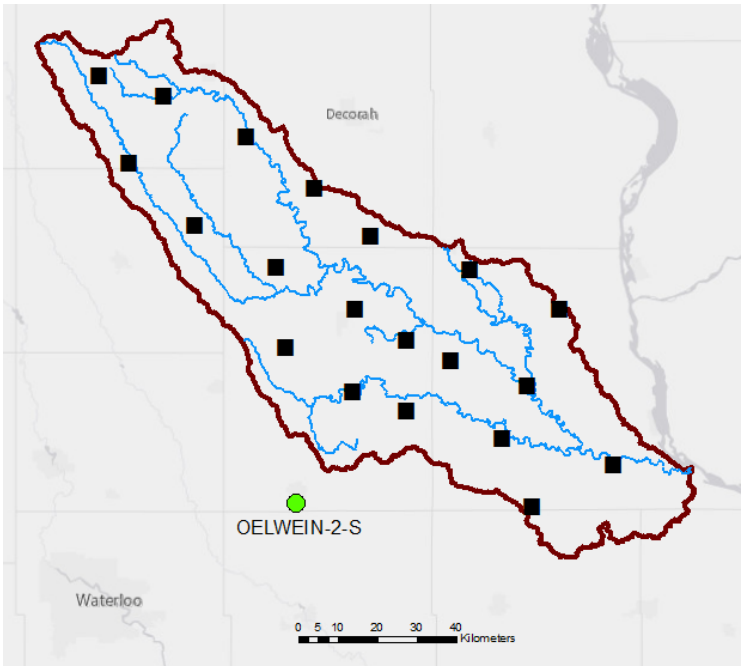

Figure 5-2 IFloodS network of in-situ soil moisture observations (squares) in the Turkey River Basin and the NWS COOP site OELWEIN-2-S (circle).

Model input forcing for this study was the National Centers for Environmental Prediction (NCEP) NEXRAD Stage IV rainfall data derived from multiple sensors (gauges and radars) over the CONUS. The reanalysis air temperature from the North American Land Data Assimilation System Phase 2 (NLDAS2) available from NASA Goddard Earth Sciences Data and Information Services Center (GES DISC) was also used. Both forcing data are in 4km, hourly, spatio-temporal resolution.

This study also makes use of data from the NWS Cooperative Observer Program (COOP). The NWS COOP is made of a network of over 7,000 volunteer climate data observers in addition to the hundreds of NWS stations. These sites record daily maximum/minimum temperatures as well as precipitation to aid in the study of various climate phenomena in the United States (Robinson, 1990). Daily precipitation from the COOP site OELWEIN-2-S in northeastern Iowa (Figure 5-2) was utilized in the synthetic study design (described in the following section).

5.4 Synthetic Soil Moisture Experiment

In order to evaluate the suitability of using soil moisture data to identify parameters in HL-RDHM, single pixel synthetic studies were conducted. Use of a single pixel reduces the complexity of a fully distributed basin, and allows for a simple, ideal case representation of the larger experiment. These single pixel experiments were carried out in two phases: 1) a sensitivity analysis of all parameters plausibly relevant to soil moisture and 2) a series of scenarios that test the ability to retrieve a prescribed parameter set.

A model pixel located near the Turkey River Basin extent was selected for the synthetic experiments. Within this pixel is the NWS COOP site OELWEIN-2-S, which has a data record that dates back to 1951. Climate data from this site were used to design 2-month long synthetic precipitation patterns of varying intensity. The temporal pattern was taken as the basin average of the 2005 May-June precipitation Stage IV hourly estimates. This pattern was linearly scaled such that the total precipitation equals the minimum, median, and high May-June precipitation totals from the COOP site. NLDAS2 temperatures from the same 2005 time period that the precipitation was based on were used to force the model in all three scenarios. The *a priori* parameter values from the NWS at this pixel were taken as the prescribed true parameters. This was done to ensure a realistic combination of the parameters, as several studies have demonstrated reasonable simulations using the *a priori* parameter sets (e.g. Nguyen *et al.*, 2015; Fares *et al.,* 2014). It should be emphasized that calibration of HL-RHDM parameters in the upper Midwest has been shown to substantially improve simulation results (Spies *et al.,* 2015), and that use of the *a priori* sets for this synthetic study is simply to provide a plausible mixture of parameters. The model was run using the *a priori* parameters, and the resulting simulated soil moisture at the four observable layers of the IFloodS instruments and simulated pixel discharge were used as "perfect observations" to complete the ideal case experiments.

Each of the 11 SAC-HTET parameters related to storage and release were perturbed one at a time to evaluate individual effects on soil moisture and discharge (at the single pixel scale). The entire plausible range for each parameter as provided in Koren *et al.* (2008) was explored (see Table 1). The median precipitation scenario described in the previous section was used to drive the model. An example conceptualization of how the *in situ*

observations in this study relate to the model parameters is provided in Figure 5-3. Although the exact relationship will vary pixel to pixel, this example shows the parameter-soil layer relationship of the synthetic experiment pixel, which provides an idea of how parameters of pixels in the Turkey River Basin are related to the IFloodS soil moisture observation layers. The model defines its own layers for internal calculations while offering the user the ability to request specific layers, which are interpolated from the model-defined soil layers.

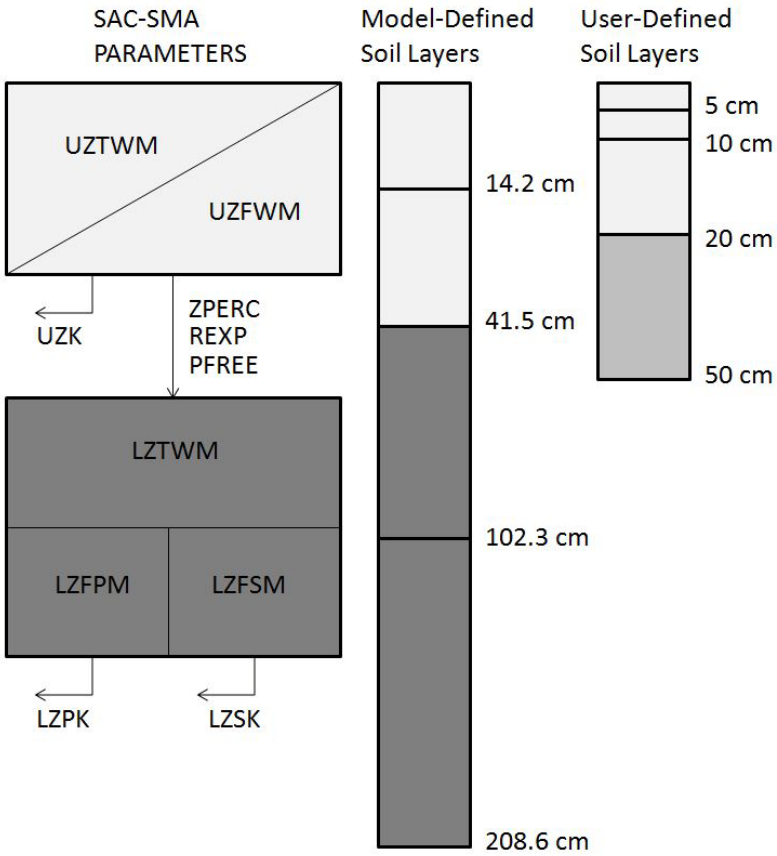

Figure 5-3 Sample (pixel at NWS COOP site OELWEIN-2-S) connection between the SAC-SMA conceptual storage parameters, model-defined soil layers, and user-defined soil layers. Light shades correspond to the upper zone conceptual storages, dark shades to lower zone storages, and the medium shade lies in both.

Figure 5-4 qualitatively shows the sensitivity of simulated soil moisture at the four observable soil layers for the IFloodS campaign. Of the 11 parameters, the storage parameters (UZTWM, UZFWM, LZTWM, LZFSM, and LZFPM) exhibit sensitivity in the simulated soil moisture at all four layers, which shows itself as a spreading in the soil moisture estimate with changing parameter values. The three free water storage parameters show lower soil moisture estimates when lower parameter values are used, and the two tension water storage parameters show higher soil moisture estimates at the lower end of the parameter spectrum. UZFWM displays the highest sensitivity for the lower parameter values, whereas the other four storage parameters are more sensitive in the higher range.

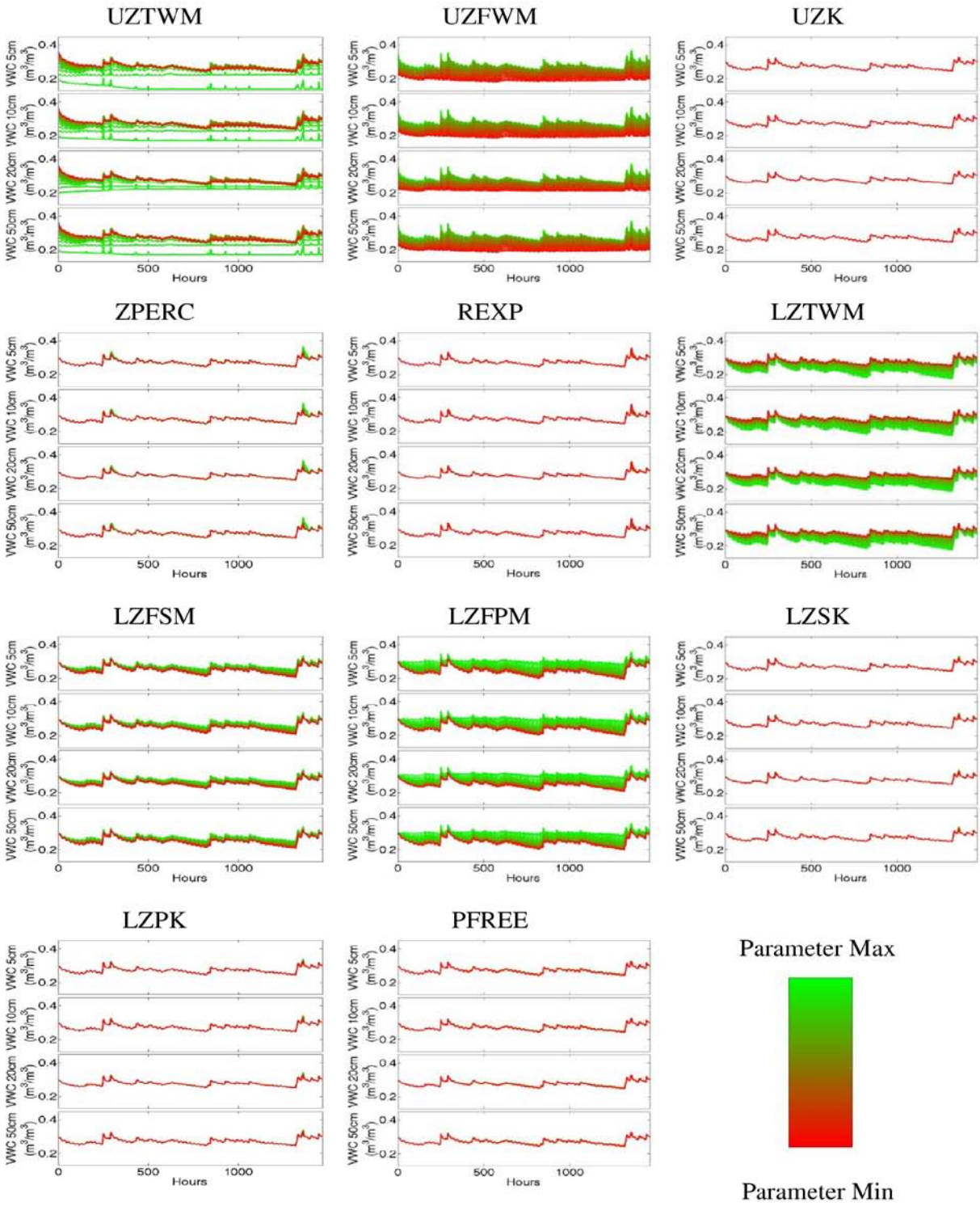

Figure 5-4 Soil moisture sensitivity at the four IFloodS sensor depths to individually changed parameters at the single pixel scale.

Sensitivity of discharge response to changing the same suite of parameters was also examined (Figure 5-5). For this experiment, single pixel runoff is considered to be "discharge," as there is no channel flow/channel routing during this step. Unlike the soil moisture signature, discharge exhibits some degree of sensitivity to all of the parameters under consideration. This figure demonstrates the potential complications of changing several SAC-HTET parameters simultaneously while using the discharge pattern as the evaluation tool for pursuing the "true" parameter values. For example, the discharge has an exceptionally similar response to the range of possible values for LZTWM, LZSK, and LZPK. The response for changing UZK also has the same shape, but opposite effect with changing parameter magnitude. It follows that there may not be sufficient information to adjust certain observed hydrograph behaviors via the proper parameter during discharge-based calibration.

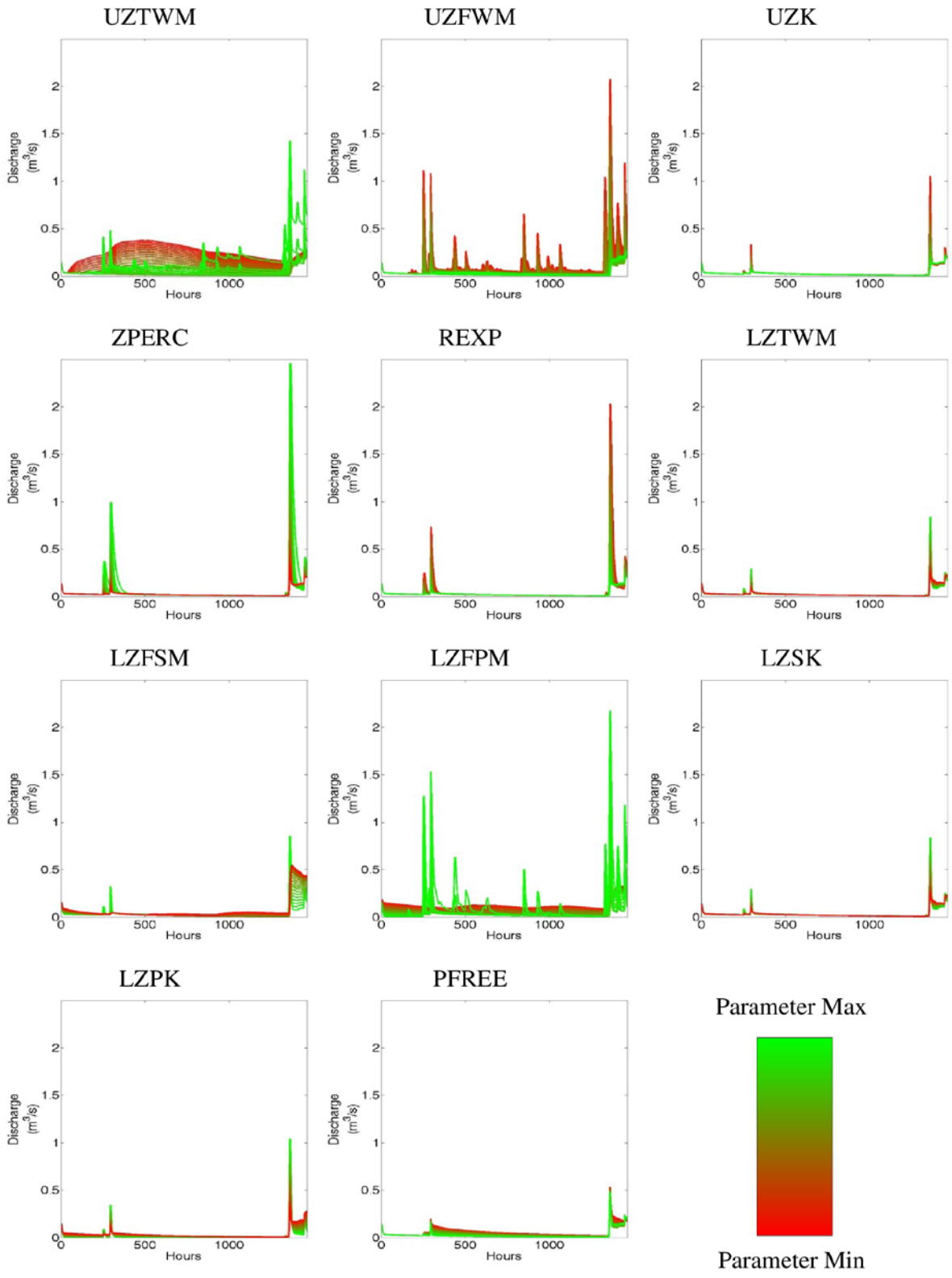

Figure 5-5 Discharge sensitivity to individually changed parameters at the single pixel scale.

To test the ability to recapture predefined parameter values at the pixel scale, SCE-UA calibration was implemented 15 separate times (five times for each of the three different precipitation intensity patterns). This was done for three cases, each defined by a different objective function. All 11 storage and release parameters were allowed to be calibrated and it was assumed that no prior information of the parameters was available so that the entire parameter space defined by the bounds in Table 1 can be explored.

For the first case, RMSE of the four observable soil moisture layers was used as the targeted objective function to minimize. Figure 5-6 shows the results of this soil moisture-based calibration in the normalized parameter space (grey markers). The results show that UZTWM, UZFWM, and LZTWM are well identified by soil moisture calibration when forced with any of the three precipitation intensities. The lower zone free storage parameters (LZFSM and LZFPM) showed a moderate spread in estimated parameter location from the 15 trials, and the remainder of the parameters showed a large spread, suggesting soil moisture-based calibration may be unreliable in their identification. The next case followed the same setup as the first with the exception of utilizing discharge RMSE for the objective function. This scenario shows some degree of spread in estimated parameters for all cases. However, it can be seen that for the highest precipitation intensity trials, UZK and UZTWM are consistently identified as being close to the true value. Given many intense precipitation events, UZTWM will likely reach its capacity multiple times, allowing for its identification, and since UZK controls the release of quickflow, it too has the necessary conditions for identification. Complimenting the rational of Hogue *et al.* (2000, 2003), who used low flow hydrograph segments to calibrate lower zone parameters, is the precise identification of LZFPM, LZFSM, and LZPK during low precipitation intensity trials.

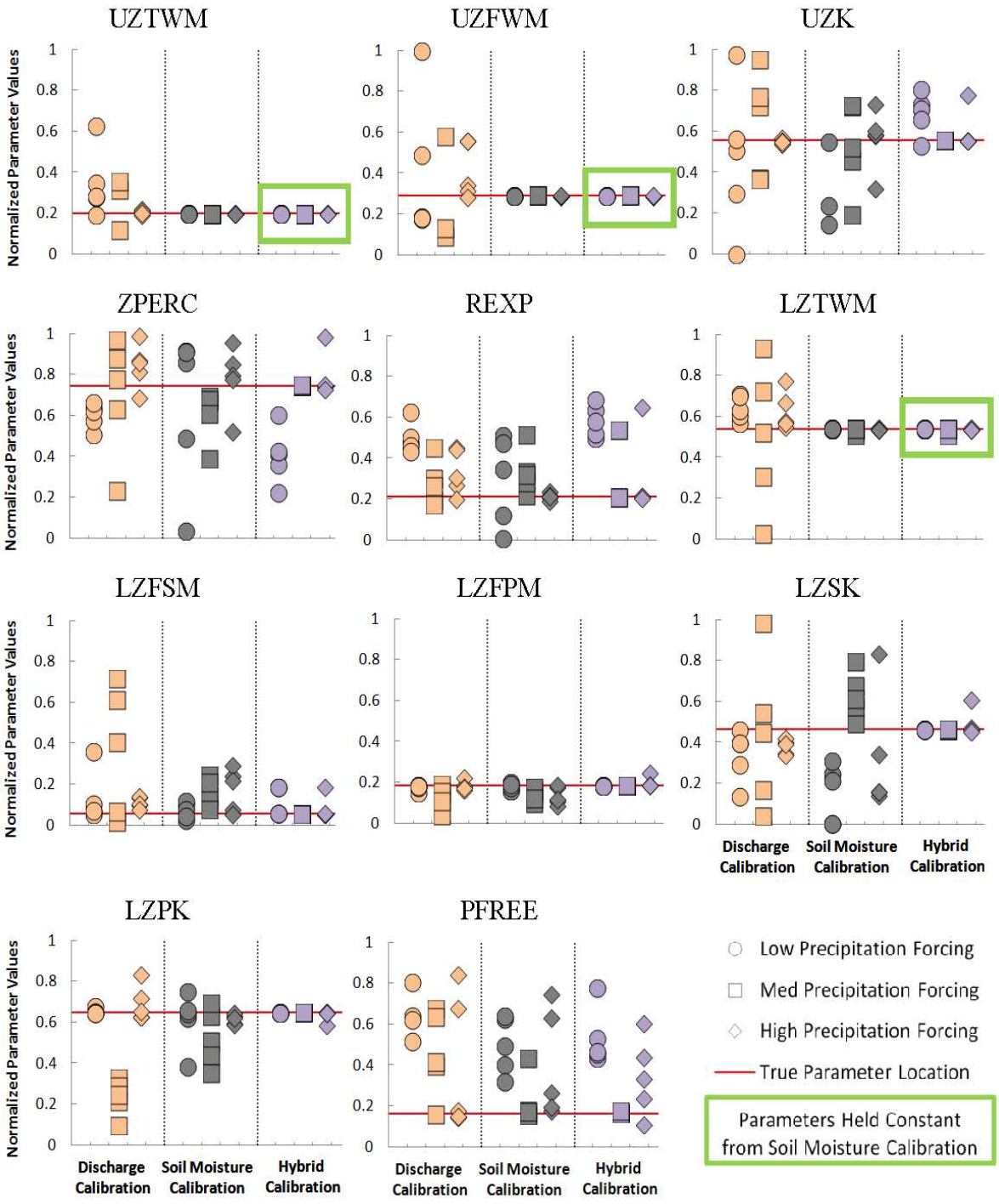

Figure 5-6 Parameter identification tests using synthetic data for a single pixel with discharge-based (orange), soil moisture-based (grey), and hybrid (purple) calibration schemes.

The results of these first two trials are consistent with the findings of Wanders *et al.* (2014), who found that discharge-based calibration was most useful for identifying parameters related to groundwater and routing whereas soil moisture-based calibration had the most positive effect on parameters related to land-surface processes. A similar connection is apparent in this experiment with the relationship soil moisture observations have to surficial processes and ET, as represented by the upper zone and tension water storages respectively. Furthermore, the discharge observations are able to provide information on groundwater and flow timing, as regulated by the lower zone and release parameters.

The final calibration case features a two-step hybrid scheme that attempts to combine the strengths of each of the first two cases. Step one is simply case one where all 11 parameters are allowed to be calibrated to find the lowest soil moisture RMSE. In step two, those parameters that are clearly and consistently identified by soil moisture calibration (i.e. UZTWM, UZFWM, and LZTWM) are held constant and the remaining 8 parameters are allowed to be calibrated according to discharge RMSE (purple markers in Figure 5-6). Compared to the first two cases, the hybrid scheme is able to more accurately and precisely identify the prescribed true parameter values with the exception of PFREE and low intensity precipitation forcing trials for UZK, REXP, and ZPERC.

5.5 Real-World Soil Moisture Experiment: IFloodS

The 20 HL-RDHM pixels collocated with the IFloodS soil moisture observations were individually calibrated using SCE-UA. Figure 5-7 highlights the simulated soil moisture time series statistics before and after each pixel was calibrated. Average improvement in

RMSE over *a priori* values after calibration is 33% with a range of 0-71%. Improvement in BIAS, CORR and R^2 is also seen for nearly all of the observation sites. All sites show an improvement of NSE over the uncalibrated simulations, although 8 of the 20 stations maintain a negative NSE value after calibration, which is unsatisfactory for this metric.

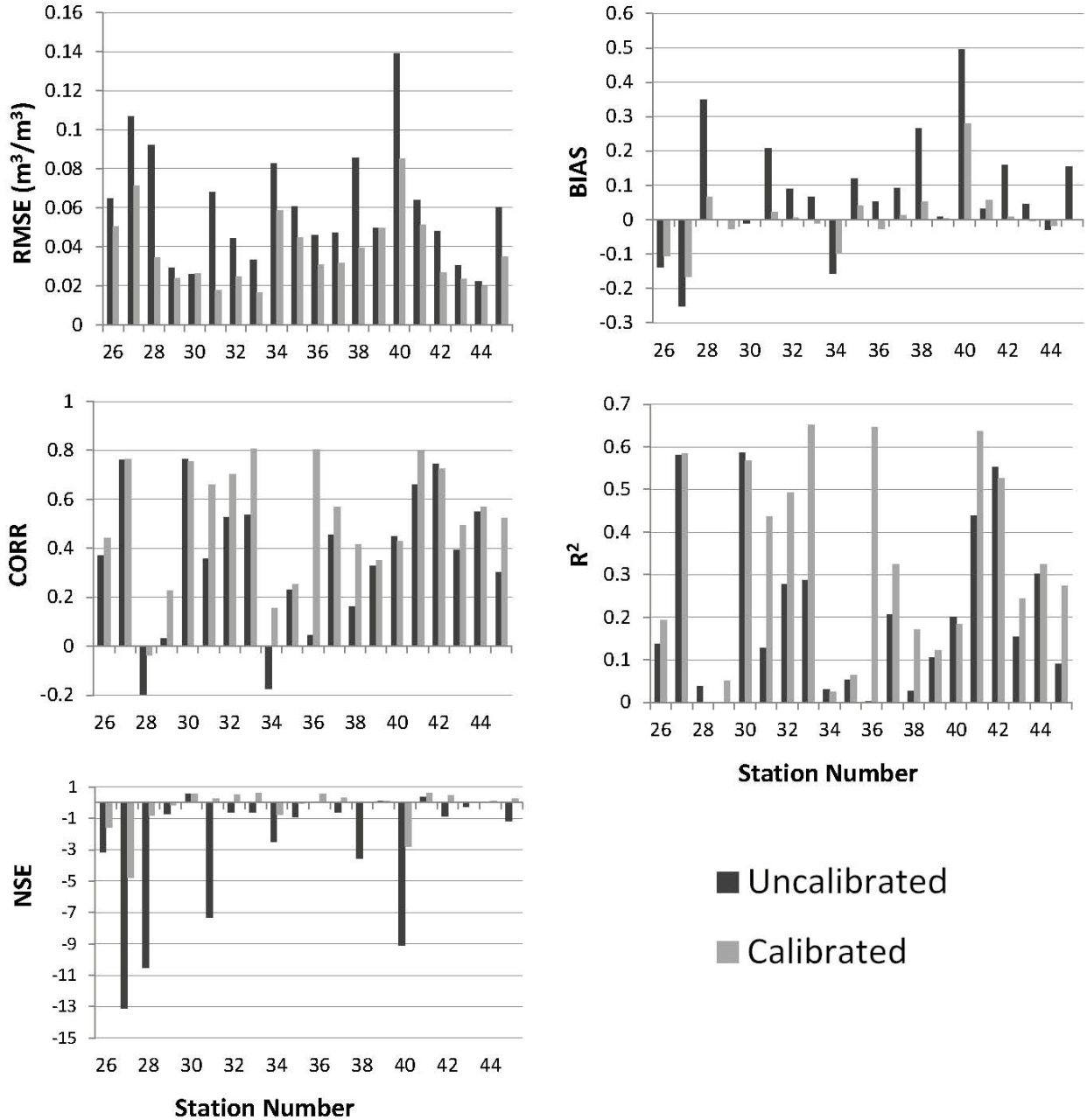

Figure 5-7 Statistics of simulated soil moisture at the 20 IFloodS sites before and after individual calibration.

Extending the single pixel calibration schemes outlined in the previous section to the full basin scale first requires interpolation of the calibration at the pixels collocated with soil moisture observations to the remaining pixels. Simulations using parameter sets derived from the three distribution methods outlined in section 2.2 were tested using the IFloodS soil moisture sites. To evaluate soil moisture simulation performance, calibrated parameters from 10 of the sites were used for distribution while the remaining 10 sites were reserved for validation. The observations were distributed to the full basin scale through inverse distance weighting, which makes it necessary to divide the stations for the two purposes as the segregation alleviates any advantage the InvDist method would gain from having a weight scheme corresponding perfectly with observation location. In addition to soil moisture simulations from the three soil moisture calibration-based schemes, simulated soil moisture using *a priori* parameters (UnCal) as well as the simulation results using outlet discharge-based only calibration (AutoCal) were evaluated.

The pixel-based RMSE for each of the five simulations is highlighted in Figure 5-8 along with a configuration of which sites were used for calibration/validation and an average RMSE of the 10 validation station simulations under each calibration scheme. The RMSE values presented represent an RMSE of the four soil moisture layers concatenated together into one time series.

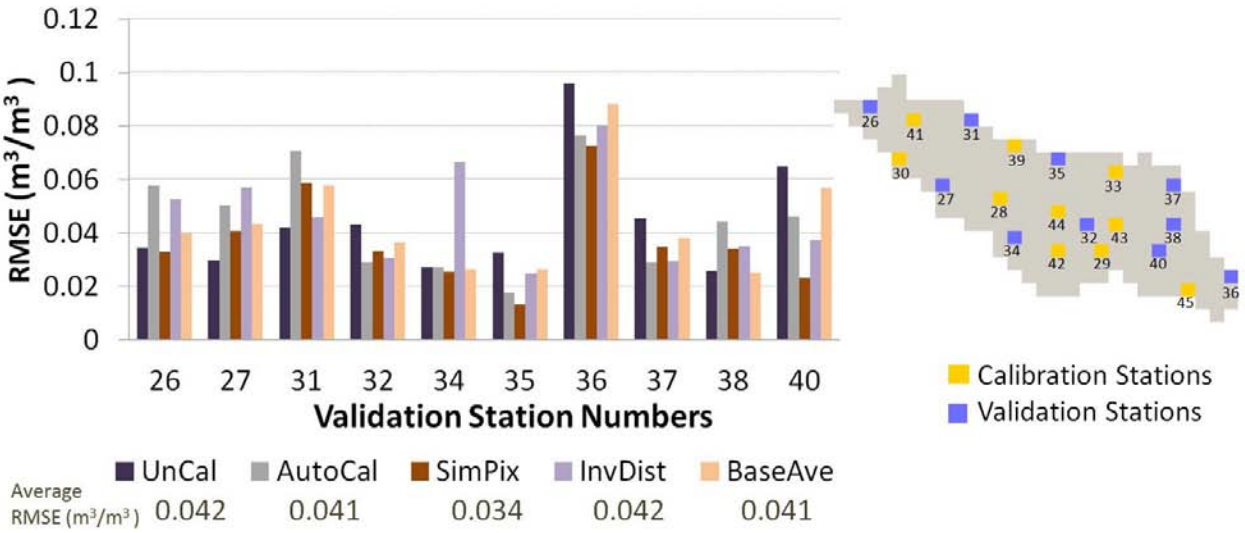

Figure 5-8 Left: Soil moisture RMSE at the 10 IFloodS sites used for validation. Right: Map of stations used for soil moisture calibration and validation.

Of the three soil moisture-based calibration experiments, the SimPix configuration showed the best performance in terms of RMSE. The central part of the basin exhibits a slight degradation for the SimPix RMSE compared to the UnCal run, but the high RMSE in the southeastern portion of the basin seen in the UnCal simulation experienced the greatest reduction for the SimPix run (Figure 5-9). The InvDist method showed some degradation in the western basin while the AutoCal and BaseAve simulations had higher RMSE in the northwestern portion of the basin compared to the UnCal simulation with a slight RMSE reduction in the southeastern region. Considering the collection of 10 validation pixels that are collocated with observations and are not subject to a possibly flawed form of observation interpolation, the SimPix method has the lowest RMSE at 5 out of the 10 station pixels, and has the lowest average RMSE of the 5 methods tested.

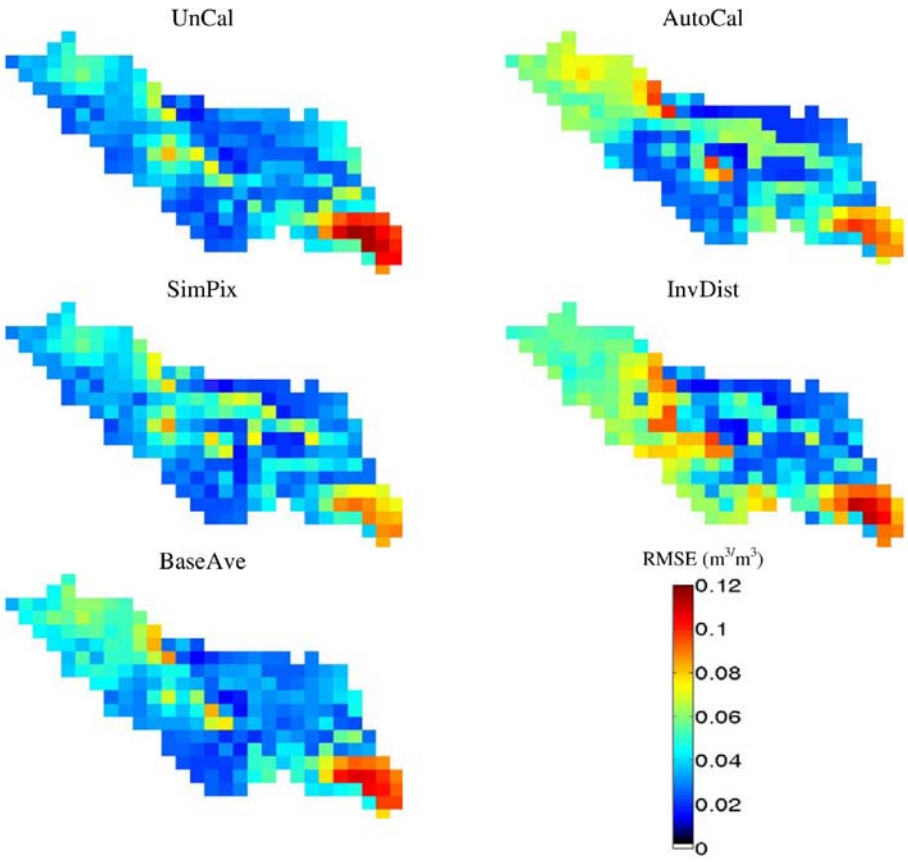

Figure 5-9 Distributed basin soil moisture RMSE using 10 IFloodS stations for calibration and 10 for validation.

Based on the results from the calibration distribution tests in section 5.1, the SimPix method was selected as the most suitable means for representing a distributed calibration through soil moisture. Therefore, the parameter grids for UZTWM, UZFWM, and LZTWM derived from the SimPix scheme were held constant and the remaining parameters were calibrated using discharge and SCE-UA to form the hybrid calibration scheme. This time, all 20 calibrated pixels were used in the parameter distribution to maximize the potential benefit of the soil moisture calibration. For both the discharge-based and hybrid

calibration methods, routing parameters were now allowed to be adjusted during the SCE-UA process.

Figure 5-10 shows the streamflow simulation results during the analysis period that follows the one year spin-up for the various calibration methods. In addition to the discharge-based and hybrid methods, the *a priori* (default) parameters and calibration using only soil moisture were evaluated.

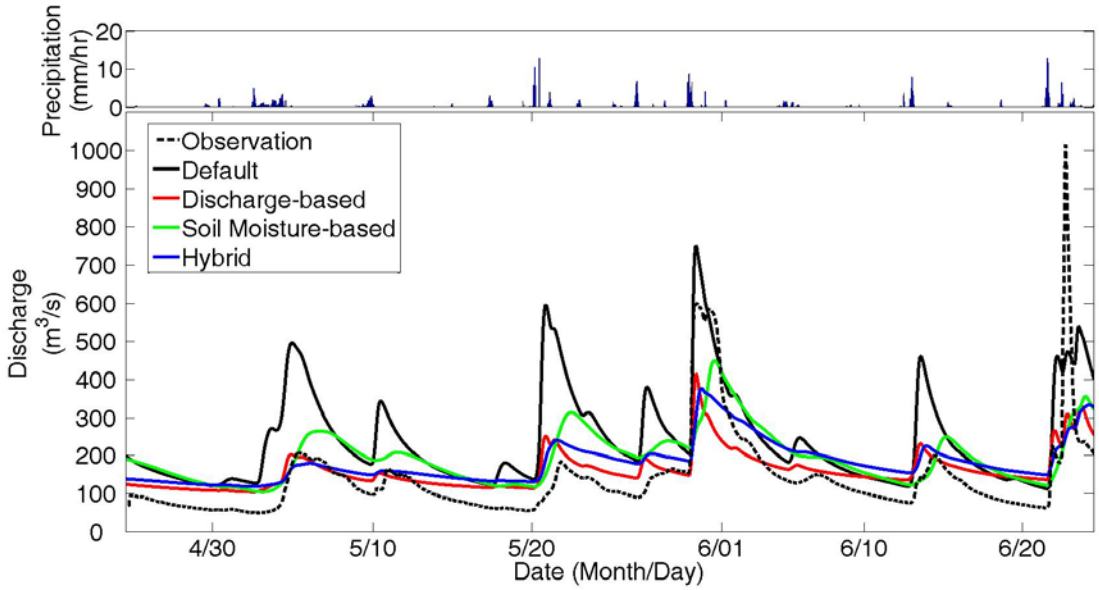

Figure 5-10 USGS observed discharge and model results for the 2013 IFloodS period used for calibration with basin average hourly precipitation from Stage IV.

Table 5-1 Statistics of simulated streamflow for the IFloodS period used for calibration

Event	Calibration Method	RMSE (m^3/s)	BIAS	CORR	R^2	NSE
2013 April-June	Default (uncalibrated)	136.14	0.73	0.71	0.51	-0.50
	Discharge-based	79.22	0.15	0.82	0.67	0.49
	Soil Moisture-based	97.91	0.40	0.70	0.49	0.23
	Hybrid	88.62	0.30	0.77	0.59	0.37

The most notable improvement over the *a priori* simulation exhibited by the other three simulations is in the reduction of bias (Table 5-1). The discharge-based, soil moisture-based and hybrid calibration simulations resulted in a 79%, 45% and 59% bias reduction respectively. It is worth noting, however, that all calibrated simulations now underestimate larger peaks while overestimating lower flows for most of the evaluation period. Marked improvement in hydrograph RMSE also resulted from all three calibration efforts with a 42%, 28%, and 35% RMSE reduction for the discharge-based, soil moisture-based and hybrid calibration simulations respectively. In terms of the RMSE performance of each simulation relative to one another, the discharge-based calibration showed the greatest improvement over the uncalibrated run followed by the hybrid calibration scheme, then the soil moisture-based calibration simulation. This pattern of improvement follows the degree of freedom each calibration scheme has compared to the others. An increase in CORR and R^2 for the discharge-based and hybrid calibration methods is shown, with the soil moisture-based calibration method CORR and R^2 being nearly equal to that of the simulation with default parameter sets. These results are aligned with the fact that the soil moisture-based calibration method does not address any routing parameters and thus does

not have the freedom to adjust hydrograph features such as peak timing like the discharge-based and hybrid schemes. The NSE of all calibrated simulations improved over the uncalibrated simulation, going from no predictive skill (negative NSE) to 0.49, 0.23 and 0.37 for discharge-based, soil moisture-based, and hybrid respectively.

Validation by means of streamflow was done to supplement the lack of soil moisture observations and to also investigate how each calibration process translates to other parts of the water cycle besides soil moisture. The three wet late spring/early summer events for the Turkey River Basin used include 1 April – 10 June 2009, 1 June – 30 July 2010, and 5 April – 5 July 2014 (Figure 5-11). In terms of observed hydrographs, the 2009 event featured a peak smaller than the magnitude of the calibration period peaks, and the 2010 and 2014 events showed peaks roughly equal to the calibration period.

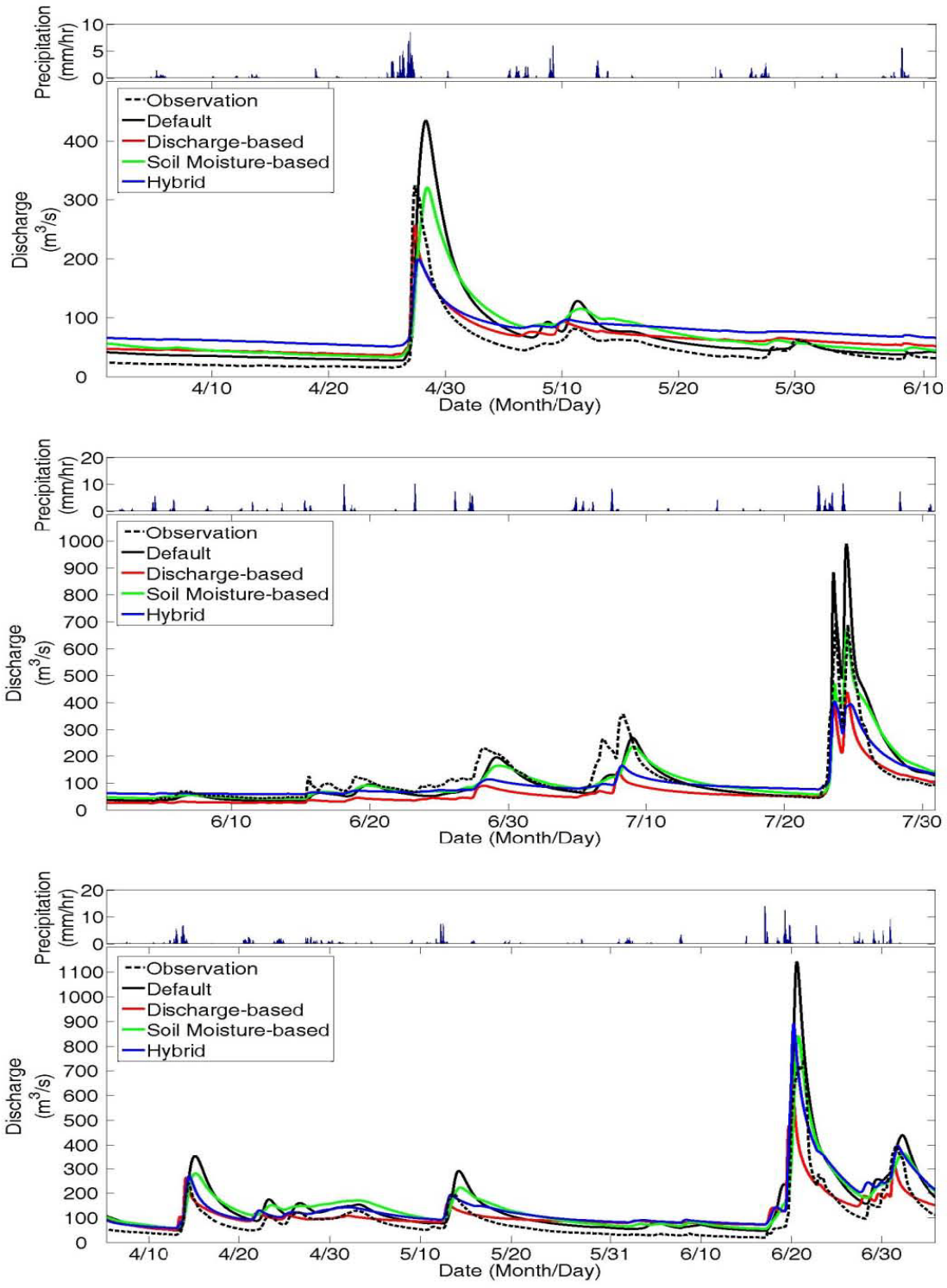

Figure 5-11 USGS observed discharge and model results for three validation events (from top to bottom: 2009, 2010, and 2014) with basin average hourly precipitation from Stage IV.

Table 5-2 Statistics of simulated streamflow for the three validation events

Event	Calibration Method	RMSE (m^3/s)	BIAS	CORR	R^2	NSE
2009 April 1-June 10	Default (uncalibrated)	41.08	0.46	0.87	0.75	0.01
	Discharge-based	22.94	0.39	0.98	0.96	0.69
	Soil Moisture-based	37.59	0.58	0.84	0.70	0.17
	Hybrid	37.62	0.68	0.95	0.90	0.17
2010 June 1 – July 30	Default (uncalibrated)	59.89	-0.01	0.90	0.82	0.63
	Discharge-based	69.46	-0.40	0.88	0.78	0.50
	Soil Moisture-based	50.23	-0.01	0.87	0.75	0.74
	Hybrid	55.19	-0.11	0.86	0.75	0.68
2014 April 5-June 5	Default (uncalibrated)	73.98	0.53	0.95	0.91	0.52
	Discharge-based	60.56	0.19	0.87	0.76	0.68
	Soil Moisture-based	64.34	0.53	0.95	0.89	0.63
	Hybrid	63.15	0.49	0.93	0.87	0.65

The simulations calibrated with soil moisture showed an 8-16% reduction in RMSE and the hybrid simulations had an 8-15% RMSE reduction (Table 5-2). For the discharge-based calibrated simulations, the RMSE shows an increase from the uncalibrated run for the 2010 event, but a 44% and 18% reduction for 2009 and 2014 respectively. No consistent bias reduction was achieved for any of the 3 calibration schemes. Correlations remained high for all three validation events and for all simulations calibrated or not (values ranged from 0.84 to 0.98) and R^2 values followed suit (values from 0.70 to 0.96). Gains from calibration over the uncalibrated run in terms of NSE were mostly positive save the discharge-based

scheme for the 2010 event. As all calibration efforts were based on RMSE, the improvement seen over the *a priori* set is anticipated in this metric. Not one calibration method can be classified as "superior" to the others in terms of streamflow simulation given the validation statistics, and in fact, the uncalibrated simulations show the best statistics in some instances.

5.6 Discussion

In this chapter, the use of concentrated *in situ* soil moisture observations for calibration of a distributed hydrologic model was investigated through the aid of data from the soil moisture network of the IFloodS field campaign. Calibration of HL-RDHM pixels collocated with the IFloodS soil moisture sensors was performed using the SCE-UA global search algorithm.

A suite of synthetic single-pixel experiments was carried out in order to 1) identify which conceptual parameters had the greatest impact on physically meaningful soil moisture and 2) establish with what procedures (if any) can prescribed conceptual parameters be retrieved using SCE-UA when forced with "perfect" precipitation and temperature and given "perfect" observations. Through a sensitivity analysis of the 11 storage and release parameters, it was found that simulated soil moisture estimates at the four observable physical soil layers were sensitive to changes of storages parameters (UZTWM, UZFWM, LZTWM, LZFPM, and LZFSM), whereas discharge showed some degree of sensitivity to changes in all storage and release parameters.

It was found that UZTWM, UZFWM, and LZTWM could be consistently and precisely identified in the ideal synthetic case using soil moisture RMSE as the objective function. The choice of objective function plays a role in which parameters were more identifiable, and because RMSE targets overall error, adjusting the storage parameters will be most effective in its reduction. It is anticipated that calibrating to an objective function that takes into account how rate of change of the soil moisture signature (i.e. CORR or NSE) would have more of an impact on some of the release parameters. The identifiably of these three parameters over the others also arises due in part to the location of the observations. With the top three observation layers within the upper zone, there are three time series providing information related to UTZWM and UZFWM. There is some information available to account for LZTWM with the deepest observation layer representing an area of the soil column between the upper and lower zones. It is likely that had the deepest observation layer not fallen partly in the area reserved for the lower zone, LZTWM may not have been as easily identified. This should be taken into consideration if only shallow observations are available. The development of the two step-hybrid calibration process led to more consistent parameter identification for all 11 storage and release parameters compared to calibration based solely on soil moisture or discharge.

This work also evaluated the ability of soil moisture-based calibrated simulations to capture streamflow patterns at the full basin scale. Several advantages of using soil moisture for calibration emerge from this experiment. Soil moisture-based calibration consistently showed improvement in simulated discharge RMSE for both calibration and validation experiments. As the soil moisture calibration had no connection to routing parameters, peak timing could not be improved, but peak magnitude was improved in most

cases. Additionally, the realized reduction in streamflow RMSE for soil moisture-based calibrated simulations was achieved even with a calibration time period that is a fraction of what has been deemed necessary for stability when calibrating with streamflow. Given that calibration was performed for a single, multi-month time period, events for validation through streamflow were selected to be similar to conditions during the IFloodS campaign. Yapo *et al.* (1996) conclude that approximately 8 years of observed streamflow are required for a relatively stable calibration. However, to satisfy the goal to calibrate within the limited time frame of the IFloodS campaign for both the soil moisture and the streamflow-based schemes, this recommendation is unattainable. Wet late spring/early summer events (similar to IFLoodS conditions) of three other years were selected for validation in an effort to compensate for the lack in the observation record. It is acknowledged that to expect high model performance, especially from the calibration schemes involving discharge, is unreasonable for conditions too dissimilar to the short calibration period. While much more investigation is needed, it may be so that less time is required to find stable parameters when calibrating with soil moisture. Given observations with a longer time period, it would be worth following the example of Yapo *et al.* (1996) to test what kind of calibration time length is required for soil moisture-based calibration. This would provide a more thorough account of how the dual calibration of soil moisture and streamflow can be merged together.

Even though RMSE was reduced for nearly all of the calibration/validation period calibrated streamflow simulations, the overall performance in terms of capturing streamflow patterns begs the question of whether or not any one (or any) of the calibration methods can be considered satisfactory. It is certainly worth exploring whether or not

extending the streamflow calibration period can enhance performance within the scope of the other evaluation metrics (particularly for the discharge-based and hybrid calibration schemes). Furthermore, this study focuses strictly on the minimization of RMSE during calibration, which puts emphasis on reducing magnitude of errors over matching hydrograph evolution. It is possible that a multi-variable, multi-objective approach that takes into account the shape of the observed hydrograph compared to the simulation (NSE, for example) could enhance the performance of the streamflow simulated with calibrated parameters. While it is not clear from this experiment that soil-moisture based or hybrid calibration of HL-RDHM can greatly enhance streamflow prediction, the added information provided by soil moisture in the calibration process improves soil moisture estimates in a distributed sense rather than scalar improvement of the basin average. Individual pixel calibration had an average improvement of 33% reduction of RMSE. This feature allows for adjustment in the representation of basin heterogeneity if needed, which is a feat that discharge-based only calibration is unable to achieve. Other studies have shown improvement in streamflow simulation using soil moisture for calibration (i.e. Campo *et al.,* 2006; Wanders *et al.*, 2014), so this objective appears attainable through additional exploration.

When considering the possibilities of calibrating ungauged basins or those with limited observations, soil moisture-based calibration becomes an attractive option. This is especially relevant with the availability of global soil moisture observations through satellite-based estimates such as SMAP and SMOS. However, when considering satellite retrieved soil moisture, certain adaptations may be necessary due to the fact that only the

top layer soil moisture is available (which may reduce meaningful connection to LZTWM) and that the temporal resolution is on the daily to multi-day scale rather than hourly.

The complex geology/topography of the basin itself presents a unique challenge in the context of this experiment. High soil moisture RMSE values in the southeast part of the Turkey River Basin (Figure 10) reveal themselves in a pattern that coincides well with the highly karstic areas highlighted in Figure 2. Currently, HL-RDHM is not formulated to directly take into account the effect that these types of formations have. It is possible that having distributed observations such as soil moisture to calibrated to can help separate out problematic areas and define proper parameter values at least in areas that are less karstic and conform to the type of processes HL-RDHM can handle. This is opposed to the alternative of trying to distinguish what portion of the hydrograph behavior is attributed to the karstic regions.

Several conclusions can be drawn from this study. Synthetic experiments fed with perfect observations revealed that three storage parameters were strongly identifiable through soil moisture calibration and that all eleven parameters were more recoverable when used in a two-step hybrid calibration with observed discharge than calibration to either variable individually. This process is supported by the findings of Bastidas et al. (1999), who found not only a reduction of computational effort when only sensitive parameters are calibrated, but also miniscule degradation in the quality of the calibration. Of the three calibration distribution methods, it was found that the SimPix method, defined on the principle of a given uncalibrated pixel's similarity to the calibrated pixels, was the most appropriate for use in distributing the calibration effects. The inclusion of soil moisture observations in the

calibration process was able to consistently reduce RMSE and increase NSE of simulated streamflow, which discharge-based calibration could not do given such a short calibration period. However, the mixed results of other evaluation metrics suggest that more investigation is needed before soil-moisture based calibration can be confidently used by itself to improve streamflow estimation with HL-RDHM. The following chapter includes a more in-depth investigation into the role that soil moisture observations play in terms of streamflow given a longer observation period but a sparser network.

5.7 Chapter 5 Synopsis

- Synthetic experiments revealed 3 model parameters that can be precisely and accurately identified with soil moisture-based calibration if given "perfect" forcing.
- A method called "SimPix" was developed as an appropriate way to distribute calibration information to pixels without observed soil moisture information, which tests showed superior to simple averaging and inverse distance weighted interpolation.
- Soil moisture-based calibration allows for a more reliable description of internal basin processes than traditional outlet streamflow-based calibration, but cannot account for hydrograph features that are routing dependant (i.e. peak timing).
- A two-step hybrid calibration procedure was introduced to combine benefits of soil moisture-based calibration and outlet streamflow-based calibration.

Chapter 6. Impact of Soil Moisture-Based Calibration and Data Assimilation on Streamflow

6.1 Introduction

While Chapters 4 and 5 highlight the improvement in simulated soil moisture that result from assimilating soil moisture observations and calibrating using soil moisture observations respectively, the question as to what happens to simulated streamflow with each of these strategies has not yet been fully addressed. This is a pivotal piece to investigate given that primary purpose of HL-RDHM is to predict streamflow. In this chapter, both methods are employed individually for the same basin and time domain to assess the individual effects on modeled streamflow.

The Russian River Basin in California is used for this investigation given the record of available data over the region. As seen in figure 6-1, 2013 was the least active out of the years with HMT soil moisture data in terms of streamflow, thus it was deemed unsuitable for a streamflow evaluation (whereas the soil moisture signals in Chapter 4 were appropriately dynamic for this year). Since 2012 shows more active streamflow activity at the beginning and end of the year, it was selected for the simulation year.

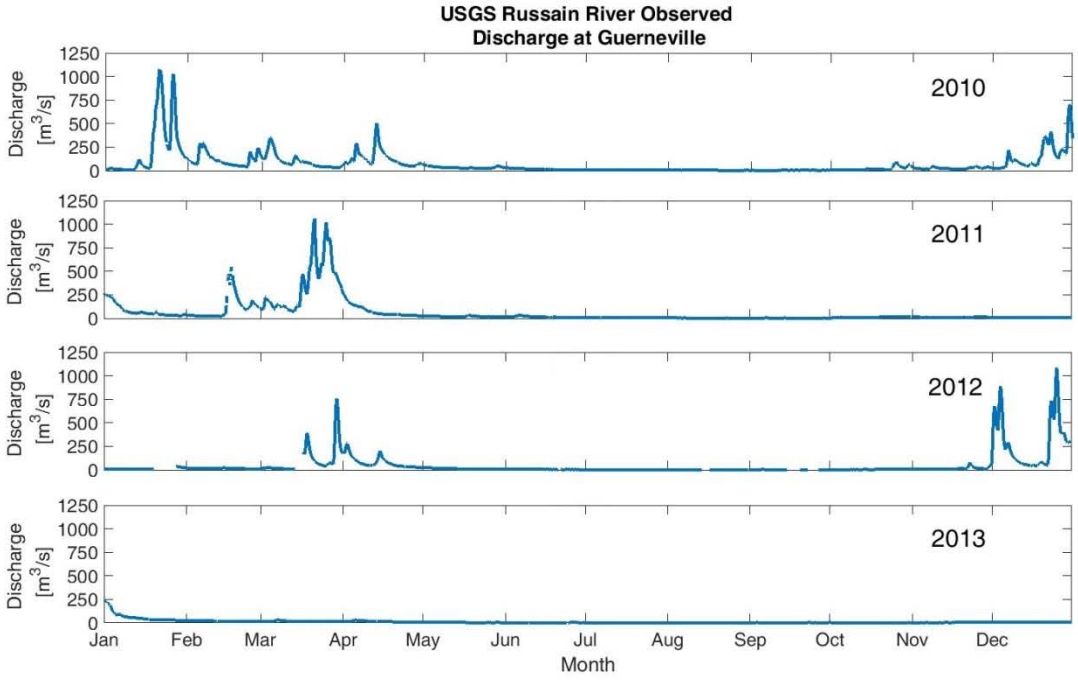

Figure 6-1 USGS observed discharge by year, 2010 – 2014.

For both sets of simulations, 2011 is used as spin-up period. The model is forced with CNRFC estimates of precipitation and temperature.

6.2 Data Assimilation Impact on Streamflow

In previous chapters, HL-RDHM was run in either an "unconnected" mode, where calculations are performed on a pixel by pixel basis (data assimilation experiments) or in a "connected" mode, where the routing scheme is activated and the model can output an outlet hydrograph (calibration experiments). In order to investigate the impacts of soil moisture data assimilation on outlet streamflow, the two options are woven together. To allow inclusion of observations that would be masked out during a connected run (either they are downstream of the USGS gauge location, or slightly outside of the basin boundary), the soil moisture data assimilation step is carried out in a rectangular window that

encompasses all HMT observations. Following the update step in the EnKF, only the ensemble mean of the states at each pixel is fed into the connected run to estimate streamflow. Additionally, the simulation uses the set of *a priori* parameter grids provided by the National Weather Service.

Figure 6-2 depicts the streamflow simulation with soil moisture assimilated compared to the control run and the USGS observations. The two wet seasons of interest are also magnified for clarity.

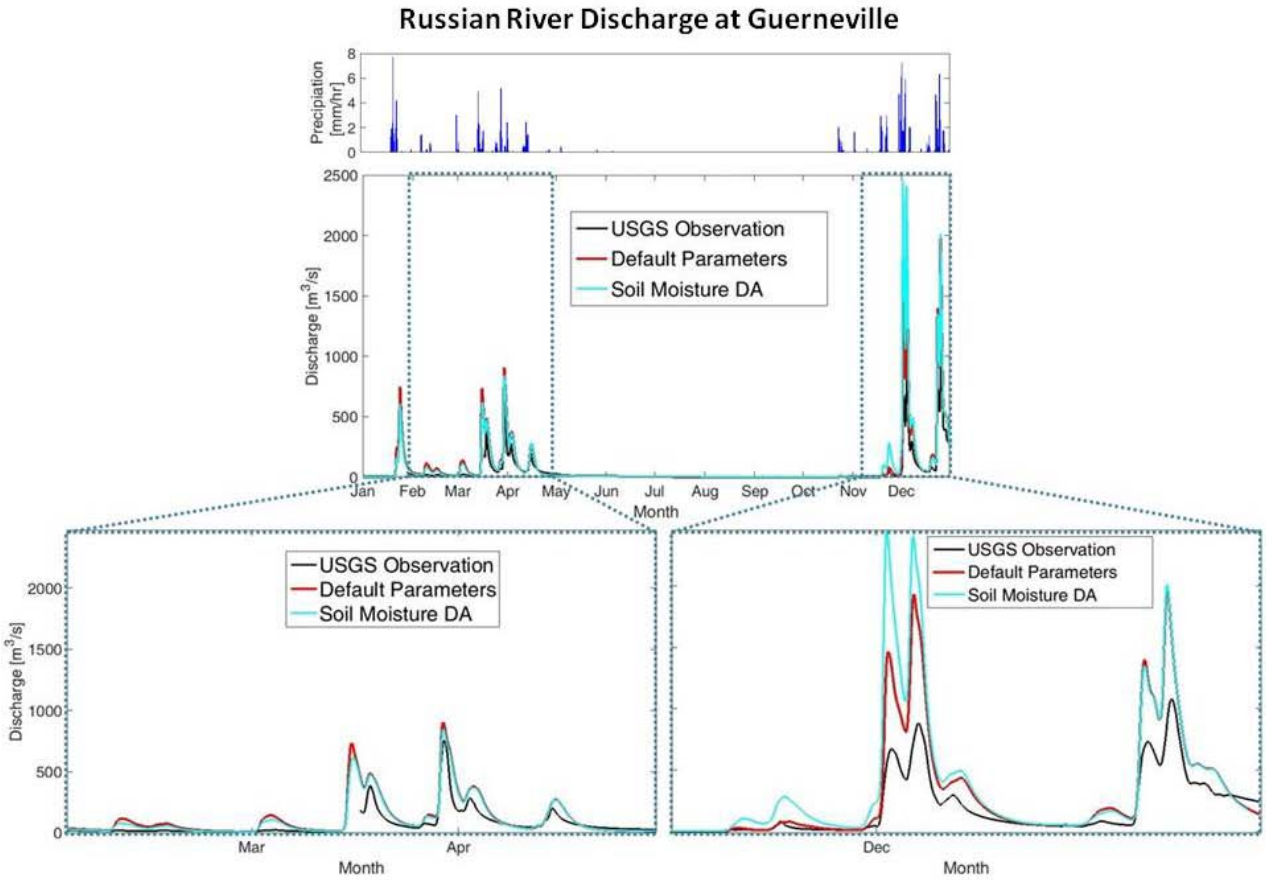

Figure 6-2 Simulated streamflow with 10 cm depth HMT soil moisture observations

assimilated at a daily frequency.

It can be seen that the early year event shows little difference in streamflow between the simulations with and without shallow layer soil moisture assimilated. Table 6-2 supports this notion with a slight increase in all performance metrics, save correlation which remained unchanged from the control run. However, the Nov-Dec simulations paint a different picture with a large increase in bias, particularly obvious in the first part of December. Although the correlation degrades for this time period, it is likely the nearly 60% increase in bias that sends the predictive skill from an already meager 0.02 NSE to an unacceptable -1.18.

6.3 Calibration Impact on Streamflow

Following the calibration strategy introduced in Chapter 5, HL-RDHM is calibrated using the 7 HMT soil moisture observation sites in the Russian River Basin. The SimPix method is used spread the calibrated information to the remaining pixels. For this case study, the 10 cm depth is used for calibration. Because deep layer observations are unavailable in this basin, only the upper zone storage parameters (UZTWM and UZFWM) are targeted. Furthermore, the hybrid calibration scheme introduced in Chapter 5 is not implemented in this chapter, as the benefits of incorporating streamflow observations in the calibration process has already been established and is not the goal of this investigation.

As in section 6.2, the year 2012 is used as for evaluation due to its relatively "active" streamflow signal compared to the other years coinciding with available HMT observations. Consequentially, 2011 is used for the calibration year as well as a spin-up

period for 2012 evaluation period. For a sanity check, Table 6-1 summarizes the simulated soil moisture RMSE improvement for the 2011 calibration period as well as the 2012 validation period. From the validation period RMSE, it can be seen that the calibration consistently improves the simulation save for the PTV site. It is worth noting that PTV site did not become active until April of 2011, therefore the calibration period is missing three months of the wet season. This may explain why the benefits of the calibration do not carry over to the validation period at this site.

Table 6-1 Uncalibrated and calibrated parameters of HMT soil moisture sites based on 2011 calibration period

SITE ID		UZTWM	UZFWM	RMSE Cal [frac]	% Reduction Cal	RMSE Val [frac]	% Reduction Val
WLS	Uncalibrated	29.14	28.00	0.11		0.13	
	Calibrated	110.50	62.45	0.09	11.7	0.11	14.3
PTV	Uncalibrated	50.03	37.00	0.17		0.14	
	Calibrated	74.23	5.00	0.17	0.1	0.15	-8.0
HLD	Uncalibrated	37.57	30.00	0.12		0.09	
	Calibrated	71.13	70.23	0.08	28.1	0.06	38.9
LSN	Uncalibrated	46.40	42.00	0.12		0.15	
	Calibrated	91.02	89.12	0.11	6.2	0.12	21.4
CZC	Uncalibrated	29.71	28.00	0.09		0.12	
	Calibrated	63.11	72.04	0.07	29.2	0.09	26.8
HBG	Uncalibrated	49.68	44.00	0.07		0.07	
	Calibrated	31.52	27.49	0.06	3.3	0.07	0.8
ROD	Uncalibrated	45.24	40.00	0.10		008	
	Calibrated	79.35	54.67	0.10	0.2	0.08	5.5

The results for the validation period (2012) for the soil moisture-based calibration simulations are shown in Figure 6-3. From here, it is evident that the calibration was able to decrease the streamflow peak overestimation for both wet periods in 2012. While the largest peak in the end of May is slightly underestimated in the calibrated simulation, it is

still closer to observed peak than the control run. Peaks of all other events in the evaluation period were overestimated in the simulation with *a priori* parameters, and while they were still overestimated in the calibrated run, they were brought much closer to observation. This is particularly evident in the RMSE and bias reduction of the late year event, both of which decreased by 40%.

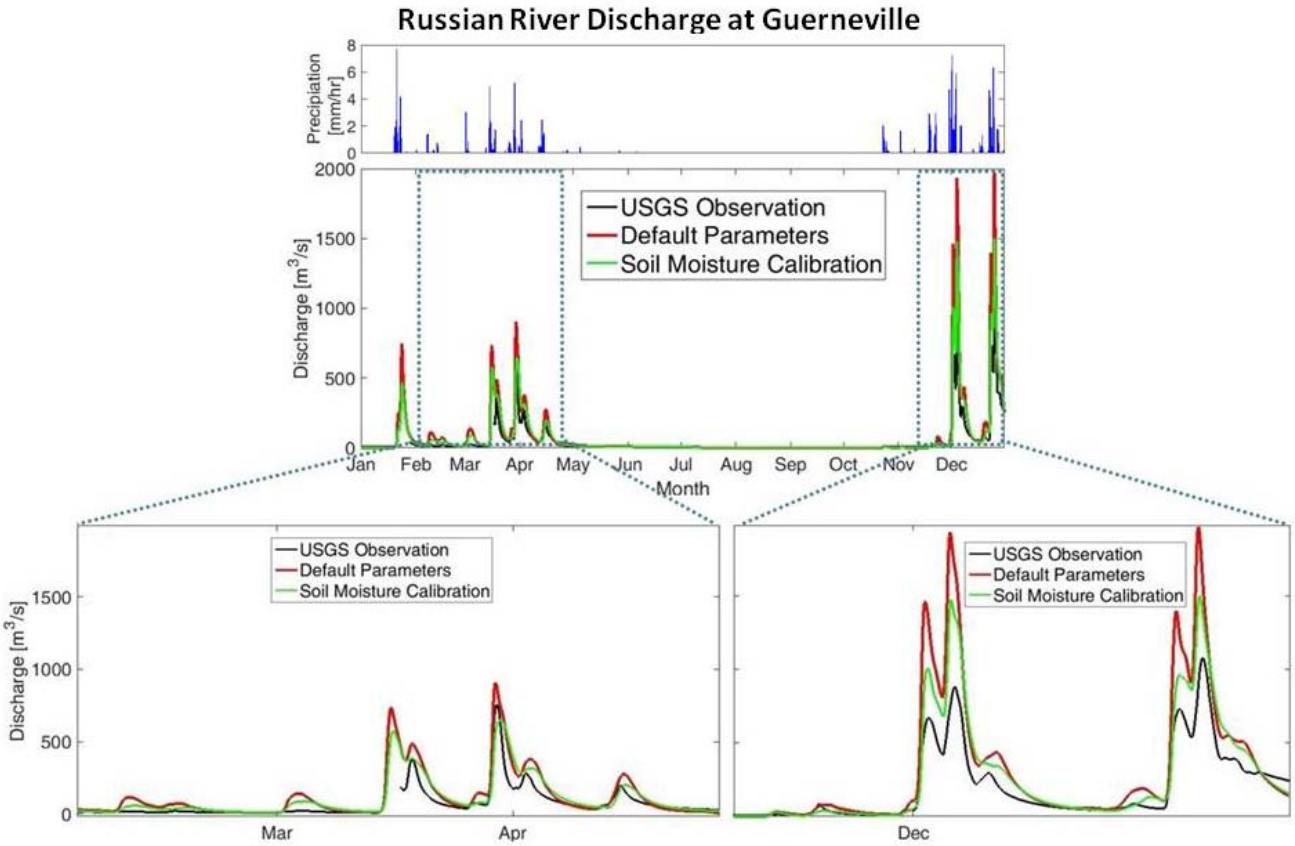

Figure 6-3 USGS observed discharge and soil moisture-based calibrated model results for wet season validation events in 2012

Overall, the soil moisture-based calibration scheme using only 7 HMT observations and the SimPix calibration spreading routine described in the previous chapter had a largely positive effect on outlet streamflow for the Russian River Basin. While not presented here, it is anticipated that implementation of the hybrid scheme that utilizes outlet streamflow to calibrate

other HL-RDHM parameters would further improve the simulation. Although the correlation is already quite high for the Nov – Dec 2012 period with a value of 0.98, calibration of routing parameters would likely improve the Feb – Apr 2012 correlation, which decreased from 0.95 to 0.90 from the control run. Nevertheless, the high performance of the simulation using only soil moisture to calibrate relevant parameters is encouraging for ungauged basin applications.

6.4 Dual-Use Impact on Streamflow

As a final test, the simulation was run employing both uses of soil moisture observations simultaneously. Daily assimilation of 10 cm HMT soil moisture observations was performed on a model run using the calibrated parameter sets. All other conditions were kept the same as in sections 6.3 and 6.4. Figure 6-4 depicts the results of dual-use of soil moisture observations for streamflow simulation.

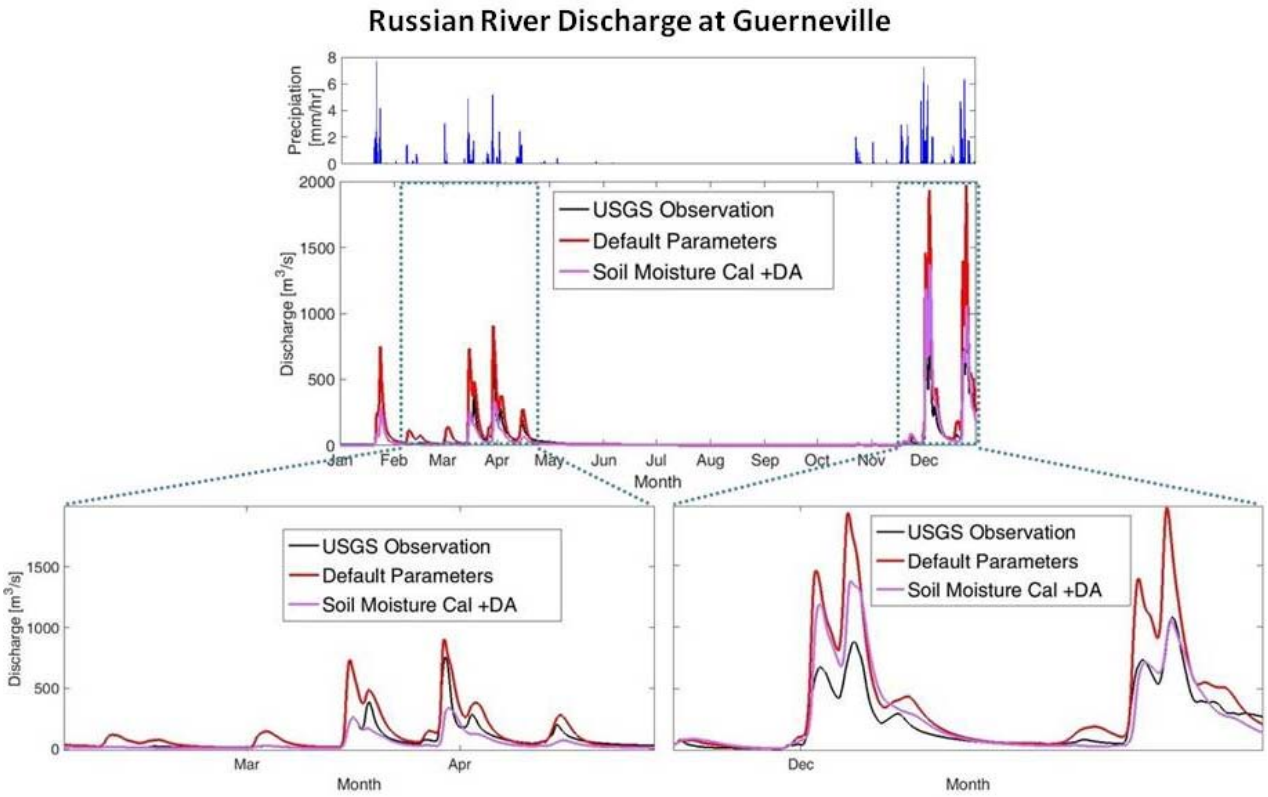

Figure 6-4 USGS observed discharge and results for model run using soil moisture-based calibration and daily soil moisture observation data assimilation

The combined use of soil observations for calibration and data assimilation together show some encouraging results in streamflow simulation. When compared to the observed USGS hydrograph, the simulation is able to accurately capture the hydrograph shape of the second wet period for December, 2012. The dual-use simulation of the wet period during the beginning of December also shows an improvement over the control run. However, for the smaller magnitude discharge in March-April, the calibrated simulation with data assimilation now underestimates the observed discharge, and by a large margin for the larger peaks.

Comparing statistical metrics of the dual-use simulation to the individual trial methods and the control run, performance is split between the evaluation periods of 2012. For the early year Feb

– April period, combining the tactics of soil moisture based calibration and data assimilation has an overall positive effect over the control run (a NSE increase from 0.56 to 0.59), with the exception of the correlation decreasing from 0.95 to 0.88. Furthermore, this period does not improve in the other metrics more than each of the tactics do individually (save for a slightly smaller magnitude bias than the assimilation only simulation). For the Nov – Dec 2012 event, the combination approach boasts the best performance metrics except for a 0.94 correlation that was edged out by the soil moisture-based calibration's correlation of 0.98.

Table 6-2 Statistical summary for streamflow simulations with assimilated 10 cm depth soil moisture and soil moisture-based calibration

Event	Simulation Method	RMSE [m^3/s]	BIAS	CORR	NSE
2012 Feb 1 – April 30	Default (uncalibrated)	67.92	0.57	0.95	0.56
	Daily Soil Moisture Assimilation	59.49	0.46	0.95	0.66
	Soil Moisture-based Calibration	61.01	0.41	0.90	0.65
	Soil Moisture-based Calibration + Assimilation	65.61	-0.43	0.88	0.59
2012 Nov 1 – Dec 31	Default (uncalibrated)	229.89	0.62	0.96	0.02
	Daily Soil Moisture Assimilation	344.56	0.99	0.91	-1.18
	Soil Moisture-based Calibration	139.01	0.37	0.98	0.64
	Soil Moisture-based Calibration + Assimilation	123.92	0.21	0.94	0.72

6.5 Discussion

In this chapter, the effects of adding soil moisture information via data assimilation, calibration, or both, were investigated in terms of outlet streamflow. Considering each of

the two methods individually, the calibration approach provides a more stable improvement in simulated hydrograph behavior compared to the data assimilation approach. While the dual-use simulation arguably showed the best statistics in the Nov – Dec period, improvement over the control run during the less intense events in the Feb – Apr period was not as considerable as each of the two methods individually.

One immediate issue that comes to mind when assimilating soil moisture without accounting for the adjustments is that an inevitable water imbalance arises in the model space. However the bigger issue that reveals itself in this study is that in the late 2012 event, the soil moisture state throughout the basin is pushed to a higher level of saturation, which consequently generates more runoff. This amplified runoff generation results in flow peaks that are higher than the control model run and further away from the USGS observation. In the dual-use simulation, this detrimental effect of assimilation is dramatically dampened, suggesting the importance of proper parameter specification prior to assimilation.

6.6 Chapter 6 Synopsis

- A large effort to interconnect the unconnected and connected mode options of HL-RDHM was successfully undertaken.
- Effects that including soil moisture information via data assimilation and/or calibration has on streamflow are examined in the Russian River Basin using HMT *in situ* soil moisture observations.
- Calibration efforts consistently improved streamflow simulations, whereas data assimilation efforts only aided the simulation when applied to a calibrated model.

Chapter 7. Discussion and Conclusions

7.1 Summary

Although challenging to measure and model, soil moisture is a key player in the hydrologic cycle. In the context of hydrologic modeling, it is one of the primary influencing factors in the partitioning of precipitation into infiltration and runoff. In this research, methods to incorporate soil moisture information in ways fitting for an operational distributed hydrologic model were investigated. Through a combined effort of synthetic and real-world data experiments, strategies to maximize the benefits of observed soil moisture use to improve simulated soil moisture were introduced. Furthermore, since the primary purpose of the model in question is to capture an outlet hydrograph, the effect of these strategies on streamflow simulations was investigated. The developed calibration scheme showed more stable performance and was deemed a necessary step in capturing observed streamflow, although both the assimilation of soil moisture and soil moisture-based calibration improved soil moisture estimates.

The following objectives outlined in Chapter 1 are addressed throughout the dissertation:

> ***1) Establish a common ground on which highly localized in situ observations, large-scale satellite-based estimates (10's of km), and medium-scale model pixels (~4km) representations of soil moisture can be compared.***

To address the issues that arise when comparing these drastically different spatial scales, a method for describing multi-scale estimates of soil properties (SMAX and SWLT) was introduced. While the HL-RDHM simulations can be and were normalized to a saturation

ratio internally within the model, the two observation sources require defining representative upper and lower bounds (saturation and wilting point, respectively) of the dynamic soil moisture space. This allowed volumetric soil moisture estimates to be transformed into a saturation ratio space to help regulate the comparison. Instead of asking "what is the exact volumetric water content" when comparing observations/simulations, the question becomes "how wet is the soil at the scale of interest." The idea that "how wet?" is more comparable at various scales than "how much?" is the basis for transforming to saturation ratio space.

A new strategy that leverages available observations and computed boundaries for the dynamic soil moisture space was introduced. This strategy not only has the capability to generalize basic soil properties at virtually any lateral scale, but it is flexible enough to be used both in heavily monitored areas and those with no observations (and anywhere in between).

Due to an apparent seasonal bias in the SMOS data, a second preprocessing step of CDF matching was performed. This rounded off the procedure to bring highly localized *in situ* probe observations, HL-RDHM pixel simulations, and coarse resolution SMOS pixels to a common ground for comparison.

2) Construct an effective assimilation framework suitable for updating conceptual model states using observed soil moisture.

In the face of challenges relevant to soil moisture data assimilation including ensemble member underdispersiveness and observations not existing at every model pixel, a

framework for a double EnKF was established in order to update all model pixels in a given time step. Measures to address underdispersiveness while respecting the expected and desired tendency for smaller variances after precipitation events and prolonged dry periods were introduced. These included implementation of a traditional inflation factor and a newly developed tracking and resampling technique. To distribute innovations of model states collocated with observations to unobserved pixels, a second EnKF step was employed. This followed a shift in the roles of the updated states in the first step to the observation ensemble for the second step.

These strategies were tested in the Russian River Basin using HMT *in situ* observations and SMOS satellite-based observations. Results show improvement in soil moisture simulation over model control runs at both stages of HMT evaluation (collocated tests and site removal tests). Tests utilizing SMOS show modest improvement with one of the seven sites (HBG) appreciably worsening with assimilation.

As discussed in De Lannoy *et al.* (2007), effectiveness within Kalman filtering is often restricted to a time length that the corrected states are dampened. This time length can be short, which seems to be the case when examining the soil moisture assimilation results presented in Chapter 4. Furthermore, Draper *et al.* (2011) show that when a hydrologic model was deprived of observations for an extended period of time (because of frozen ground in the winter in their study), the model land-surface drifted back to its original, biased condition. They go on to suggest a bias-aware strategy rather than using soil moisture observations to correct on-the-go through assimilation.

3) Assess the value that comes with incorporating soil moisture information into the calibration processes of a distributed hydrologic model.

In pursuit of this objective came several unique contributions of this work. First, a sensitivity analysis using a synthetic experiment revealed which parameters within HL-RHDM can be accurately and precisely identified using soil the observed soil moisture signal as a calibration guide. Second, a method based on the level of similarity between a calibrated and uncalibrated pixel called SimPix was developed to spread calibration efforts to unobserved pixels. This structure allowed the assumption of the standard calibration method for HL-RDHM that states the spatial relationship of *a priori* parameters is correct to be loosened. Such an enhancement helps to improve simulations, especially in areas where soil surveys may be incorrect or incomplete without having additional knowledge of the physical characteristics of the area that only an expert of that basin would have. Finally, a two-step hybrid calibration procedure that targets specific soil storage parameters with the soil moisture signal and then calibrates remaining parameters with observed discharge was introduced. When observed discharge is available for calibration, its inclusion helps to correct for hydrograph features that soil moisture cannot easily correct such as peak timing (typically adjusted with routing parameter calibration).

Even though the two study basins in this dissertation are monitored with a stream gauge at the basin outlet, calibration using basin internal information, like soil moisture, provides the ability to correct for disaggregated processes. In the Russian River Basin, for example, a modeling challenge is presented by two large reservoirs in addition to a water diversion project that brings water from outside of the basin into the northeastern part of the basin

(http://cw3e.ucsd.edu/FIRO/firo_introduction.html). Currently, HL-RDHM does not have the capability to account for such structures that influence the behavior of the outlet hydrograph. Until those capabilities are included, the soil-moisture based calibration prevents the soil storage parameters from being used to compensate for discrepancies between the modeled and observed hydrograph.

4) Investigate what improvements (if any) can be achieved in terms of streamflow prediction when soil moisture observations are assimilated into a distributed hydrologic model.

The aftermath effects on streamflow of adding soil moisture information through data assimilation, calibration, and dual-use was explored. Simulations using only data assimilation showed a largely detrimental effect of increasing outlet streamflow when the control run already overestimated. The soil moisture-based calibration produced outlet streamflow simulations that were consistently an improvement over the control run. When the two strategies were combined, results were even better than the two methods separately for the largest event examined. Although results of the dual-use test were not as impressive as the individual strategies for the less intense event, there was still improvement over the control run. This suite of experiments suggests that soil moisture data assimilation has the potential to improve streamflow simulation, but it is a necessary condition that the parameters first be properly specified. Therefore, soil moisture-based calibration appears to be a more reliable method for enhancing streamflow simulation and perhaps even a prerequisite to soil moisture data assimilation to prevent detrimental effects on streamflow.

7.2 Recommendations for Future Research

The work here suggests that using soil moisture observations for calibration of a distributed hydrologic model may be more fruitful than data assimilation, especially in regards to improving simulated streamflow. However, the effort in this area largely focuses on use of *in situ* soil moisture networks. In the future, implementation of the newly developed hybrid calibration scheme using satellite-based soil moisture may provide similar benefits to areas not graced with soil moisture probe networks. Testing of a suitable objective function is a necessary precursor for such a study, since the satellite observations are only available on a daily basis at best (versus the hourly frequency of the *in situ* observations used here). Such testing is particularly of interest in areas subject to rapidly changing soil conditions such as intense rainstorms and/or quickly drying soils. These scenarios present phenomena that are particularly important in characterizing free water storages, yet observation frequencies of 1-3 days may not be able to resolve such events.

Based on the outcomes of this work, it is not recommended that the role of satellite-based soil moisture observations take the form of data assimilation in an operational streamflow model. While minimal improvement in soil moisture simulations was achieved with satellite-based soil moisture data assimilation, the corresponding improvement in streamflow was highly conditional on proper characterization of parameters. Therefore, further efforts geared towards incorporating satellite-based soil moisture observations into a distributed hydrologic model may be better suited for calibration.

As briefly mentioned in Chapter 4, another direction of future research related to this work may be the implementation of a localization scheme during the second (lateral innovation) EnKF step. Particularly when using satellite-based retrievals, localization may help to remove spurious correlations between locations that are largely unrelated. While execution of localization in data assimilation has largely been the focus of atmospheric studies (Hamill *et al.,* 2001; Hautekamer and Mitchell, 2001; Petrie 2008; Bishop and Hodyss, 2009; and Anderson, 2012), several studies have begun investigating localization techniques within land surface (De Lannoy *et al.,* 2007; Sahoo *et al.,* 2013) and hydrologic models (Rassmussen *et al.*, 2015). It is anticipated that such an effort could enhance the double EnKF assimilation process discussed in this work.

REFERENCES

Alfieri, L., P. Claps, P. D'Odorico, F. Laio, and T. M. Over, 2007: An analysis of soil moisture feedback on convective and stratiform precipitation, *Journal of Hydrometeorology,* **9**, 280-291.

Anderson, E., 1973: National Weather Service River Forecast System-Snow Accumulation and Ablation Model, *Technical Memo.* NOAA, Silver Spring, MD, pp. 217.

Anderson, J., 2012: Localization and sampling error correction in Ensemble Kalman Filter data assimilation, *Monthly Weather Review,* **140**(7), 2359-2371.

Anderson, J. L. and S. L. Anderson, 1999: A Monte Carlo implementation of the nonlinear filtering problem to produce ensemble assimilations and forecasts, *Monthly Weather Review,* **127**, 2741-2758.

Bastidas, L., H.V. Gupta, S. Sorooshian, W.J. Shuttleworth, and Z.L. Yang, 1999: Sensitivity Analysis of Land-Surface Schemes Using Multi-Criteria Methods. *Special GCIP Issue, Journal of Geophysical Research*, **104**(D16), 19481-19490.

Bishop, C. H., and D. Hodyss, 2009: Ensemble covariances adaptively localized with ECO-RAP. Part 2: A strategy for the atmosphere. *Tellus,* **61A,** 97-111.

Bergström, S., G. Lindström, and A. Pettersson, 2002: Multi-variable parameter estimation to increase confidence in hydrological modeling, *Hydrological Processes,* **16,** 413-421.

Brazil, L. E., and M. D. Hudlow, 1981: Calibration procedures used with the National Weather Service Forecast System, *Water and Related Land Resources*, pp. 457-466.

Brocca, L., S. Hasenauer, T. Lacava, F. Melone, T. Moramarco, W. Wagner, W. Dorigo, P. Matgen, J. Martinez-Fernandez, P. Llorens, J. Latron, C. Martin, and M. Bittelli, 2011: Soil moisture estimation through ASCAT and AMSR-E sensors: An intercomparison and validation study across Europe, *Remote Sensing of Environment,* **115**(2011), 3390-3408.

Brock, F., K. Crawford, R. Elliott, G. Cuperus, S. Stadler, H. Johnson, and M. Eilts, 1995: The Oklahoma Mesonet: A technical overview, *Journal of Atmospheric and Oceanic Technology,* **12**, 5-19.

Campo, L., F. Caparrini, and F. Castelli, 2006: Use of multi-platform, multi-temporal remote-sensing data for calibration of a distributed hydrological model: an application in the Arno basin, Italy, *Hydrological Processes,* **20**, 2693-2712.

Cao, W., W. Bowden, T. Davie, and A. Fenemor, 2006: Multi-variable and multi-site calibration and validation of SWAT in a large mountainous catchment with high spatial variability, *Hydrological Processes,* **20**, 1057-1073.

Chen, F., W. T. Crow, P. J. Starks, and D. N. Moriasi, 2011: Improving hydrologic predictions of a catchment model via assimilation of surface soil moisture. Advances in Water Resources, **34**, 526-536.

Chen, F., K. Mitchell, J. Schaake, Y., Xue, H-L. Pan, V. Koren, Q. Duan, M. Ek, and A. Betts, 1996: Modeling of land surface evaporation by four schemes and comparison with FIFE observations, *Journal of Geophysical Research,* **101**(D3), 7251-7268.

Chu, W., X. Gao, and S. Sorooshian, 2010: Improving the shuffled complex evolution scheme for optimization of complex nonlinear hydrological systems: Application to the calibration of the Sacramento soil-moisture accounting model, *Water Resources Research,* **46**, W09530.

Clausnitzer, V., J. W. Hopmans, and D. R. Nielsen, 1992: Simultaneous scaling of soil water retention and hydraulic conductivity curves, *Water Resources Research,* **28**(1), 19-31.

Cooper, V., V. Nguyen, and J. Nicell, 1997: Evaluation of global optimization methods for conceptual rainfall-runoff model calibration, *Water Science and Technology,* **36**(5), 53-60.

Cooper, V., V. Nguyen, and J. Nicell, 2007: Calibration of conceptual rainfall-runoff models using global optimization methods with hydrologic process-based parameter constraints, *Journal of Hydrology,* **334**(3-4), 455-466.

Crow, W. T. and D. Ryu, 2009: A new data assimilation approach for improving runoff prediction using remotely sensed soil moisture retrievals, *Hydrology and Earth System Sciences,* **13**, 1-16.

Das, N., B. Mohanty, M. Cosh, and T. Jackson, 2008: Modeling and assimilation of root zone soil moisture using remote sensing observation in Walnut Gulch Watershed during SMEX04, *Remote Sensing of Environment,* **112**(2008), 415-429.

De Lannoy, G., R. Reichle, P. R. House, V. R. N. Pauwels, and N. E. C. Verhoest, 2007: Correcting for forecast bias in soil moisture assimilation with the ensemble Kalman filter, *Water Resources Research*, **43**, W09410.

Demir, I., H. Conover, W. Krajewski, B. Seo, R. Goska, Y. He, M. McEniry, S. Graves, and W. Petersen, 2015: Data Enabled Field Experiment Planning, Management, and Research using Cyberinfrastructure, *Journal of Hydrometerology,* **16,** 1155-1170.

Desilets, D., Zreda, M., and T. P. A. Ferre, 2010: Nature's neutron probe: Land surface hydrology at an elusive scale with cosmic rays, *Water Resources Research,* **46**, W11505.

Downer, C. and F. Ogden, 2004: GSSHA: Model to simulate diverse stream flow producing processes, *Journal of Hydrologic Engineering*, **9**(3), 161-174.

Draper, C., J. F. Mahfouf, J. C. Calvet, E. Martin, and W. Wagner, 2011: Assimilation of ASCAT near-surface soil moisture into the SIM hydrological model over France, *Hydrol. Earth Syst. Sci.,* **15**, 3829-3841.

Drusch, M., E. F. Wood, and H. Gao, 2005: Observation operators for the direct assimilation of TRMM microwave imager retrieved soil moisture, *Geophysical Research Letters,* **32**, L15403.

Duan, Q., S. Sorooshian, and V. Gupta, 1992: Effective and efficient global optimization for conceptual rainfall-runoff models, *Water Resources Research,* **28**(4), 1015-1031.

Duan, Q., S. Sorooshian, and V. Gupta, 1994: Optimal use of the SCE-UA global optimization method for calibrating watershed models, *Journal of Hydrology,* **158**, 265-284.

Entekhabi, D., E. G. Njoku, P. E. O'Neill, K. H. Kellogg, W. T. Crow, W. N. Edelstein, J. K. Entin, S. D. Goodman, T. J. Jackson, J. Johnson, J. Kimball, J. R Piepmeier, R. D. Koster, N. Martin, K. C. McDonlad, M. Moghaddam, S. Moran, R. Reichle, J. C. Shi, M. W. Spencer, S. W. Thurman, L. Tsang, and J. Van Zyl. 2010: The Soil Moisture Active Passive (SMAP) mission. *Proceedings of the IEEE,* **98**(5), 704-716.

Evensen, G., 1994: Sequential data assimilation with a nonlinear quasi-geostrophic model using Monte Carlo methods to forecast error statistics, *Journal of Geophysical Research – Oceans* **99**, 10143-10162.

Fares, A., R. Awal, J. Michaud, P-S. Chu, S. Fares, K. Kodama, M. Rosener, 2014: Rainfall-runoff modeling in a flashy tropical watershed using the distributed HL-RDHM model, *Journal of Hydrology,* **519**, 3436-3447.

Flores, A. N., R. L. Bras, and D. Entekhabi. 2012: Hydrologic data assimilation with a hillslope scale-resolving model and L band radar observations: Synthetic experiments with the ensemble Kalman filter. *Water Resources Research,* **48**, W08509.

Ford, T. W., A. D. Rapp, S. M. Quiring, and J. Blake, 2015: Soil moisture-precipitation coupling: observations from the Oklahoma Mesonet and underlying physical mechanisms, *Hydrology and Earth System Sciences,* **19**, 3617-3631.

Franz, K.J. and L. Karsten, 2013: Calibration of a distributed snow model using MODIS snow covered area data, *Journal of Hydrology*, **494**, 160-175. doi:10.1016/j.jhydrol.2013.04.026

Frye, J. D. and T. L. Mote, 2009: Convection initiation along soil moisture boundaries in the southern Great Plains, *Monthly Weather Review,* **138**, 1140-1141.

Gan, T. and G. Biftu, 1996: Automatic calibration of conceptual rainfall-runoff models: optimization algorithms, catchment conditions, and model structure, *Water Resources Research,* **32**(12), 3513-3524.

Gijsman, A. J., S. S. Jagtap, and J. W. Jones, 2002: Wading through a swamp of complete confusion: how to choose a method for estimating soil water retention parameters for crop models, *Europ. J. Agronomy,* **18(**2003), 77-106.

Gupta, H.V., L. Bastidas, S. Sorooshian, W.J. Shuttleworth, and Z.L. Yang, 1999: Parameter Estimation of a Land-Surface Scheme Using Multi-Criteria Methods, *Special GCIP Issue of the Journal of Geophysical Research-Atmospheres,* **104**(D16), 19491-19503.

Gupta, H., S. Sorooshian, and P. Yapo, 1998: Toward improved calibration of hydrologic models: Multiple and noncommensurable measures of information, *Water Resources Research*, **34**(4), 751-763.

Hamill, T. M, J. S. Whitaker, and C. Snyder, 2001: Distance-dependent filtering of background error covariance estimates in an Ensemble Kalman Filter, *Monthly Weather Review,***129** (11), 2776-2790.

Han, E., V. Merwade, and G. C. Heathman, 2012: Implementation of surface soil moisture data assimilation with watershed scale distributed hydrological model, *Journal of Hydrology*, **416-417**, 98-117.

Hautekamer, P. L. and H. L. Mitchell, 1998: Data assimilation using an Ensemble Kalman Filter technique, *Monthly Weather Review,* **126** (3), 796-811.

Hautekamer, P. L. and H. L. Mitchell, 2001: A sequential Ensemble Kalman Filter for atmospheric data assimilation, *Monthly Weather Review,* **129**, 123-137.

Hogue, T., S. Sorooshian, and H. Gupta, 2000: A multistep automatic calibration scheme for river forecasting models, *Journal of Hydrometeorology,* **1**(6), 524-542.

Hogue, T., H. Gupta, S. Sorooshian, and C. Tomkins, 2003: A multi-step automatic calibration scheme for watershed models, *Calibration of Watershed Models: water Science and Application Series,* No. 6, American Geophysical Union, 165-174.

Hsu, K. J. Li, and S. Sorooshian, 2012: To improve model soil moisture estimation in arid/semi-arid region using in situ and remote sensing information, *Paddy and Water Environment,* **10**(3), 165-173.

Immerzeel, W., and P. Droogers, 2008: Calibration of a distributed hydrological model based on satellite evapotranspiration, *Journal of Hydrology,* **349**, 411-424.

Isenstein, E., S. Wi, Y. Ethan Yang, and C. Brown, 2015: Calibration of a distributed hydrologic model using streamflow and remote sensing snow data, *World Environmental and Water Resources Congress* **2015,** 973-982.

Ivanov, V., S. Fatichi, G. Jenerette, J. Espeleta, P. Troch and T. Huxman, 2010: Hysteresis of soil moisture spatial heterogeneity and the "homogenizing" effect of vegetation, *Water Resources Research,* **46**, W09521.

Keefer, T., M. Moran, and G. Paige, 2008: Long-term meteorological and soil hydrology database, Walnut Gulch Experimental Watershed, Arizona, United States, *Water Resources Research,* **44**, W05S07.

Kerr, Y. H, P. Waldteufel, P. Richaume, J-P. Wigneron, P. Ferrazzoli, A. Mahmoodi, A. A. Bitar, F. Cabot, C. Gruhier, S. E. Juglea, D. Leroux, A. Mialon, and S. Delwart, 2012: The SMOS Soil Moisture Retrieval Algorithm, *Geoscience and Remote Sen.,* **50**(5), 1384-1403.

Kerr, Y., P. Waldteufel, J.-P. Wigneron, S. Delwart, F. Cabot, J. Boutin, M.-J. Escorihuela, J. Font, N. Reul, C. Gruhier, S. Enache Juglea, M. Drinkwater, A. Hahne, M. Martín Neira, & Susanne Mecklenburg. 2010: The SMOS mission: New tool for monitoring key elements of the global water cycle. *Proc. of the IEEE,* **98***,* 666-687.

Koren, V., F. Moreda, and M. Smith, 2008: Use of soil moisture observations to improve parameter consistency in watershed calibration, *Physics and Chemistry of the Earth*, Parts A/B/C 33(17-18), 1068-1080.

Koren, V., S. Reed, M. Smith, Z. Zhang, D.J. Seo, 2004. Hydrology laboratory research modeling system (HL-RMS) of the US National Weather Service. *Journal of Hydrology*, **291**, 297–318.

Koren, V., Smith, M., Cui, Z. 2014. Physically-based modifications to the Sacramento Soil Moisture Accounting Model. Part A: modeling the effects of frozen ground on the runoff generation process, *Journal of Hydrology,* **519**, 3475-3491.

Koren, V., Smith, M., Cui, Z., Cosgrove, B. 2007. Physically-based modifications to the Sacramento Soil Moisture Accounting Model: modeling the effects of frozen ground on the rainfall-runoff process. NOAA Technical Report NWS 52.

Koren, V., M. Smith, Z. Cui, B. Cosgrove, K. Werner, and R. Zamora, 2010: Modification of Sacramento Soil Moisture Accounting Heat Transfer Component (SAC-HT) for enhanced evapotranspiration. NOAA Technical Report NWS 53.

Koren, V., M. Smith, and Q. Duan, 2003: Use of a priori parameter estimates in the derivation of spatially consistent parameter sets of rainfall–runoff models, Q. Duan, H. Gupta, S. Sorooshian, A. Rousseau, and R. Turcotte, *Calibration of Watershed Models: Water Science and Application Series*, No. 6, American Geophysical Union, 239-254.

Kosugi, K., and J. W. Hopmans, 1998: Scaling water retention curves for soils with lognormal pore-size distribution, *Soil Sci. Soc. Am. J.,* **62**, 1496-1505.

Krajewski, W., B. Seo, R. Goska, I. Demir and M. Elsaadani, 2013: Precipitation datasets the GPM Iowa Flood Studies (IFLoodS) field experiment. *EGU General Assembly 2013*, Vienna, Austria. [Available online at http://meetingorganizer.copernicus.org/EGU2013/EGU2013-11303.pdf].

Lee, H., D. Seo, and V. Koren, 2011: Assimilation of streamflow and in situ soil moisture data into operational distributed hydrologic models: Effects of uncertainties in the data and initial model soil moisture states, *Advances in Water Resources,* **34**(2011), 1597-1615.

Liang, X. and Z. Xie, 2001: A new surface runoff parameterization with subgrid-scale soil heterogeneity for land surface models, *Advances in Water Resources,* **24**(2001), 1173-1193.

Libra, R., 2005: Living in Karst. Iowa Field Conference for Public Policy Makers October 11-12, *Iowa Geological Survey Guidebook Series,* **25**, 48 p.

Merlin, O., A. Chehbouni, G. Boulet, and Y. Kerr, 2006b: Assimilation of disaggregated microwave soil moisture into a hydrologic model using coarse-scale meteorological data, *Journal of Hydrometeorology*, **7**, 1308-1322.

Moriasi, D. N.; Arnold, J. G.; Van Liew, M. W.; Bingner,R. L.; Harmel, R. D.; Veith, T. L., 2007: Model Evaluation Guidelines for Systematic Quantification of Accuracy in Watershed Simulations, *Transactions of the ASABE*, **50** (3), 885–900.

National Weather Service (NWS), 2011: Hydrology Laboratory-Research Distributed Hydrologic Model (HL-RDHM) User Manual V. 3.2.0.

Nguyen, P., A. Thorstensen, S. Sorooshian, K. Hsu, and A. AghaKouchak, 2015: Flood forecasting and inundation mapping using HiResFlood-UCI and near real-time satellite precipitation data: the 2008 Iowa flood, *Journal of Hydrometeorology,* **16**, 1171-1183.

Petrie, R., 2008: Localization in the Ensemble Kalman Filter, *Ms. Thesis, Department of Meteorology, University of Reading, UK.*

Rasmussen, J., H. Madsen, K.H. Jensen, and J. C. Refsgaard, 2015: Data assimilation in integrated hydrological modeling using ensemble Kalman filtering: evaluating the effect of ensemble size and localization on filter performance, *Hydrol. Earth Syst. Sci.,***19**, 2999-3013.

Reichle, R., and R. D. Koster, 2004: Bias reduction in short records of satellite soil moisture, *Geophys. Res. Lett.,***31**, L19501.

Reichle, R. H., D. B. McLaughlin, and D. Entekhabi, 2002a: Hydrologic data assimilation with the ensemble Kalman filter. *Monthly Weather Revue*, **130,** 103-114.

Rientjes, T., L. Muthuwatta, M. Bos, M. Booij, and H. Bhatti, 2013: Mulit-variable calibration of a semi-distributed hydrological model using streamflow data and satellite-based evapotranspiration, *Journal of Hydrology,* **505**, 276-290.

Robinson, D., 1990: The United States Cooperative Climate-Observing systems: Reflections and recommendations, *Bulletin American Meteorological Society,* **71**(6), 826-831.

Santanello Jr., J., C. Peters-Lidard, M Garcia, D. Mocko, M. Teschler, M. Moran, and D. Thoma, 2007: Using remotely-sensed estimates of soil moisture to infer soil texture and hydraulic properties across a semi-arid watershed, *Remote Sensing of Environment,* **110**(1), 79-97.

Sahoo, A. K., G. J. M. De Lannoy, R. H. Reichle, and P. R. House, 2013: Assimilation and downscaling of satellite observed soil moisture over the Little River Experimental Watershed in Georgia, USA, *Advances in Water Resources,* **52**(2013), 19-33.

Saxton, K. E., and W. J. Rawls, 2006: Soil water characteristic estimates by texture and organic matter for hydrologic solutions, *Soil Sci. Soc. Am. J.,* **70**, 1569-1578.

Saxton, K.E., W.J. Rawls, J.S. Romberger, and R.I. Papendick, 1986: Estimating generalized soil water characteristics from texture, *Trans. ASAE,* **50**, 1031-1035.

Schaefer, G., M. Cosh, and T. Jackson, 2007: The USDA Natural Resources Conservation Service Soil Climate Analysis Network (SCAN), *Journal of Atmospheric and Oceanic Technology*, **24**, 2073–2077.

Schwaller, M., and K. Morris, 2011: A ground validation network for the Global Precipitation Measurement Mission, *Journal of Atmospheric and Oceanic Technology,* **28**, 301-319.

Scott, B., T., Ochsner, B. Illston, C. Fiebrich, J. Basara, and A. Sutherland, 2013: New soil property database improves Oklahoma Mesonet soil moisture estimates, *Journal of Atmospheric and Oceanic Technology,* **30**(11), 2585-2595.

Shafii, M., and F. De Smedt, 2009: Multi-objective calibration of a distributed hydrological model (WetSpa) using a genetic algorithm, *Hydrology and Earth System Sciences,* **13,** 2137-2149.

Simmons, C. S., D. r. Nielsen, and J. W. Biggar, 1979: Scaling of field-measured soil water properties, *Hilgardia,* **47**(4), 77-174.

Smith, M., Koren, V., Zhang, Z., Zhang, Y., Reed, S., Cui, Z., Moreda, F., Cosgrove, B., Mizukami, N., Anderson, E., DMIP 2 Participants, 2012. Results of the DMIP 2 Oklahoma experiments. *Journal of Hydrology*, **418–419**, 17-48.

Sorooshian, S., Q., Duan, and V. Gupta, 1993: Calibration of rainfall-runoff models: application of global optimization to the Sacramento Soil Moisture Accounting Model, *Water Resources Research,* **29**, 1185-1194.

Spies, R.R, K. J. Franz, T.S. Hogue, and A.L. Bowman, 2015: Distributed hydrologic modeling using satellite-derived potential evapotranspiration, Journal of Hydrometeorology, 16(1),129-146. DOI 10.1175/JHM-D-14-0047.1

Sutanudjaja, E. H., L. P. H. van Beek, S. M. de Jong, F. C. van Geer, and M. F. P. Bierkens, 2014: Calibrating a large-extent high-resolution coupled groundwater-land surface model using soil moisture and discharge data, *Water Resources Research,* **50**, 687-705.

Tapiador, F., F. Turk, W. Petersen, A. Hou, E. Garcia-Ortega, L. Machado, C. Angelis, P. Salio, C. Kidd, G. Huffman, and M. Castro, 2012: Global precipitation measurement: Methods, datasets and applications, *Atmospheric Research,* **104-105**, 79-97.

Van Dam, J., J. Huygen, J. Wesseling, R. Feddes, P. Kabat, and P. Van Waslum, 1997: Theorogy of SWAP version 2.0: Simulation of water and plant growth in the soil-water-atmosphere-plant environment. Technical Document 45. Wageningen Agricultural University and DLO Winand Staring Centre, The Netherlands.

Van Der Knijff, J., Younis, J., and A. De Roo, 2010: LISFLOOD: a GIS-based distributed model for river basin scale water balance and flood simulation, *International Journal of Geographical Information Science,* **24**(2), 189-212.

Vrugt, J., H. Gupta, L. Bastidas, W. Bouten, and S. Sorooshian, 2003: Effective and efficient algorithm for multiobjective optimization of hydrologic models, *Water Resources Research,* **39**(8), 1214

Vrugt, J., H. Gupta, W. Bouten, and S. Sorooshian, 2003: A shuffled complex evolution metropolis algorithm for estimating posterior distribution of watershed model parameters, *Calibration of Watershed Models: Water Science and Application Series*, No. 6, American Geophysical Union, 105-112.

Wanders, N., M. Bierkens, S. de Jong, A. de Roo, and D. Kaarssenberg, 2014: The benefits of using remotely sensed soil moisture in parameter identification of large-scale hydrological models, *Water Resources Research,* **50**, 6874-6891.

Walker, J. P., and P. R. Houser, 2005: Hydrologic data assimilation, Chapter 2. In *Advances in Water Science Methodologies,* Aswathanarayana, A. (ed), A. A. Balkema, The Netherlands, pp. 25-48.

Warrick, A. W., G.J. Mullen, and D. R. Nielsen, 1977: Scaling field-measured soil hydraulic properties using a similar media concept, *Water Resources Research,* **13**, 355-362.

Whitaker, J.S. and T. M. Hamill, 2002: Ensemble data assimilation without perturbed observations, *Mon. Wea. Rev.* **130**, 1913-1924 (2002).

Wood, E., D. Lettenmaier, and V. Zartarian, 1992: A land-surface hydrology parameterization with subgrid variability for general circulation models, *Journal of Geophyscial Research,* **97**(D3), 2717-2728.

Yapo, P., H. Gupta, and S. Sorooshian, 1996: Automatic calibration of conceptual rainfall-runoff sensitivity to calibration data, *Journal of Hydrology*, **181,** 23-48.

Yapo, P., H. Gupta, and S. Sorooshian, 1998: Mulit-objective global optimization for hydrologic models, *Journal of Hydrology,* **204,** 83-97.

Zamora, R., F.M. Ralph, E. Clar, and T. Schneider, 2011: The NOAA Hydrometeorology Testbed soil moisture observing networks: Design instrumentation, and preliminary results, *Journal of Atmospheric and Oceanic Technology,* **28**, 1129-1140.

Zamora, R., E. Clark, E. Rogers, M. Ek, T. Lahmers, 2014: An examination of meteorological and soil moisture conditions in the Babocomari River Basin before the flood event of 2008, *Journal of Hydrometeorology,* **15**, 243-260.

Zhang, C., R. Wang, and Q. Meng, 2015: Calibration of conceptual rainfall-runoff models using global optimization, *Advances in Meteorology,* **2015**, 545376.